ERDC/GSL TR-13-24

Geotechnical and Structures Laboratory

US Army Corps
of Engineers®
Engineer Research and
Development Center

ERDC
INNOVATIVE SOLUTIONS
for a safer, better world

Evaluation of Precast Panels for Airfield Pavement Repair

Phase II: Results of Accelerated Pavement Testing

Lucy P. Priddy, Peter G. Bly, Christopher J. Jackson,
and Tony N. Brogdon

September 2013

The US Army Engineer Research and Development Center (ERDC) solves the nation's toughest engineering and environmental challenges. ERDC develops innovative solutions in civil and military engineering, geospatial sciences, water resources, and environmental sciences for the Army, the Department of Defense, civilian agencies, and our nation's public good. Find out more at www.erdc.usace.army.mil.

To search for other technical reports published by ERDC, visit the ERDC online library at http://acwc.sdp.sirsi.net/client/default.

ERDC/GSL TR-13-24
September 2013

Evaluation of Precast Panels for Airfield Pavement Repair

Phase II: Results of Accelerated Pavement Testing

Lucy P. Priddy and Peter G. Bly

Geotechnical and Structures Laboratory
US Army Engineer Research and Development Center
3909 Halls Ferry Road
Vicksburg, MS 39180-6199

Tony N. Brogdon

Information Technology Laboratory
US Army Engineer Research and Development Center
3909 Halls Ferry Road
Vicksburg, MS 39180-6199

Christopher J. Jackson

Applied Research Associates
Aircraft Operating Surfaces Research Group
Engineering Science Division
104 Research Road, Bldg. 9742
Tyndall AFB, FL 32403-5319

Report 2 of a series

Prepared for Headquarters, Air Force Civil Engineer Center
Tyndall Air Force Base, FL 32403-5319

Abstract

During the period May through August 2012, researchers of the US Army Engineer Research and Development Center (ERDC) in Vicksburg, MS conducted accelerated pavement testing using a C-17 load cart to evaluate the performance of a precast portland cement concrete (PCC) pavement repair system. The system was originally developed by the Air Force Research Laboratory (AFRL) in 2009 but was modified in a joint venture between AFRL and ERDC in 2011 and 2012 as Phase 1 of this project. Three PCC precast panel repairs were performed using the modified system. The precast repairs evaluated were a single-panel, a double-panel, and a quad-panel repair, which simulated repairing a quarter, a half, and a full pavement slab, respectively. Simulated C-17 traffic was applied to the repaired surfaces to determine if the precast panel repairs were suitable for withstanding aircraft traffic for emergency or contingency airfield operations. This report presents the results of accelerated pavement testing including the passes-to-failure, surface deterioration, load-transfer efficiency, deflections, and stress-strain measurements during trafficking. Results of this investigation will be used to further refine the design of the precast panel repair system.

Contents

Figures and Tables

Figures

Tables

Preface

The US Army Engineer Research and Development Center (ERDC) was tasked by Headquarters, U.S. Air Force Civil Engineer Center (AFCEC), to develop and evaluate precast portland cement concrete (PCC) panels for rapidly repairing damaged PCC airfield pavements. The results of this evaluation were used to determine whether the precast system of repair met the requirements defined by the AFCEC for use in contingency environments. The technical manager for this project was Dr. Craig Rutland of the AFCEC, Tyndall Air Force Base, FL. The ERDC technical manager for this project was Jeb S. Tingle, Engineer Systems and Materials Division (ESMD), Geotechnical and Structures Laboratory (GSL).

This report was written for use by the US Air Force's (USAF) pavement evaluation teams, contingency readiness groups, base civil engineers, major command pavement engineers, Rapid Engineer Deployable, Heavy Operational Repair Squadron, Engineer (RED HORSE) Squadrons, and Prime Base Engineer Emergency Force (BEEF) Units. Additional users of this report include Army, Navy, and Marine Corps units charged with the repair and sustainment of damaged airfield pavements.

This publication was prepared by personnel of ERDC's GSL, ESMD, Airfields and Pavements Branch (APB). The findings and recommendations presented in this report are based upon full-scale tests and analyses conducted at the ERDC during May through August 2012. The principal investigators for this project were Peter G. Bly and Lucy P. Priddy, APB and Christopher J. Jackson, Applied Research Associates (ARA). The lead engineering technician was Quint S. Mason, APB. Instru-mentation support was provided by Tony N. Brogdon and Harold T. Carr, ERDC, Information Technology Laboratory. Technical assistance for this work was provided by numerous civil engineering technicians and summer students of the APB, and numerous personnel from the ERDC Directorate of Public Works (DPW). Additional field testing support was provided by Mike L. Chapman, Timothy M. Flynn, and Scott C. Smith of the Air Force Research Laboratory during panel construction and panel placement. Priddy, Bly, Jackson, and Brogdon prepared this report under the supervision of Dr. Gary L. Anderton, Chief, APB; Dr. Larry N. Lynch, Chief, ESMD; Dr. William P. Grogan, Deputy Director, GSL; and Dr. David W. Pittman, Director, GSL.

COL Kevin J. Wilson was Commander and Executive Director of ERDC.
Dr. Jeffery P. Holland was Director.

Recommended changes for improving this publication in content and/or format should be submitted on DA Form 2028 (Recommended Changes to Publications and Blank Forms) and forwarded to Headquarters, US Army Corps of Engineers, ATTN: CECW-EW, 441 G Street NW, Washington, DC 20314.

Unit Conversion Factors

Multiply	By	To Obtain
cubic feet	0.02831685	cubic meters
cubic inches	1.6387064 E-05	cubic meters
cubic yards	0.7645549	cubic meters
degrees Fahrenheit	(F-32)/1.8	degrees Celsius
Feet	0.3048	meters
gallons (US liquid)	3.785412 E-03	cubic meters
Inches	0.0254	meters
pounds (force)	4.448222	newtons
pounds (force) per foot	14.59390	newtons per meter
pounds (force) per inch	175.1268	newtons per meter
pounds (force) per square foot	47.88026	pascals
pounds (force) per square inch	6.894757	kilopascals
square feet	0.09290304	square meters
square inches	6.4516 E-04	square meters
tons (force)	8,896.443	newtons

Definitions

California Bearing Ratio (CBR): A measure of the bearing capacity of soil based upon its shearing resistance. The CBR value is calculated by dividing the unit load required to force a standard piston into the soil being evaluated by the unit load required to force the same piston the same depth into a standard sample of crushed stone and multiplying the result by 100 percent.

Coverage: One application of the load wheel over a single point in the portion of the traffic lane that receives the maximum amount of traffic. For a normally distributed traffic pattern, the test section's pass-to-coverage ratio is determined by dividing the total number of passes in one distribution pattern of traffic by the number of times the load wheel passes over the peak traffic lane. For the six-wheel load cart, the number of coverages must be determined from a scale drawing of the wheel pattern layout and traffic lane distribution. For this test, the pass-to-coverage ratio was calculated as 1.12 for the C-17 load cart.

Elastic deflection: Temporary vertical deformation of the PCC panels and/or the sublayer soil under the load from the heavy weight deflectometer (HWD) or load cart. In this report, elastic deflections were measured using the HWD.

Load cart: A specially constructed vehicle used in engineering tests for simulating aircraft taxiing and braking operations. For this test, the C-17 load cart was used for trafficking operations.

Pass: One traverse of a load wheel across a given length of runway, taxiway, or test section surface.

Pattern: The completion by the test load cart of one simulated normal distribution of traffic in a test lane.

Plastic/permanent deformation: The permanent change in elevation of the subgrade soil resulting from load applications.

Subgrade: An area of soil processed under controlled conditions to provide a desired bearing capacity upon which the test section was constructed. Typically, it is the bottom layer of a foundation or pavement structure.

Test section: A PCC surfaced airfield section. In this test, a 60-ft-wide by 100-ft-long test section built for conducting PCC slab repairs and for trafficking with simulated C-17 aircraft loads.

Test wheel: The main load-bearing wheel on the load cart. In this test, the six actual C-17 aircraft wheels mounted on a load cart.

Traffic lane: That portion of the test section that is subjected to the moving test wheel load of the load cart.

1 Introduction

Problem

Military personnel need expedient methods for conducting partial- and full-slab replacements of portland cement concrete (PCC) pavements in contingency environments. The nature of contingency operations precludes the long-term closure of pavement surfaces, particularly the runway and primary taxiway pavements. In these environments, flight operations must be restored in the shortest timeframes possible, often with only 4 to 6 hr available to complete repairs. Traditional repair methods using conventional PCC, high early-strength concrete, or proprietary cementitious repair materials are the most broadly practiced methods. Disadvantages to using conventional cast-in-place PCC include long curing durations and difficulty in placement during all weather conditions.

Precast concrete panel technology offers a method to eliminate the issues of traditional cast-in-place PCC repair in contingency environments. Panels can be cast before installation using locally available PCC, allowed to cure to their ultimate strength, and stockpiled on site for future use. Panels can be designed to be placed with readily available construction equipment within a narrow construction or repair window either alone or in series with additional precast panels. Prior to recommending the use of precast panel technology for PCC pavement repair in contingency environments, traffic testing was required to validate the precast system's performance. Based on the results, specifications for preparing and using precast panels were provided to military personnel.

The Phase I report ERDC/GSL TR-13-XX, "Evaluation of Precast Panels for Pavement Repair Phase I: System Optimization and Test Section Construction" documented the first phase of a research effort to improve a prototype precast panel system to repair damaged airfield pavements initially created by the Air Force Research Laboratory (AFRL) in 2009. The Phase I report documented the modification and optimization of the system, test section construction, and field installation of panels. This Phase II report documents the performance of the precast panel repairs under simulated full-scale C-17 aircraft traffic.

Objectives and scope of the current investigation

The objective of the research was to develop a precast PCC system to be used for rapid airfield repair work by deployed warfighters for contingency or other expedient repairs. Attributes for an acceptable system include:

- Is easily fabricated under adverse field conditions,
- Uses locally available materials,
- Is capable of long-term storage,
- Is ready for use in a moment's notice,
- Allows for rapid installation in multiple repair geometries,
- Minimizes equipment required for installation,
- Minimizes specialized training, and
- Provides sufficient service life under the prospective aircraft traffic.

To verify the objectives above, the precast PCC system developed during Phase I of this project was used to construct precast panels for full-scale performance evaluation. Three different repair configurations were conducted to evaluate the capability of the repair system to perform single- and multiple-panel repairs. The completed repairs were trafficked under simulated C-17 aircraft traffic to determine their performance. Results of the testing were then analyzed to verify if the precast panel system met the attributes outlined above.

This report describes the physical and geometrical properties of the precast panels in Chapter 2. The construction of the full-scale test section and installation of the panel instrumentation are presented in Chapter 3. Chapter 4 describes the accelerated pavement testing including traffic application, data collection, and failure criteria. Chapter 5 summarizes the visual deterioration observations during the traffic tests, and Chapter 6 summarizes settlement and faulting results. Nondestructive test results are presented in Chapter 7, and Chapter 8 presents the instrumentation data collected. Analyses of results are presented in Chapter 9. Pertinent conclusions and recommendations are presented in Chapter 10.

2 Panel Descriptions

In 2011, the combined ERDC and AFRL research team improved the US Air Force's current precast repair system. A major modification made to the system was adding a second panel design that allowed the system to connect multiple panels together to complete larger repairs. The original panel design, now referenced as the "standard" panel, was carried over (with slight modifications) and was applied for both single- and multiple-panel repairs. This panel had load transfer dowels integrated mid-depth on both transverse edges. The dowels selected were 1-in. diameter, 22-in. long, and were epoxy coated. The dowels provided load transfer between the precast panel and the surrounding pavement and between the precast panel and another precast panel. The second panel was called a "terminal" panel, which was designed for multiple-panel repairs only. Load transfer dowels were only placed on one transverse edge, while the other transverse edge had formed dowel receptacles for connecting to a standard panel to facilitate a larger repair.

Both panels were slightly less than 10-ft-wide by 10-ft-long to ensure fit and ease of placement within a 10-ft by 10-ft saw cut repair area with a 0.375-in.-wide joint around each panel. The panels each measured 9-ft 11-1/4 in. by 9-ft 11-1/4 in. by 11 in. Each panel weighed approximately 13,600 lb. Panels were designed such that load transfer dowels were only oriented parallel to the direction of traffic; no load transfer dowels were installed perpendicular to the direction of traffic (on the longitudinal edges).

Both panel types are shown in Figure 1. Details of reinforcement and panel dimensions are presented in Figures 2 and 3. During August through October 2011, ERDC personnel cast two terminal and five standard panels. The panels were prepared at the ERDC in Vicksburg, MS. Each panel required approximately 3.5 yd^3 of a locally available 5,000 psi minimum compressive strength ready mixed concrete with a #67 limestone. The average 28-day measured compressive strength was 5,710 psi by ASTM C39. Further details of the panel designs and their fabrication are provided in the Phase I report and are not presented herein.

Figure 1. Precast concrete panel types.

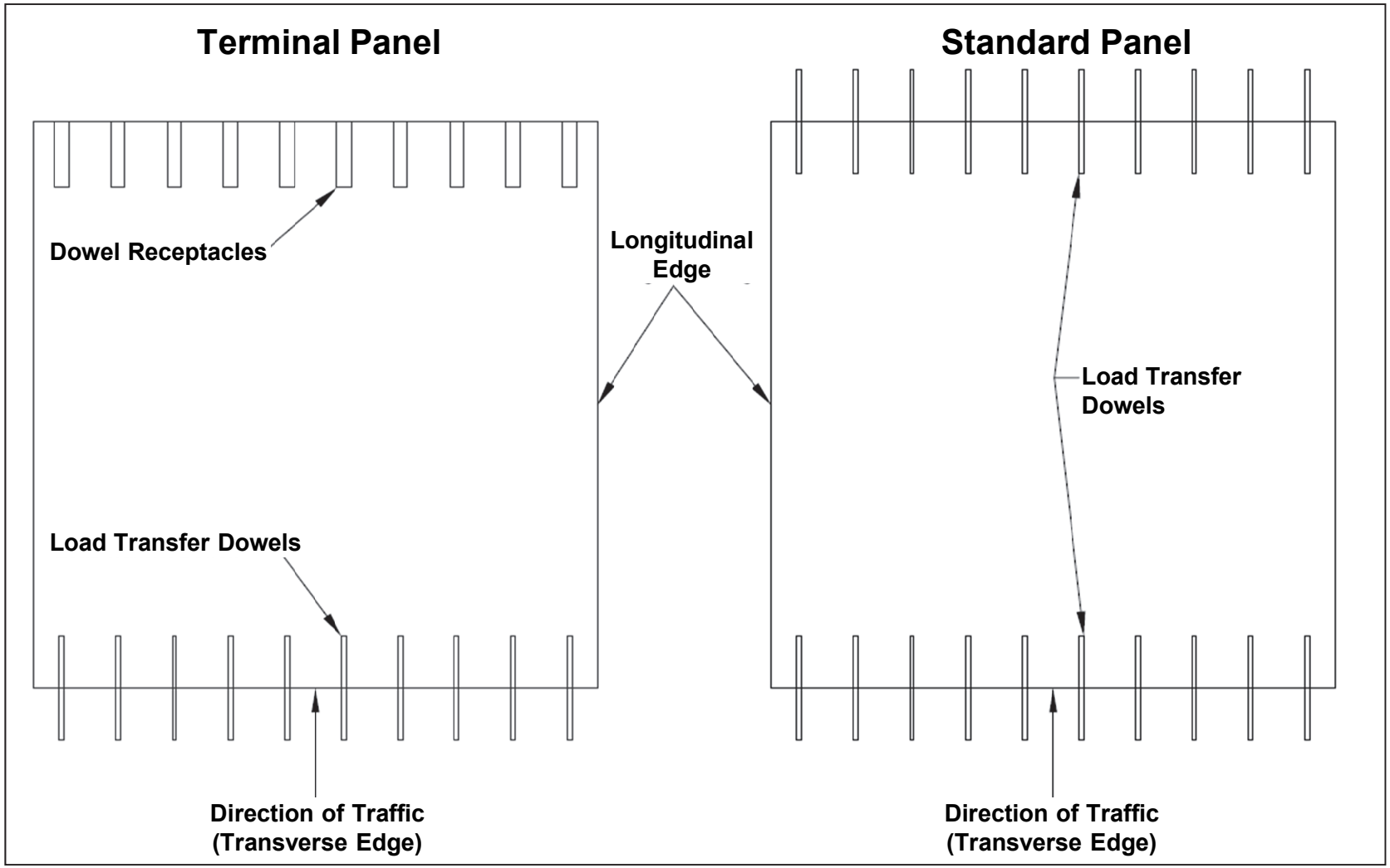

Figure 2. Rebar layout for standard precast panel.

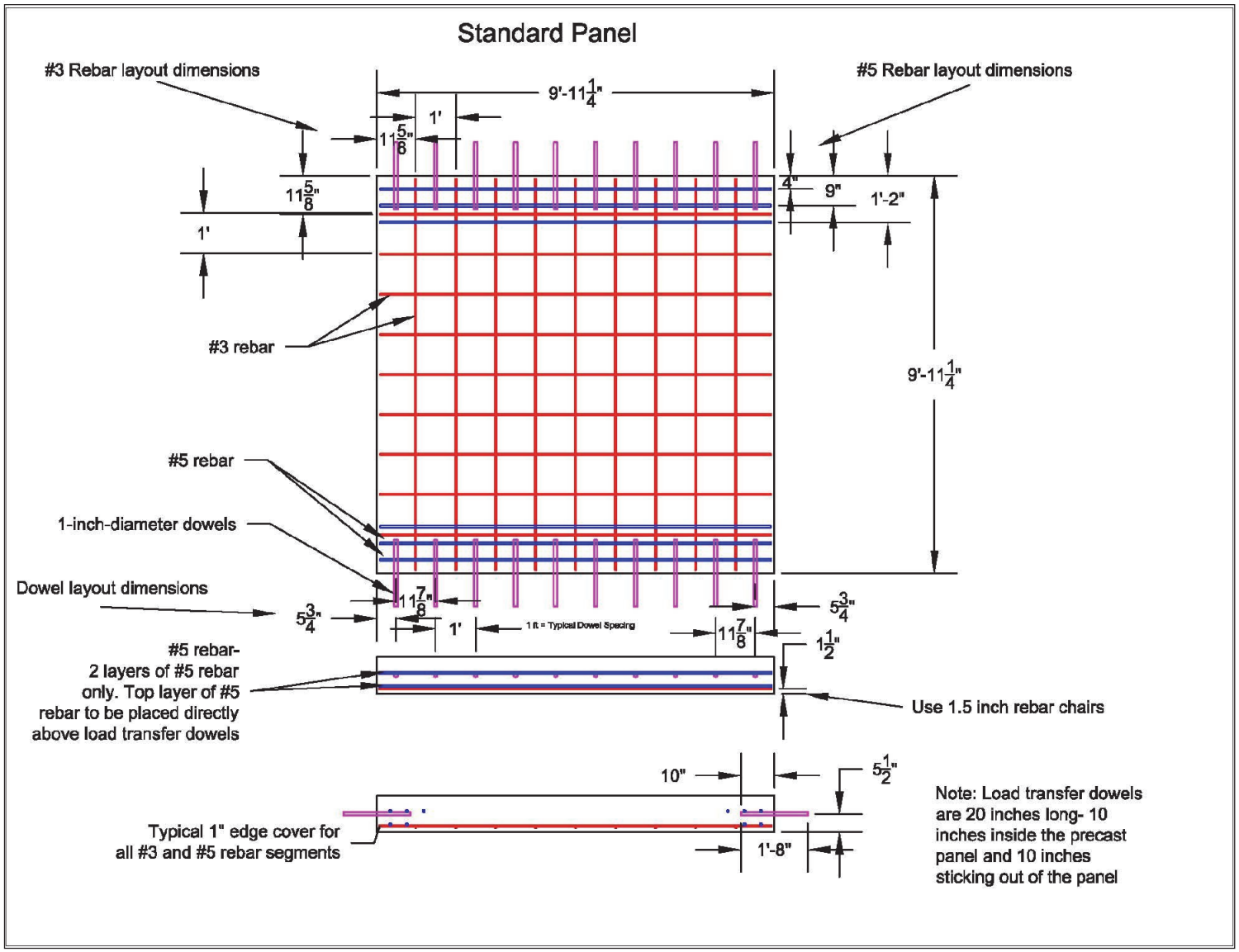

Figure 3. Rebar layout for standard precast panel.

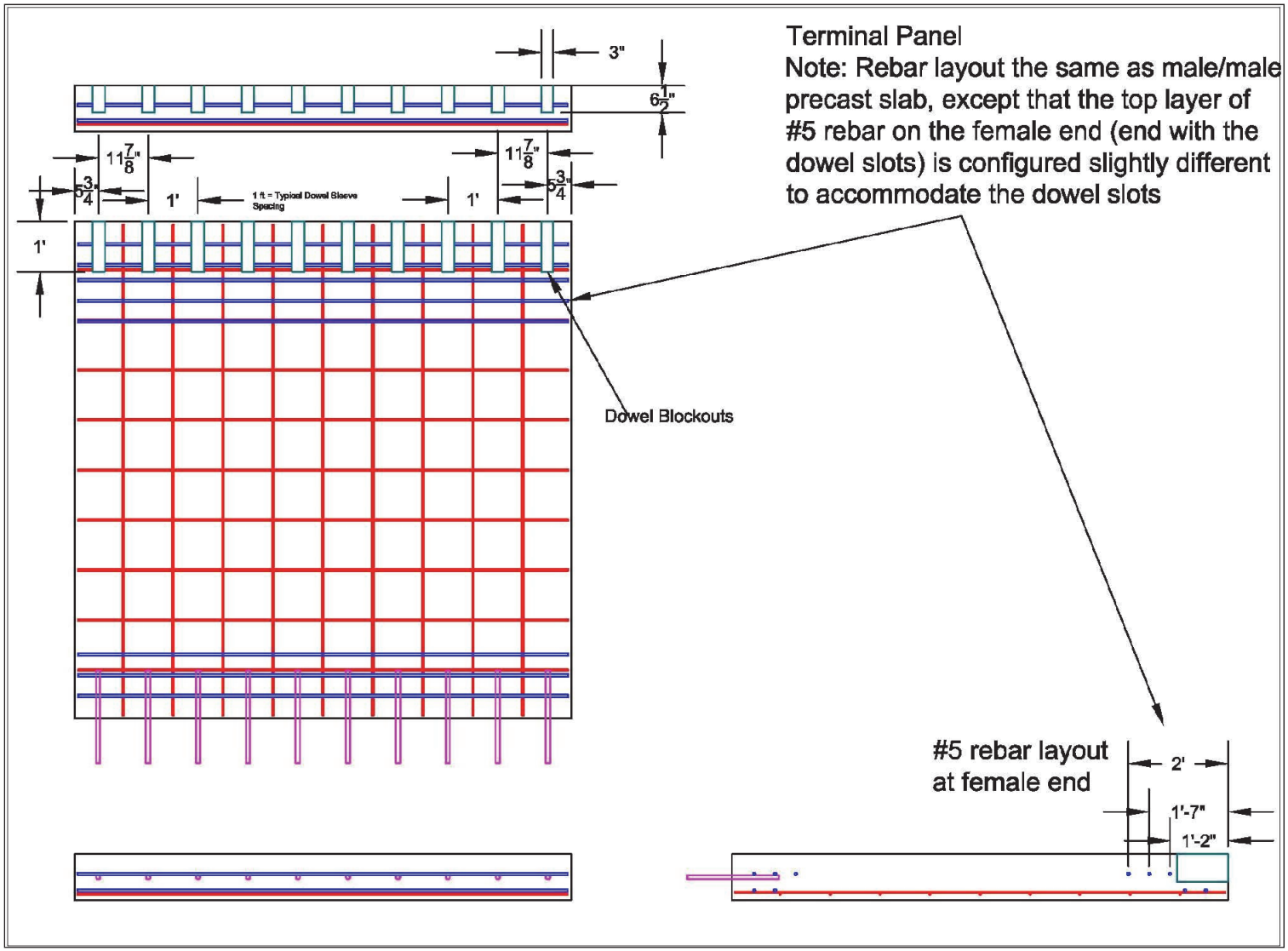

3 Field Testing

Test section construction and panel installation

General test section design

A 60-ft-wide by 100-ft-long PCC test section was constructed at the ERDC in Vicksburg, MS, from April through July 2011. The PCC test section was designed to consist of fifteen 20-ft-wide by 20-ft-long slabs, each 14-in.-thick placed over a compacted well-graded crushed limestone base (with a soil classification of GW) over a low-plasticity clay subgrade (with a soil classification of CL). Seven of the precast panels fabricated were installed in the test section as shown in Figure 4. As shown in the cross-section view of the test section (Figure 5), the precast panels were thinner than the test section PCC and where placed over a thin (3-in.) layer of flowable fill backfill. A brief description of the general repair process is provided in this section. Detailed descriptions of the construction of the test section are provided in the Phase I report.

Sublayer instrumentation

Just prior to the placement of the surface PCC, the prepared base was instrumented with 9-in.-diam Geokon® earth pressure cells (EPC) capable of measuring up to 200 psi that were installed at the base-PCC interface at 10 locations as shown in Figure 6. These EPCs were placed to monitor the stress distribution provided by the panels under loading.

PCC surface instrumentation

Following the placement and curing of the PCC, selected PCC slabs were instrumented with 20 surface strain gauges as shown in Figure 6. The foil strain gauges were manufactured by Vishay Micro-Measurements. An EP-08-40CBY-120 gauge with a resistance of 120 ohms ±0.2 percent and gauge factor of 2.075 ±0.5 percent from Lot Number A19AP152 was used. The procedure for installing gauges was prescribed by Vishay in their literature "Tech Note TT611." The gauges were placed in the transverse direction, wired, waterproofed with sealant coatings, and covered with aluminum tape to aid in additional waterproofing and acted as electrical noise barriers. Finally, a neoprene rubber patch was applied as a mechanical barrier to protect the gauges from abrasion during trafficking.

Figure 4. PCC panel layout-plan view.

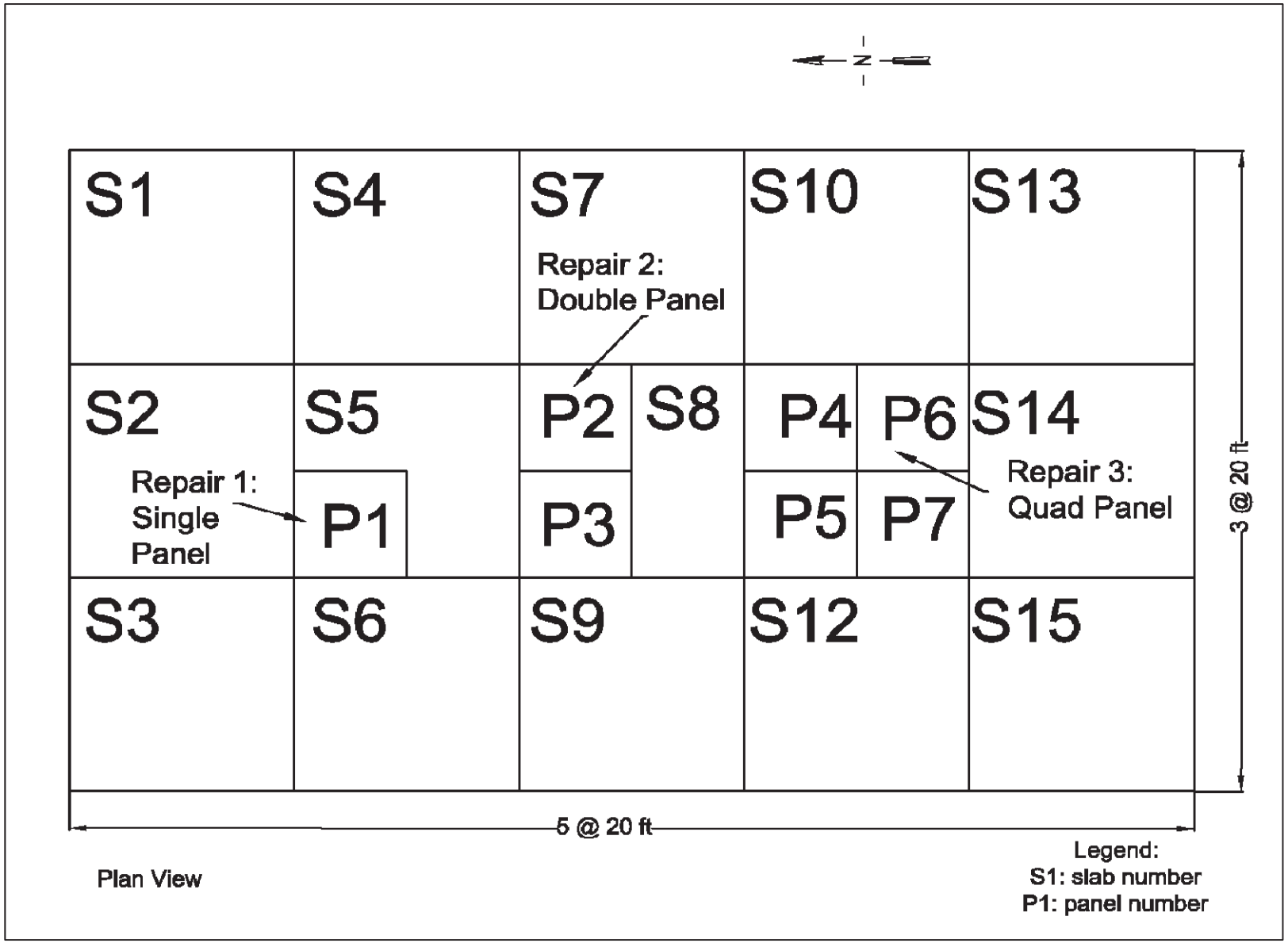

Figure 5. PCC panel layout-profile view.

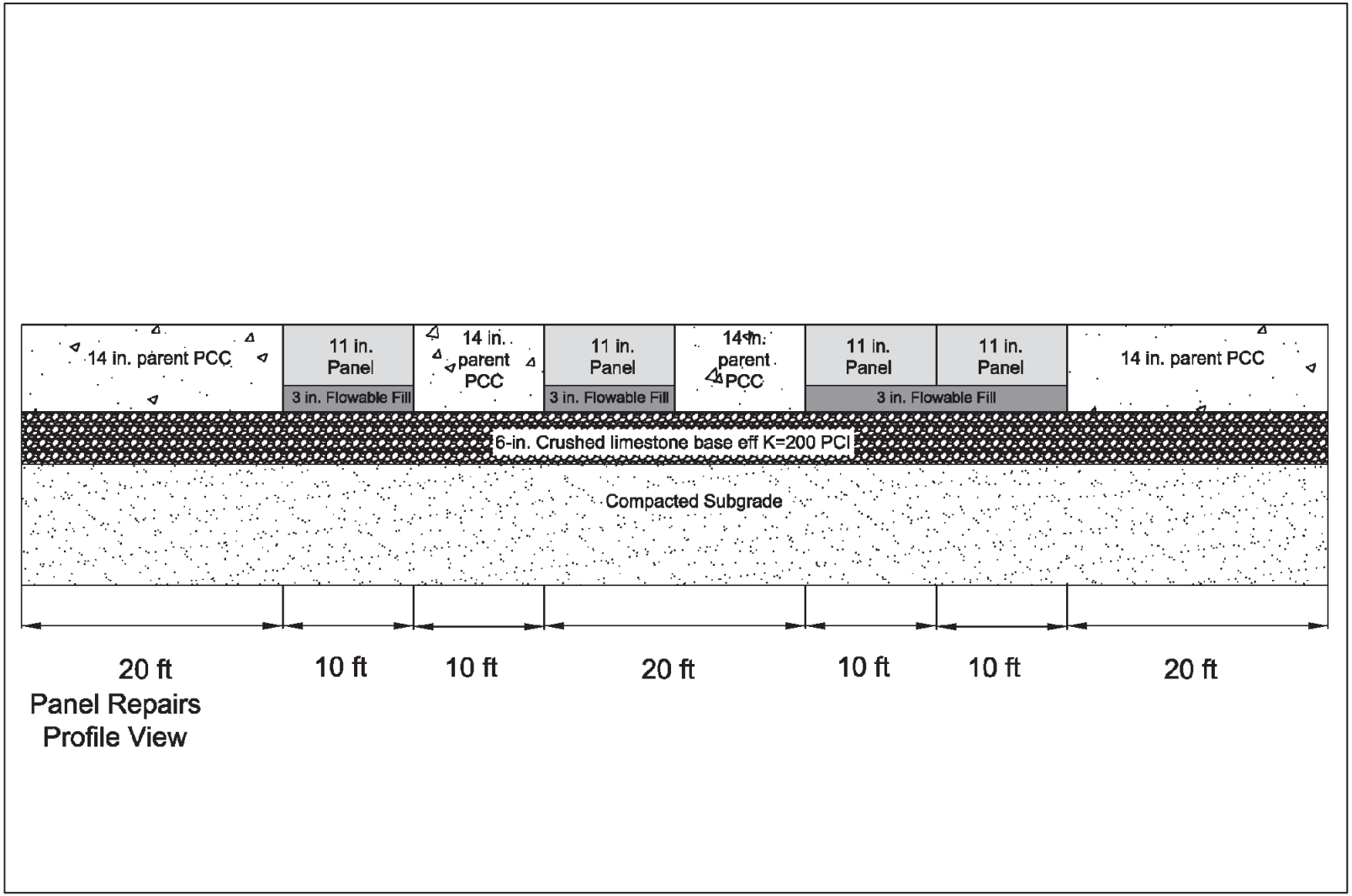

Figure 6. Instrumentation layout.

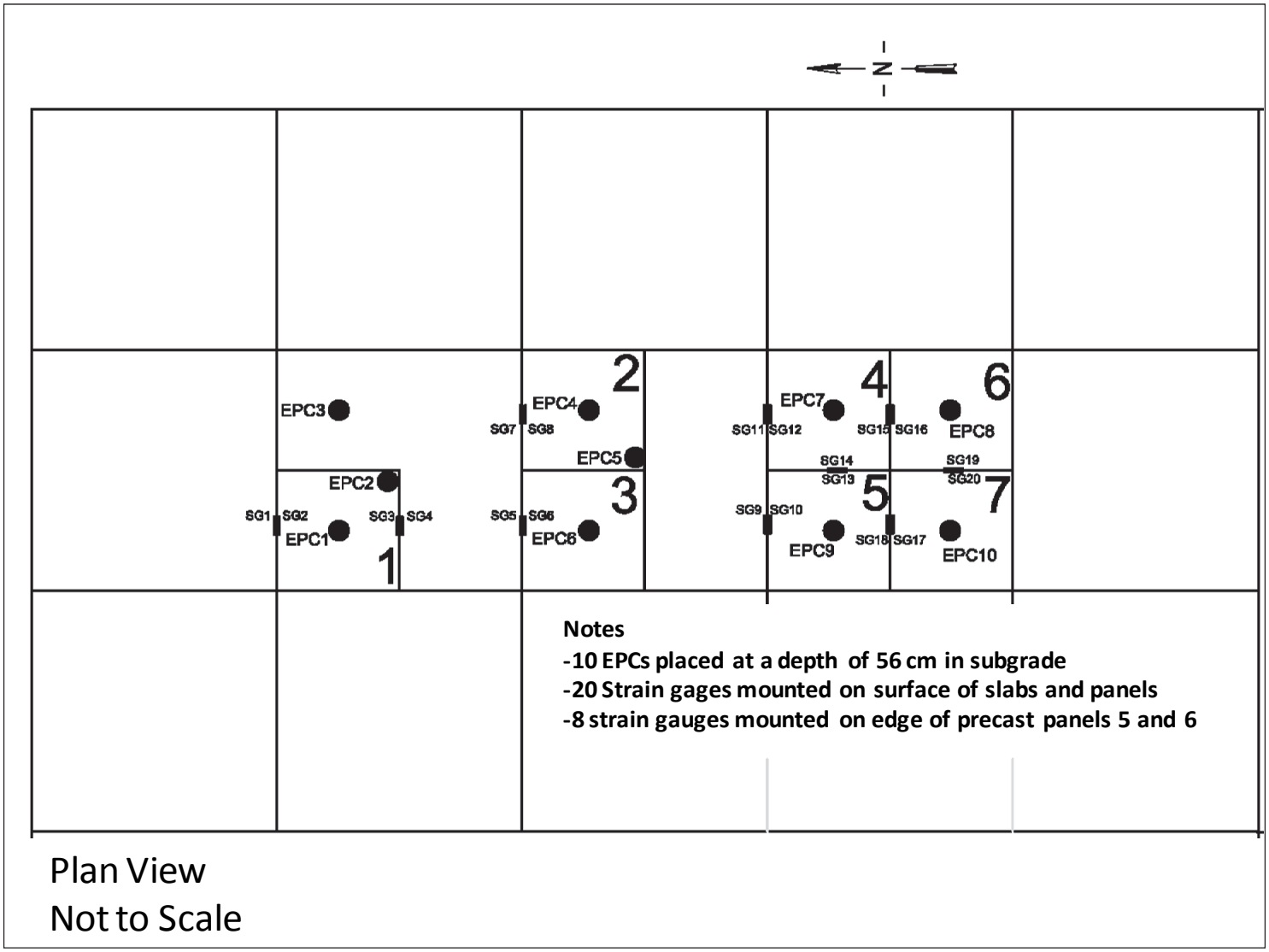

Precast panel instrumentation

The precast panels were instrumented with eight strain gauges mounted on the sides of two precast panels centered 1 in. from the top and bottom of the panel vertically and centered horizontally. The foil strain gauges used were also manufactured by Vishay Micro-Measurements. An EP-08-40CBY-120 type of gauge with a resistance of 120 ±0.2 percent and gauge factor of 2.075 ±0.5 percent from Lot Number A19AP152 was used. Each gauge location was prepared in a similar manner previously described with the exception of the application of the neoprene rubber patches. During trafficking, the EPCs were programmed to collect data at a rate of 1 kHz (or 1,000 samples per second). During nondestructive testing, EPC data were collected at a rate of 5 kHz. Strain gauge data were collected at a rate of 5 kHz for both trafficking and nondestructive testing.

Field testing—precast panel repairs

Following the 28-day curing period for the PCC, three areas were marked in the test section to represent damaged pavement. Repair 1 (Panel 1) simulated a 10 ft x 10 ft replacement using a single panel. Repair 2 (Panels 2 and 3) simulated a 10 ft x 20 ft replacement along a joint requiring two panels. Repair 3 simulated a 20 ft x 20 ft replacement requiring four panels (Panels 4, 5, 6, and 7). All repairs were conducted during October through November 2011 by a team of 12 ERDC and AFRL personnel.

The repair installation procedure consisted of first saw cutting 10-ft x 10-ft square PCC areas and saw cutting dowel receptacles in the parent PCC. Each square was removed by installing concrete expansion anchors. A crane was used to remove the pavement in single sections in lieu of breaking out the pavement and excavating the pieces. Once removed, the dowel receptacles were prepared by removing the PCC with jackhammers. Then the repair areas were backfilled with a 3.0-in.-thick layer of flowable fill to provide full and uniform support beneath the panels. Panels were then lowered into the prepared repair areas. Once the panels were leveled, the dowel receptacles were filled with a cementitious, rapid-setting repair grout, and the joints were sealed. The flowable fill and the dowel receptacles were then allowed to cure prior to the application of traffic. Detailed descriptions and step-by-step instructions of the panel installation process were provided in the Phase I portion of this report. The completed repairs are presented in Figure 7.

Figure 7. Completed Repairs 1-3.

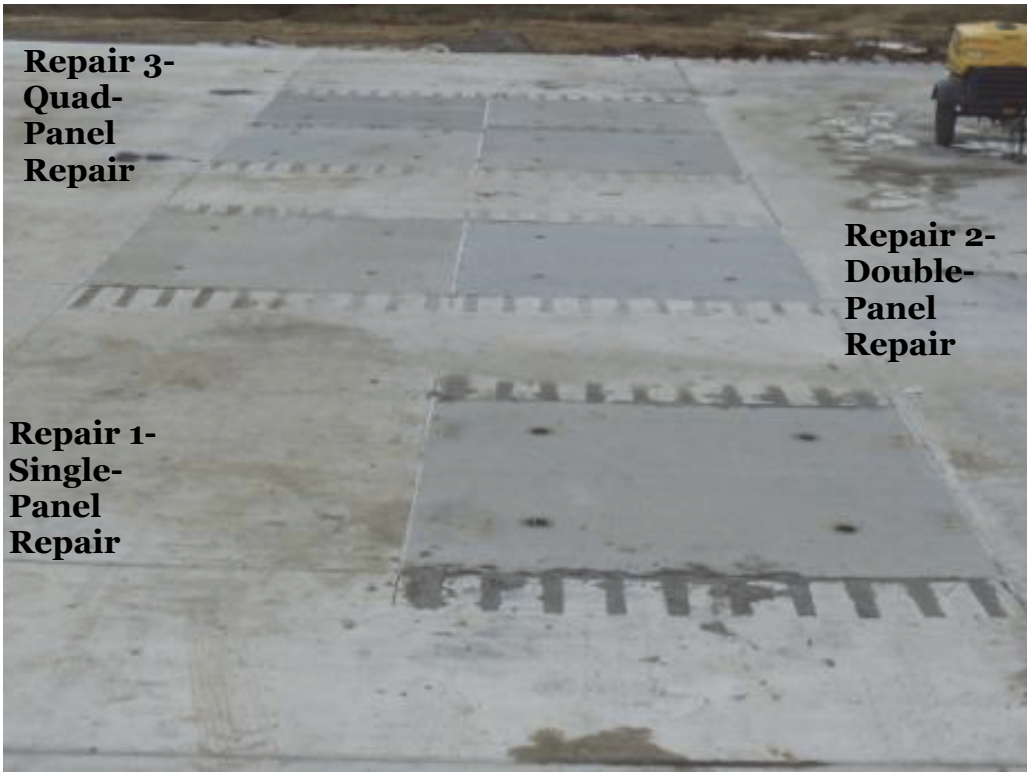

4 Accelerated Pavement Testing

The precast panel repairs were trafficked with simulated C-17 aircraft loading using a load cart and an approximated normally distributed traffic pattern. The deterioration of each repair was monitored closely during traffic application. In addition to the load cart testing, nondestructive testing techniques and instrumentation were used to monitor changes in the repairs' load transfer efficiency, stiffness, and stress and strains as a function of traffic applications. The collected data were used to perform analyses to understand the performance of the panels under aircraft traffic and also to assist in any future design work for precast panels. The remainder of this chapter details the trafficking procedure, data collection process, and failure criteria used.

Load cart description

A multiple-wheel C-17 load cart was used to simulate one-half the main gear of a C-17 fully loaded to its maximum gross ramp weight of 586,000 lbs. Figure 8 illustrates the geometrical arrangement of the C-17 landing gear. The multiple-wheel C-17 load cart (Figure 9) simulated only one-half of the main gear with a test weight of 269,560 lbs. Individual wheel loads were approximately 44,930 lbs across two triple wheels in tandem gear (6 tires total). The gear used 50-in.-diam; 21-in.-wide; 20-ply tires maintained within normal inflation range (138 to 144 psi) during testing.

Traffic operations

Simulated normally distributed traffic was applied across a 9-ft-wide traffic lane, as shown in Figure 10. The pattern simulated the traffic distribution patterns, or wander width, typically seen when aircraft taxi to and from an active runway. The width of each lane corresponded to a contact width of 18 in. (not the overall published tire width of 21 in.) of the C-17 tires when fully loaded. The normally distributed traffic patterns were simplified for ease of use by the load cart operator. Traffic was applied by driving the load cart forward and then backward over the length of the test section and then shifting the path of the load cart laterally approximately one tire width (18 in.) on each forward pass. Tracking guides were attached to the load cart to assist the driver in shifting the load cart the proper amount for each forward pass. This procedure was continued until one pattern of traffic was

completed. One complete pattern consisted of 28 passes, which resulted in the application of a maximum of 25 coverages. Traffic was continued on each item in this manner until one pattern was applied to the test item, and the pattern was repeated for 10,000 passes or until failure occurred, whichever came first.

Figure 8. Spatial layout of C-17 landing gear.

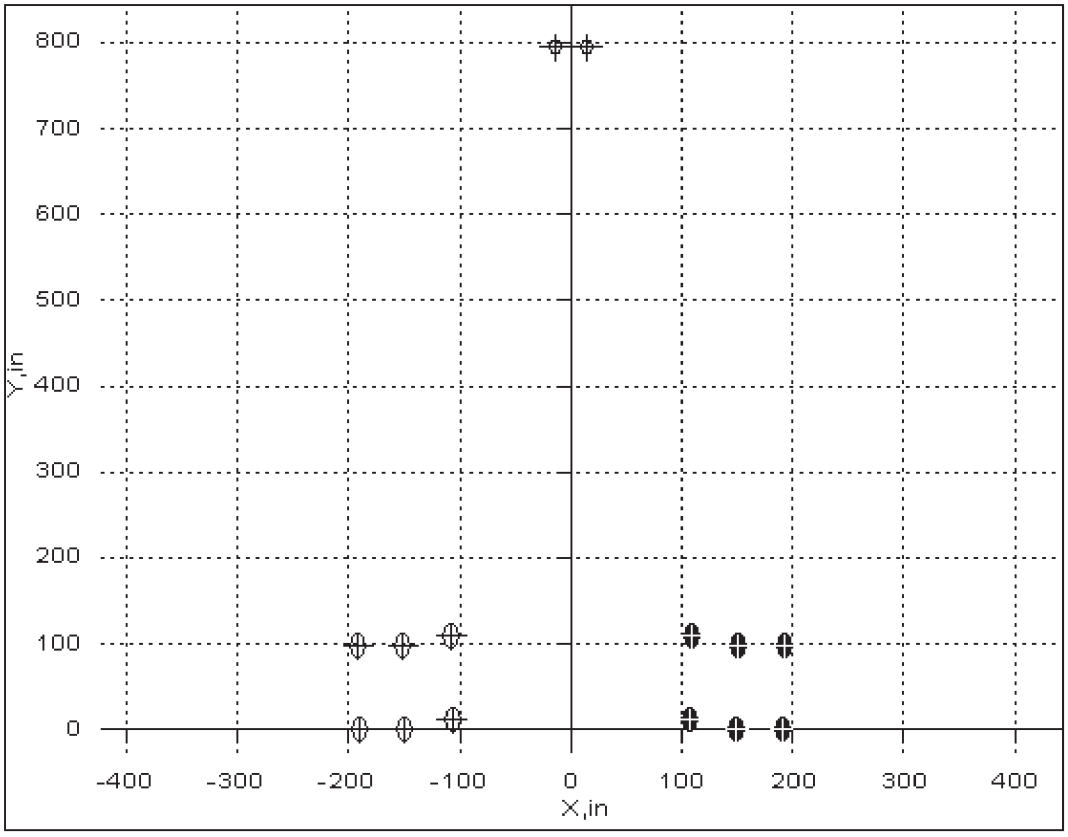

Figure 9. C-17 load cart on test section.

Figure 10. C-17 pattern on test section.

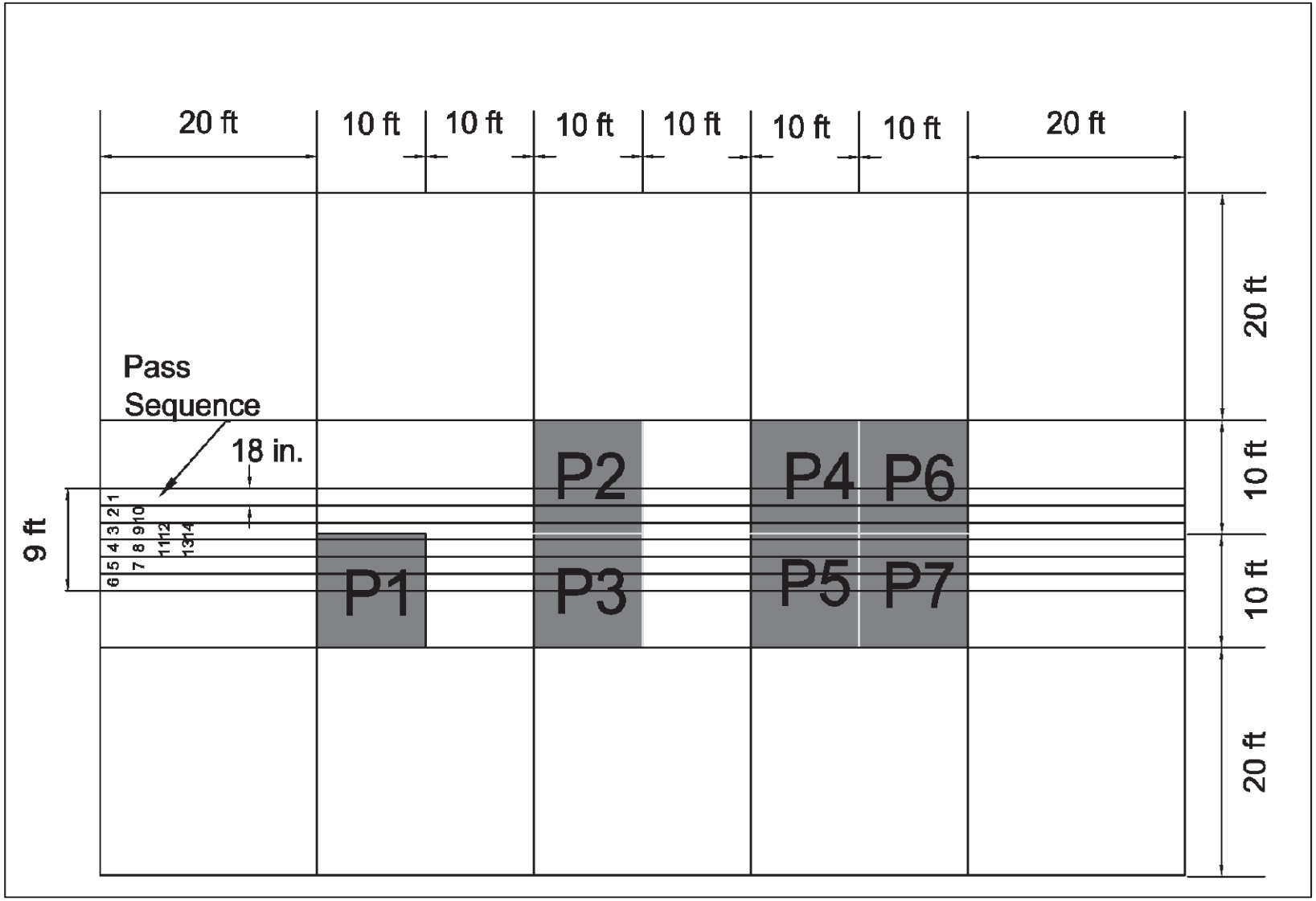

Data collection procedures

Data were collected periodically during trafficking, and the precast panels were inspected for damage during all trafficking intervals. Data collected included:

- Pavement condition surveys of the parent slabs and precast panels during trafficking;
    - Photographs during trafficking showing damage over time
    - Crack monitoring
- Heavy weight deflectometer (HWD) measurements;
    - Load transfer tests on existing slabs to establish baseline values
    - Center plate measurements in the center of each slab and precast panel to measure changes in stiffness with traffic
    - Load transfer tests on parent slab and at joints of connected panels in both the longitudinal and transverse directions
    - Corner deflection tests to monitor loss of support
- EPC data collection during trafficking in the centers of slabs, centers of precast panels, and corners and edges of panels to understand the stress distribution;
- Strain gauge data collection during trafficking to understand strains at the edges of panels; and
- Faulting and settlement measurements to determine changes in slab elevations.

Test data were collected after a predetermined number of passes as shown in Table 1 until failure or 10,000 passes were completed. Results and analyses of the data collected are presented in the following chapters.

Failure criteria

Pavement performance data were collected periodically during trafficking, and the panels and test section slabs were inspected for distresses. It was anticipated that the panels would fail as a result of surface deterioration from overloading the pavement (resulting in load-related surface distresses), loss of base support under the panels (resulting in faulting or settlement of the slabs), or from lack of load transfer at the joints (resulting in spalling, faulting, or settlement).

Table 1. Trafficking data collection intervals.

Static Data Collection Pass Level	Dynamic Data Collection Pass Interval
0	-
112	113-140
238	239-266
462	463-490
910	911-938
1,120	1,121-1,149
1,400	1,401-1,428
1,680	1,681-1,708
1,960	1,961-1,989
2,240	2,240-2,268
2,800	2,801-2,828
3,360	3,361-3,377
4,200	4,201-4,228
5,600	5,601-5,628
7,100	7,101-7,128
8,400	8,401-8,428
10,000	No data collected

Visual inspections were performed at selected traffic intervals to identify specific distresses associated with high foreign object debris (FOD) potential such as cracking, spalling, corner breaks, and shattered slabs. Cracking was considered minor unless development of associated spalls resulted in the accumulation of debris or cracks with widths greater than 1 in. Spalled materials have the potential to be sucked into jet engines or damage propellers and rotors of aircraft. Additionally, spalled concrete and wide cracks present a tire hazard because of the potential for the sharp edges to cut aircraft tires. When distresses posed high FOD potential or tire hazards were identified, the repair was considered failed.

The repairs were also monitored for failure due to high surface roughness. High surface roughness is associated with significant elevation changes, resulting from either settlement of the pavement from a weak foundation or significant abrupt surface deterioration. Elevation changes in excess of 3 in. are unacceptable for the C-17 aircraft because of the potential of damaging the landing gear. If elevation changes in excess of 3 in. or more occurred in this evaluation, the repair was considered failed. Other aircraft have different elevation change values and would need to be considered differently.

5 Surface Deterioration Results

The precast panel repairs and surrounding pavement were monitored using standard pavement condition survey procedures to identify common airfield pavement distresses and their severities. Changes to severity levels of distresses observed were monitored during trafficking. Using these distresses, the pavement condition index (PCI) for each panel was calculated during trafficking using pavement management software (PAVER). Because accelerated trafficking was completed, some climate and other related PCC distresses were not expected, since the test section would not be able to accumulate this type of damage in the short testing duration.

Pavement condition prior to traffic

Test section construction

A transverse cold joint was required in the center of Slab 2 (slab layout presented in Figure 4), after the final concrete delivery during test section construction was delayed for over 90 minutes. This joint was constructed approximately 8 ft from the N joint of Panel 1. The partially placed slab was cut back 2 ft from the face of the concrete face to provide a smooth, vertical face. No tie bars were installed prior to the completion of the slab to maintain its structural integrity.

Repairs after installation

Prior to application of traffic, a small patch was conducted in Repair 3 in the NW corner of Panel 4. The thin piece of concrete that formed the exterior most dowel slot receptacle wall was damaged (Figure 11). Cracking was noticed before the panel's installation, but the concrete piece fully dislodged during the installation. The damage was sustained between the time in which the panel was constructed to after off-loading, when the panel was transported to the test section site, but the source is unknown. A rapid-setting cementitious repair material, Pavemend 15.0™, was used to repair the damaged pavement after installation and was placed when the dowel bar receptacles were filled. Because of this distress, a slight decrease in condition occurred due to the patch with a calculated PCI of 90. The other repairs were in good condition with no visible distresses; thus the repairs were considered in brand new condition (PCI=100).

Figure 11. Damaged and repaired dowel bar receptacle on panel 4.

Additionally, when the test section was saw cut to generate the repair areas, overcuts (kerfs) from the corners of the repairs extended approximately 12 to 15 in. into the parent PCC (Figure 12). This overcutting was necessary to provide the full depth cut using a round saw blade to fully free the demolished concrete. During trafficking, cracks extended from these overcuts.

Figure 12. Saw cuts at corners of panels.

Pavement condition during traffic

Each of the three repair configurations constructed withstood different amounts of traffic before failing. The failure modes are detailed below:

- Repair 1: A total of 5,600 C-17 passes were applied to Repair 1 prior to failure due to a high-severity shattered slab for the parent slab and the precast panel.
- Repair 2: A total of 10,000 passes were applied to Repair 2 prior to failure due to high-severity joint spalls and deterioration of the dowel receptacles in the parent slab (high FOD potential).
- Repair 3: A total of 7,100 passes were applied to Repair 3 prior to failure due to a high-severity joint spalling along the south edge of the repair (high FOD potential).

Details of distresses noted during trafficking and their calculated PCI are presented in Table 2. Based on the performance of the panels under traffic, load related distresses were minor until approximately 2,800 passes, when spalling along corners and joints increased in severity.

Table 2. Summary of repair performance.

Panel	Repair	Pass Level	Distress Description	PCI (%)
1	1	0	None	100
2	2		None	100
3			None	
4	3		During placement, the NW corner was broken at the outside dowel slot. A low-severity patch was noted for this repair in good condition.	90-pretraffic patch in one panel
5			None	
6			None	
7			None	
1	1	112	Low-severity cracking was noticed in the parent slab extending to the N joint of the panel.	86
2	2		A low-severity crack was noticed in the parent slab between Panel 1 and Panel 2 running from the saw cut in the parent slab.	100
3			None	
4	3		The low-severity patch in the NW corner was in good condition. A low-severity crack was noticed in the parent slab between Panels 2 and 3 and 4 and 5 extending to the saw cut.	90

Panel	Repair	Pass Level	Distress Description	PCI (%)
5			None	
6			None	
7			None	
1	1	238	No change.	86
2	2		No change.	100
3			No change.	
4	3		Minor spalling was noticed on N joint and NW corner (not recorded as a distress following PCI procedures for minor spalls).	90
5			Minor spalling on N joint and SE corner was noticed (not recorded as a distress following PCI procedures for minor spalls).	
6			Minor spalling on S joint was noticed (not recorded as a distress following PCI procedures for minor spalls).	
7			Low-severity spalling on S joint of parent slab.	
1	1	462	No change.	86
2	2		Low-severity spalling noted on S joint.	89
3			Low-severity spalling noted on S joint.	
4	3		The patch in NW corner was in good condition.	87
5			No change.	
6			No change.	
7			Low severity joint spall noted on SE corner.	
1	1	910	FOD developing in parent slab due to medium-severity corner crack in NE corner of the parent slab. A crack connects this distress to the panel. A low-severity spall is developing in the NE corner of the panel.	80
2	2		No change.	89
3			No change.	
4	3		No change.	78
5			A hairline crack was noticed in the NE corner.	
6			Cracks were noticed in the SE corner creating a low-severity corner spall.	
7			A low-severity crack was noticed in the parent slab south of the panel between dowel slots.	
1	1	1,120	FOD noticed from saw overcut in parent slab NE of panel.	80
2	2		No change.	89
3			No change.	
4	3		No change.	65
5			No change.	

Panel	Repair	Pass Level	Distress Description	PCI (%)
6			Low-severity crack noticed from S joint through parent slab to S edge of test section (longitudinal crack).	
7			Low-severity crack extended from S joint through parent slab to S edge of test section.	
1	1	1,400	No change.	80
2	2		Low-severity joint spall noticed on S joint in panel.	89
3			Low-severity joint spall noticed on S joint in panel.	
4	3		No change.	59
5			No change.	
6			Low-severity corner spall in SE corner producing small FOD. Low-severity spalling and cracking in dowel slots were noticed on the S edge.	
7			Low-severity corner spall in SE corner producing small FOD. Low-severity spalling and cracking in dowel slots were noticed on the S edge.	
1	1	1,680	FOD produced NE of panel in parent slab.	80
2	2		No change.	89
3			No change.	
4	3		No change.	59
5			No change.	
6			Low-severity corner spall in SE corner producing small FOD. Low-severity spalling and cracking in dowel slots were noticed on the S edge.	
7			Low-severity corner spall in SE corner producing small FOD. Low-severity spalling and cracking in dowel slots were noticed on the S edge.	
1	1	1,960	No change.	80
2	2		Hairline cracks noticed in NW corner of panel.	84
3			No change.	
4	3		No change.	59
5			Low-severity spalling and cracking noticed in SE corner near repair.	
6			No change.	
7			No change.	
1	1	2,240	No change.	80
2	2		Low-severity corner spall noticed in NW corner.	84
3			No change.	
4	3		No change.	59
5			No change.	

Panel	Repair	Pass Level	Distress Description	PCI (%)
6			No change.	
7			No change.	
1	1	2,800	A low-severity corner spall approximately 6 in. long was noted in the NE corner of the panel. A 6-in.-long low-severity corner spall was also noted along the NE edge of the panel. A 3-ft-long transverse crack was noticed from the E edge of the panel progressing towards the panel center. A high-severity corner spall was noted in the NW corner of the panel. Additional distresses were noted in the parent slab N of the panel including a 5.5-ft-long medium-severity longitudinal crack and a medium-severity joint spall 4-ft long and 1.5-ft wide along the cold joint in the parent slab. A medium-severity diagonal crack approximately 8 ft long was noted extending from the saw overcut to the N edge of Repair 2 in the parent slab containing the panel. Another diagonal crack (low-severity) was noted running from the E edge of Panel 1 E towards the E joint of the parent slab.	72
2	2		A medium-severity joint spall approximately 3 in. long was noted on the SW edge of the panel. On the N panel joint, a 6-in.-long low-severity joint spall was noted. A low-severity corner spall approximately 1 ft long was noted in the NW corner of the panel.	62
3			Medium-severity joint spall approximately 3.5 ft long was noted in the NE joint. A low-severity crack was noted approximately 1 ft long progressing towards the panel center from the NW joint. A low-severity longitudinal crack was noted that extended from the overcut from Panel 1 through the parent slab to Panel 3.	
4	3		A high-severity corner spall was noted in the SE corner approximately 1 ft long. This spall was located near the patch which was beginning to deteriorate and produce FOD.	25- although this repair was considered in serious condition, trafficking was continued. The repair was inspected more often to remove FOD and prevent damage to the tires.
5			A high-severity corner spall was noted in the NE corner approximately 2.5 ft long. A longitudinal crack was noted from the N joint in the center progressing approximately 7 ft towards the center of the panel. A 1.5-ft-long low-severity joint spall was noted on the NW edge, and a 1-ft-long low-severity joint spall was noted on the center of the west edge.	
6		2,800	A medium-severity joint spall approximately 1-ft long was noted on the E edge in the center, and a high-severity corner spall was noted on the SE corner. In the parent slab S of the panel, a 19-ft-long low-severity longitudinal crack was also noted along with a high-severity joint spall on the N edge of the parent slab.	25

Panel	Repair	Pass Level	Distress Description	PCI (%)
7			A medium-severity joint spall approximately 6 in. long was noted on the central portion of the E edge. A high-severity corner spall was noted in the NE corner approximately 1 ft in length. A medium-severity corner spall was noted on the N edge towards the NW corner approximately 6 in. in length.	
1	1	3,360	A low-severity transverse crack extended from the E edge of the pavement and was 5 ft long. A low-severity diagonal crack was noted extending from the center of the N edge towards the W edge of the panel.	59
2	2		The medium-severity joint spall on the SW edge of the panel produced additional FOD.	62
3			A low-severity joint spall approximately 4 in. long was noted along the center of the W edge of the panel.	
4	3		Additional FOD noted on SE edge from high-severity joint spall in the panel. A high-severity joint spall approximately 4 ft long was noted in the parent slab S of the panel.	25- although this repair was considered in serious condition, trafficking was continued. The repair was inspected more often to remove FOD and prevent damage to the tires.
5			The low-severity longitudinal crack extended towards the panel center. The joint spalling along the NW edge progressed transforming into a low-severity corner spall.	
6			A new low-severity joint spall was noted on the SW edge of the panel. Additional FOD was produced along the S edge of the panel in the parent slab from the dowel receptacles.	
7			New medium-severity joint spalls were noted on the NW and SW edges of the panel.	
1	1	4,200	The spalling along the NE corner included a medium-severity corner break. The panel was considered a low-severity shattered slab with the intersection of the longitudinal crack with a transverse crack.	0-The PCI was calculated as 0 due to the low-severity shattered slab; however, the repair was not considered failed as the cracks were hairline. The distresses were low- and medium-severity. The panel required more frequent inspection to remove FOD.
2	2		No change.	62
3			No change.	
4	3		The patch in the SW corner continued to deteriorate.	7- although this repair was considered failed by traditional PCI procedures, trafficking was continued. The repair was inspected more often to remove FOD and prevent
5			A low-severity longitudinal crack was noted in the center of the panel. A low-severity joint spall was noted near the NE corner on the E edge of the panel.	
6			A low-severity corner break was noted in the SW corner of the panel. FOD production continued on the S side of the panel in the parent slab.	

Panel	Repair	Pass Level	Distress Description	PCI (%)
7			FOD production continued on the S side of the panel in the parent slab due to the dowel receptacles.	damage to the tires.
1	1	5,600	The panel was considered a high-severity shattered slab. FOD production on the NE corner was considered high. The panel was considered failed. The parent slab N of the repair was also considered failed due to cracking and spalling. Spalling in the parent slab where the panel was placed increased in severity to high as well.	0
2	2		A medium-severity corner break was noted on the SW corner. A high-severity joint spall was noted on the E edge. Spalling on the edges of the parent slabs and Repairs 2 and 3 continued to progress. The low-severity longitudinal crack between the repairs in the parent slab continued across the slab.	21- although this repair was considered in serious condition, trafficking was continued. The repair was inspected more often to remove FOD and prevent damage to the tires.
3		5,600	A low-severity joint spall was noted on the E edge of the panel. A medium-severity joint spall was noted on the W edge of the panel near the NW corner and a low-severity joint spall was noted towards the SW corner on the W edge.	21
4	3		A high-severity joint spall was noted on the SE corner of the panel with high FOD production.	0
5			A high-severity corner spall was noted on the NE corner of the panel. A medium-severity corner spall was noted on the NW corner of the panel.	
6			A medium-severity joint spall was noted on the E edge of the panel. A high-severity corner spall was noted in the SE corner of the panel, and a low-severity corner spall was noted in the SW corner of the panel. Spalling continued in the parent slab south of the repair with high- and medium-severity joint spalls noted due to the dowel receptacles.	
7			A high-severity corner spall was noted in the NE corner and NW corner of the panel. A medium-severity spall was noted on the W edge of the panel.	
1	1	7,100	Panel considered failed. No additional data collected.	0
2	2		No change.	21- although this repair was considered in serious condition, trafficking was continued. The repair was inspected more often to remove FOD and prevent damage to the tires.
3			No change.	
4	3		Additional FOD produced by distresses. Repair considered failed.	0

Panel	Repair	Pass Level	Distress Description	PCI (%)
5			Additional FOD produced by distresses. Repair considered failed.	
6			Additional FOD produced by distresses. Repair considered failed.	
7			Additional FOD produced by distresses. Repair considered failed.	
1	1	8,400	Panel considered failed. No additional data collected.	0
2	2		Additional FOD was noted in distresses.	21- although this repair was considered in serious condition, trafficking was continued. The repair was inspected more often to remove FOD and prevent damage to the tires.
3			Additional FOD was noted in distresses.	
4	3		Panel considered failed. No additional data collected.	0
5			Panel considered failed. No additional data collected.	
6			Panel considered failed. No additional data collected.	
7			Panel considered failed. No additional data collected.	
1	1	10,000	Panel considered failed. No additional data collected.	0
2	2		FOD production continued. Repair considered failed due to condition of NW portion of the N joint with deterioration of the parent pavement and dowel slots.	0
3			FOD production continued. Repair considered failed.	
4	3		Panel considered failed. No additional data collected.	0
5			Panel considered failed. No additional data collected.	
6			Panel considered failed. No additional data collected.	
7			Panel considered failed. No additional data collected.	

The double-panel repair outperformed both the single- and the quad-panel repair with almost twice the traffic application for the double-panel repair compared to the single-panel repair. This was attributed to a better quality flowable fill placed under Repair 2 compared to the other repairs. Additionally, the cold joint north of Repair 1 and the quality of construction of the parent slab in which this repair was conducted, contributed to the poorer performance of this panel. The parent slab cracked and spalled early in the trafficking of the panels. This deterioration may have accelerated the failure of this repair located less than 10 ft away.

Overcutting resulted in uncontrolled cracking, with cracks progressing from partial saw cuts in the parent slabs. Intermediate distresses in the parent slabs are presented in Figure 13. Figure 14 presents photos of the distresses contributing to the failure of the repairs in both the panels and parents slabs. To control cracking in the parent slabs for long-term use, it may be necessary to extend the saw cuts the remaining distance to the joint and apply joint sealant.

Cracking and spalling between the dowel slots and deterioration of the dowel slot material contributed to the failure of all three repairs, as can be seen in Figure 13, Figure 14, and Table 2. In particular, the spalling of the joint south of Panels 6 and 7 in the quad panel resulted in a shorter repair life. A spall repair may have resulted in longer panel life, but a repair was not made to understand the passes to failure of the repairs. This deterioration led to the failure of the double-panel repair. It is recommended that further research be done to determine the most efficient doweling configuration, in terms of a maximized spacing with minimized number and length that does not significantly reduce the number of allowable passes.

Despite the documented deterioration, the current panel design (including dowel spacing and dowel slot patching method) allowed at least 5,000 passes of C-17 traffic prior to failure with the potential to withstand more traffic.

Figure 13. Parent slab distresses after 2,800 passes: (a) longitudinal crack in parent slab south of Repair 2 extending from saw overcut; (b) longitudinal crack in parent slab between Repairs 2 and 3 extending from saw overcut; (c) diagonal crack in parent slab extending from NE edge of Repair 1 extending from saw overcut; (d) diagonal crack in parent slab from SE edge of Repair 1 to Repair 2 extending from saw overcut and spalling and cracking between saw overcuts on SE corner of Repair 1; (e-f) spalling and cracking in parent slab north of Repair 1 near construction cold joint.

Figure 14. Repair failure details: (a) Repair 1-Panel 1: high-severity corner break/spall and shattered parent slab; (b) Repair 2: diagonal cracking in parent slab between Repairs 1 and 2 and cracking and spalling of Panel 2 due to the parent slab deterioration; (c) close-up of the cracking and deterioration in the parent slab and dowel slots and corner of Panel 2; (d) Repair 3 Panels 6 and 7: high-severity spalling in corner of Panels 6, 7, and the parent slabs south of the repair.

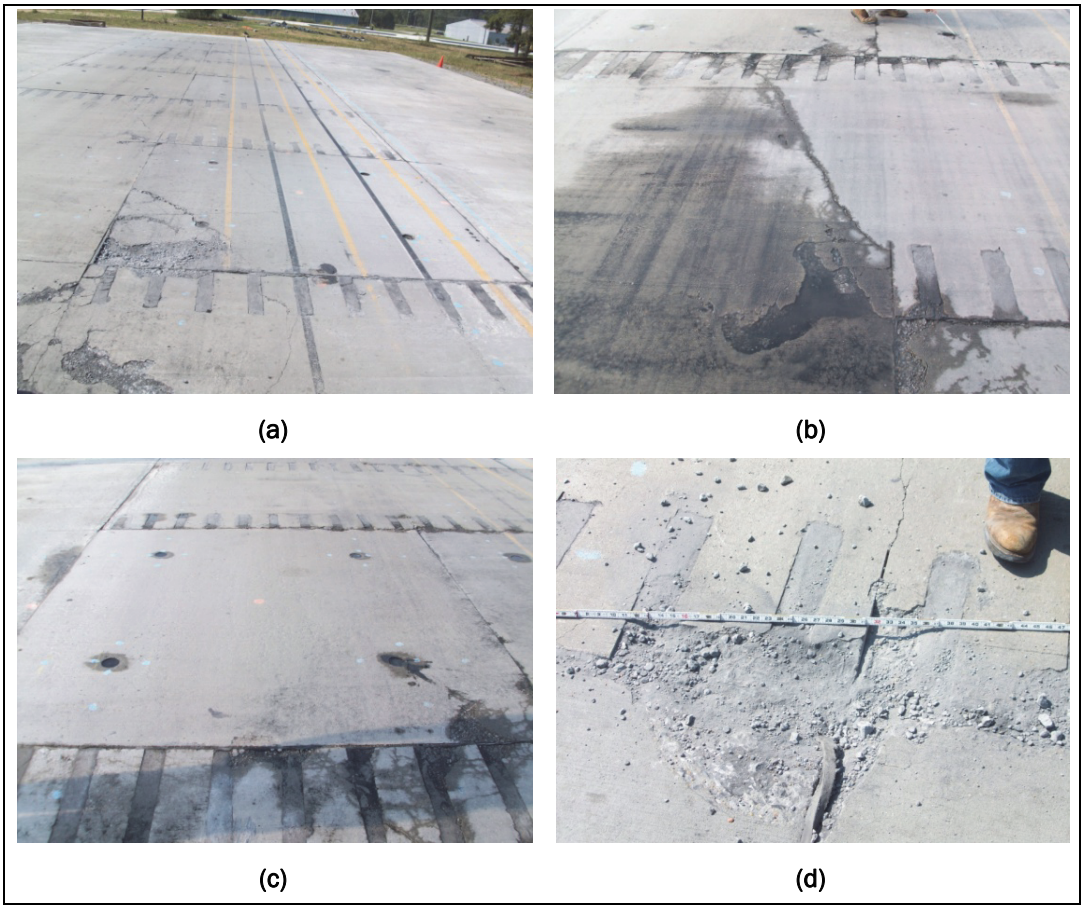

(a) (b)

(c) (d)

6 Settlement and Faulting Results

In addition to the observed surface distresses, measurements were taken to monitor any elevation differences of the panels during trafficking. Faulting was considered an upward elevation change between slabs at a joint, and settlement was considered a negative elevation difference at a joint. These distresses are commonly encountered in PCC pavements and are usually caused by upheaval (faulting), consolidation, or loss of support (settlement). Elevation differences are important measurements to determine if aircraft can safely operate on the paved surface; since large differences can cause tire hazards and place large stresses on landing gear.

During trafficking, data were collected at selected pass intervals shown in Table 1 to monitor the surface elevation of the repairs. Differences in elevation were made using a 10-ft straight edge and hand ruler. The straight edge was placed at two locations across the joints on every edge of the panel (1 ft from the corners). A series of six measurements spaced at 12-in. intervals were made at preset intervals marked on the surface of the test sections shown in Figure 15 to monitor changes in the surface elevation and any rotation of the panel. The maximum measurement (elevation difference) was identified for each set of measurements.

The peak elevation differences for each set of measurements are presented in Table 3. Negative differences represent changes in elevation due to settlement or loss of material. The data shows the panels moved very little during trafficking. None of the repairs had settlement or faulting in excess of 3.0 in., indicating that the panels did not fail due to roughness. The differences in elevation appear to be very minimal indicating that the flowable fill provided adequate support for the panels and that loss of subgrade support and excess material loss did not occur during trafficking. Additionally, the results show that the dowels provided successful load transfer across the transverse joints.

Figure 15. Locations of faulting and settlement measurements.

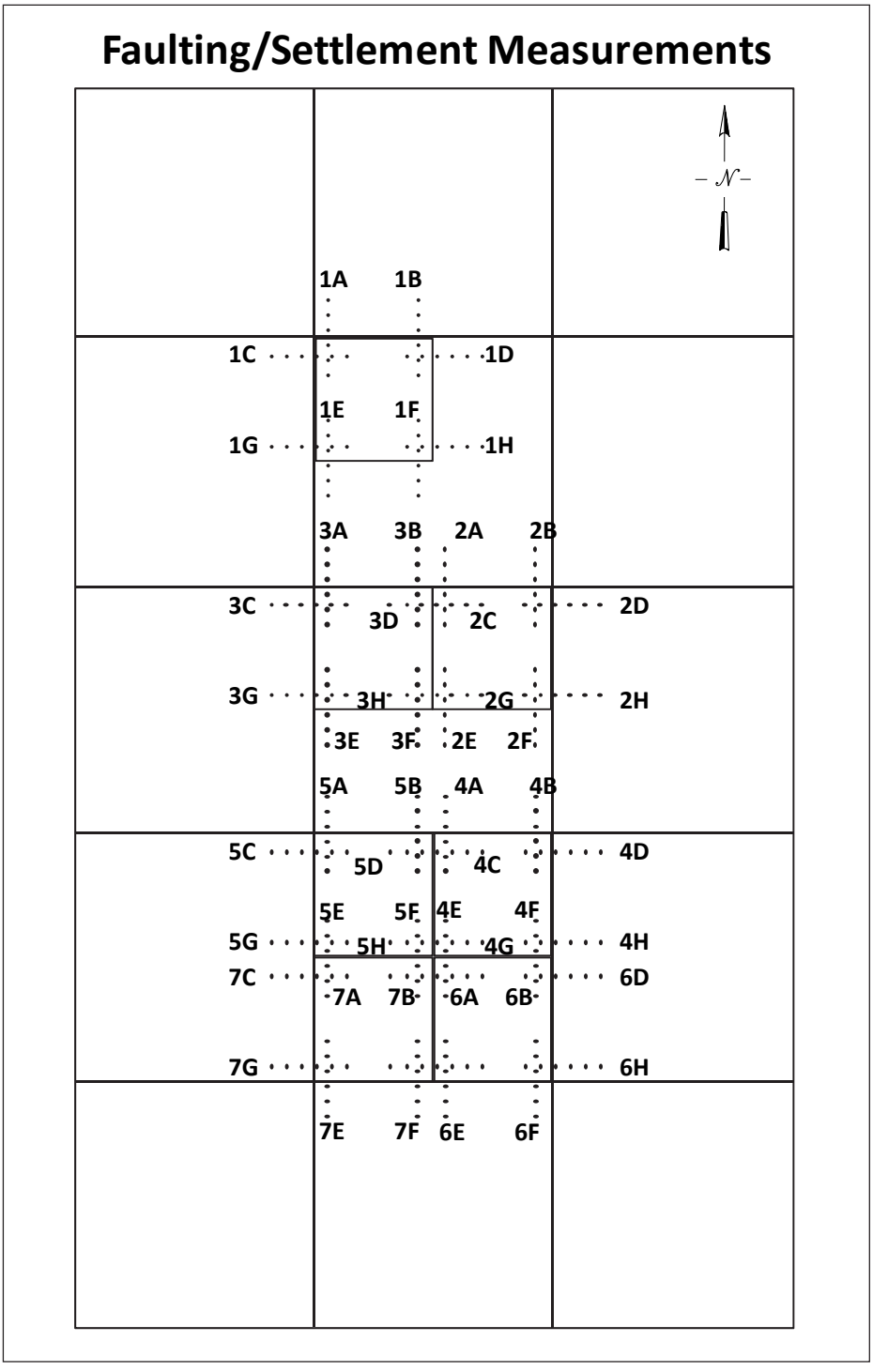

Table 3. Elevation measurement intervals.

Repair	Test Location	Initial Installation Measurement, in.	Maximum Measurement, in.	Elevation Difference from Installation, in.
Repair 1	1a	0.375	0.375	0.000
	1b	0.1875	0.4375	-0.250
	1c	0.25	0.375	-0.125
	1d	0.25	0.625	-0.375
	1e	0.5	0.5	0.000
	1f	0.125	0.375	-0.250
	1g	0.3125	0.375	-0.063
	1h	0.5	0.5625	-0.063
Repair 2	2a	0.5	0.5625	-0.063
	2b	0.375	0.4375	-0.063
	2c	0.125	0.1875	-0.063
	2d	0.1875	0.25	-0.063
	2e	0.375	0.5	-0.125
	2f	0.3125	0.375	-0.063
	2g	0.125	0.1875	-0.063
	2h	0.375	0.375	0.000
	3a	0.25	0.3125	-0.063
	3b	0.4375	0.5	-0.063
	3c	0.1875	0.1875	0.000
	3d	0	0.0625	-0.063
	3e	0.3125	0.5	-0.188
	3f	0.1875	0.375	-0.188
	3g	0.5	0.5625	-0.063
	3h	0.0625	0.3125	-0.250
Repair 3	4a	0.125	0.1875	-0.063
	4b	0.125	0.1875	-0.063
	4c	0.125	0.1875	-0.063
	4d	0.25	0.625	-0.375
	4e	0.125	0.25	-0.125
	4f	0.0625	0.125	-0.063
	4g	0.0625	0.1875	-0.125
	4h	0.125	0.1875	-0.063
	5a	0.125	0.375	-0.250
	5b	0.125	0.1875	-0.063
	5c	0.3125	0.3125	0.000

Repair	Test Location	Initial Installation Measurement, in.	Maximum Measurement, in.	Elevation Difference from Installation, in.
	5d	0.0625	0.125	-0.063
	5e	0	0.125	-0.125
	5f	0.0625	0.1875	-0.125
	5g	0.375	0.375	0.000
	5h	0.0625	0.125	-0.063
	6a	0.125	0.1875	-0.063
	6b	0.125	0.1875	-0.063
	6c	0.0625	0.125	-0.063
	6d	0.125	0.25	-0.125
	6e	0.125	0.1875	-0.063
	6f	0.1875	0.1875	0.000
	6g	0	0.0625	-0.063
	6h	0.0625	0.1875	-0.125
Repair	Test Location	Initial Installation Measurement, in.	Maximum Measurement, in.	Elevation Difference from Installation, in.
Repair 3 (cont.)	7a	0.13	0.33	-0.21
	7b	0.13	0.19	-0.06
	7c	0.25	0.31	-0.06
	7d	0.13	0.17	-0.04
	7e	0.25	0.31	-0.06
	7f	0.06	0.19	-0.13
	7g	0.31	0.31	0.00
	7h	0.13	0.25	-0.13

7 Nondestructive Testing

Nondestructive tests (NDT) were performed to determine the structural capacity of the repaired pavement. Response data were used to determine the structural capacity and the operational effectiveness of the precast panel repair methods in terms of stiffness, load-transfer efficiency, and joint stiffness. These items are commonly used for monitoring the effectiveness of traditional PCC pavement repairs and were applied to precast panels for comparison purposes. Recent investigations into precast panels also recommend monitoring precast panel repairs using these NDT methods.

Equipment used

NDT were completed with a Dynatest model 8081 heavy weight deflectometer (HWD). The HWD uses heavy weights dropped onto a padded plate (11.8 in. diameter) to measure the pavement's response to a dynamic load. The applied force and the pavement deflections, respectively, are measured with load cells and velocity transducers (geophones). The drop height of the weights can be varied from 0 to 15.7 in. to produce a force from 0 to approximately 50,000 lb. The system is controlled with a laptop computer that also records the loading and pavement deflections. The HWD is shown in Figure 16 during testing on a PCC test section.

Figure 16. HWD test device.

Prior to conducting repairs and following the completion of traffic testing, the HWD was used to obtain deflection basins for the parent PCC slabs. Locations of the HWD on the test section are provided in Figure 17 (numbered from 1 to 15). Test 6 was not conducted because of the construction joint.

In addition to backcalculating modulus values for pavement layers, the HWD was also used to measure the decay in stiffness with repeated applications of traffic. The stiffness properties of PCC significantly impact the distribution of aircraft loads between slabs and panels. Thus, the repair stiffness values were determined with traffic applications and compared to the parent PCC. Repair stiffness was monitored through center, corner, and joint deflection measurements. Deflection measurements were conducted in the center of each panel and at selected parent PCC locations (marked 1-10 in Figure 18) at various traffic intervals (shown previously in Table 1). Other deflection tests were conducted during the same traffic intervals including load transfer efficiency (LTE) and corner deflections, which will be detailed in the following sections.

Backcalculation of moduli for the test section

The recorded HWD deflections and known pavement structure layer thicknesses were used to backcalculate the elastic modulus of each pavement layer for the parent PCC and for the precast panels. The back-calculated moduli before and after trafficking are presented in Table 4. CBR values from dynamic cone penetrometer (DCP) tests prior to the construction of the PCC layer are provided for comparison against the backcalculated results for the parent slabs. The average DCP values (37 percent base and 14 percent subgrade) were converted into modulus values using the relationship presented in Equation 1.

$$\text{DCP estimated modulus} = 1500 * \text{CBR (\%)} \quad (1)$$

The backcalculated base and subgrade moduli for the parent slabs are similar to the DCP-estimated values, with only a slight reduction to the respective values after traffic. This indicates that there was not a substantial loss in foundation support beneath the test section due to environmental factors that could contribute to early deterioration of the repairs.

Figure 17. Locations of HWD tests pre-repair and post-test.

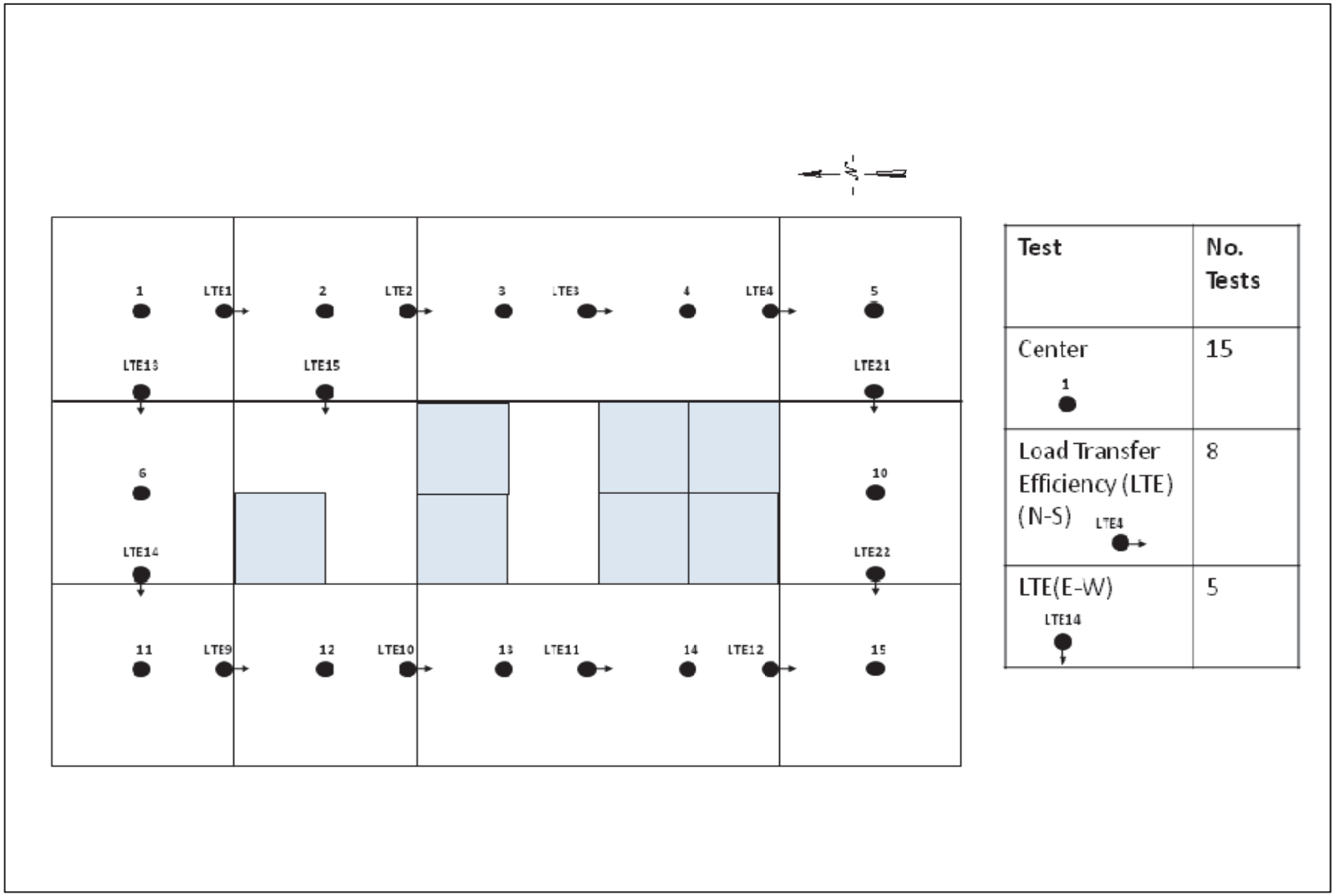

Test	No. Tests
Center 1	15
Load Transfer Efficiency (LTE) (N-S) LTE4	8
LTE(E-W) LTE14	5

Figure 18. Location of ISM, corner deflection, and LTE HWD tests.

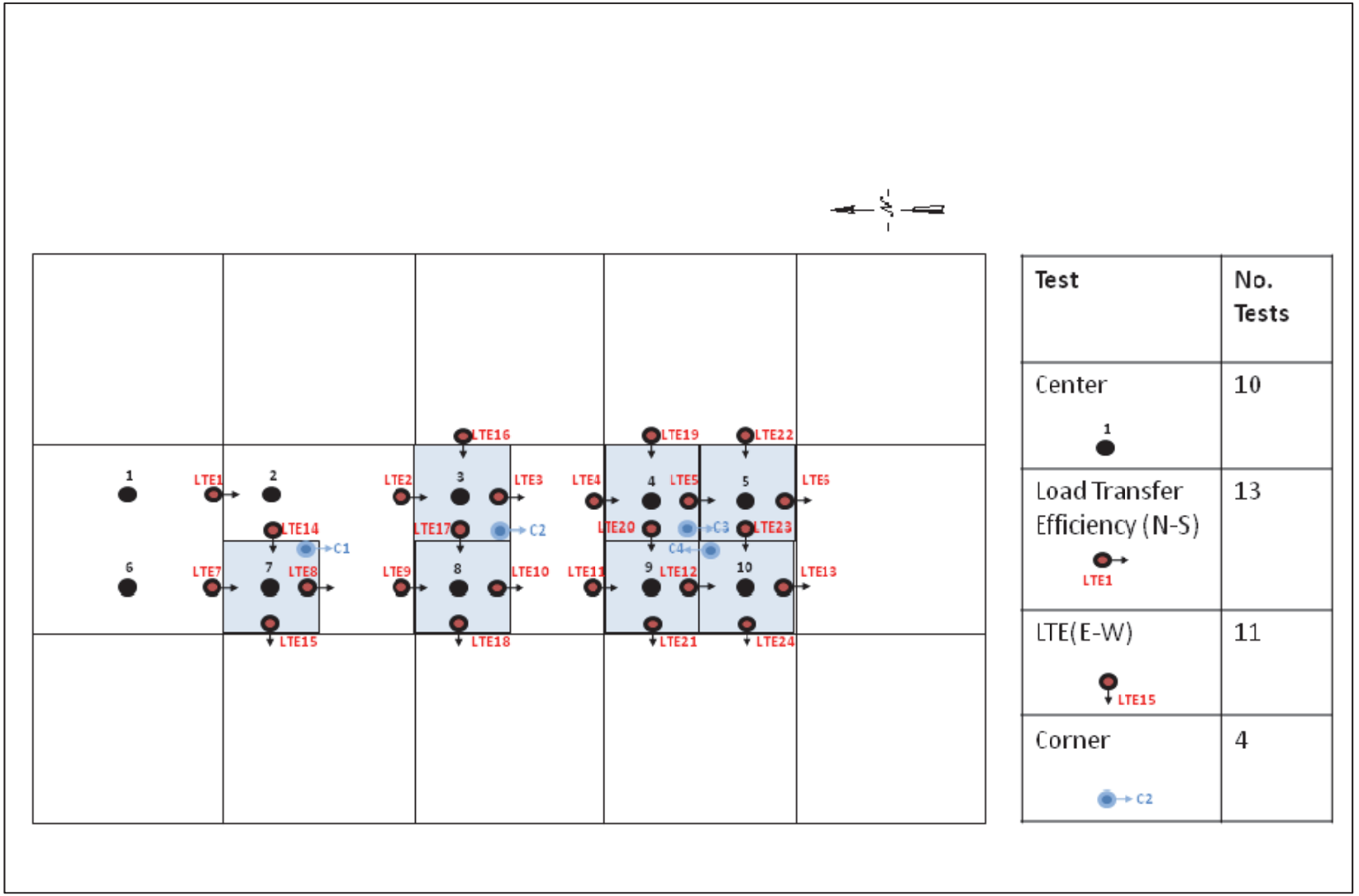

Table 4. Summary of modulus values.

Test	PCC Modulus, psi	Backcalulated HWD		DCP-estimated	
		Base Modulus, psi	Subgrade Modulus, psi	Base Modulus, psi	Subgrade Modulus, psi
Pre-repair slabs	5,000,000	49,276	24,453	55,000	21,000
Post-traffic slabs	5,000,000	48,333	23,737	55,000	21,000
Pre-repair panels	6,248,706	54,892	24,453	n/a	n/a
Post-traffic panels	2,545,719	33,488	11,560	n/a	n/a

The backcalculated moduli for the precast panels show significant loss in strength during trafficking. This is attributed to the deterioration of the panels and cracking of the flowable fill during trafficking.

The equivalent PCC thickness of the panel system (panel plus the flowable fill) was calculated based on the HWD deflections using Ioannides et al. (1992) equivalent thickness solution for multi-layered pavements. This solution uses the assumptions that the equivalent PCC would have the same modulus of elasticity, Poisson's ratio, and modulus of subgrade reaction as the multi-layered system. The equivalent thickness calculated for the panel repair was 11.02 in. indicating that the contribution of the 3-in. flowable fill layer was negligible and that the reinforcement did not allow a reduction in panel thickness. The flowable fill provided similar base moduli (3 in. of flowable fill and 6 in. of compacted aggregate) to the compacted aggregate alone as shown in Table 4.

Center slab deflections and impulse stiffness modulus

Center slab deflections recorded at the maximum HWD load level (measured at the first sensor) are presented in Figure 19. Deflections were normalized to a force of 50,000 lb to provide a comparison of the test data that varied in maximum force from approximately 39,000 to 57,500 lb. Normalized deflection values for each panel and pass level are also presented in Table 5. Figure 19 shows the general trend that as traffic applications increased, the deflections also increased for all repairs and adjacent pavement (parent PCC). This figure also shows that lower deflections were recorded for Panels 2 and 3 of Repair 2, slightly better than parent slab deflections. The highest deflections were recorded for Panel 1 of Repair 1 and Panels 4, 5, and 7, of Repair 3.

Figure 19. Normalized deflections for panels with traffic passes.

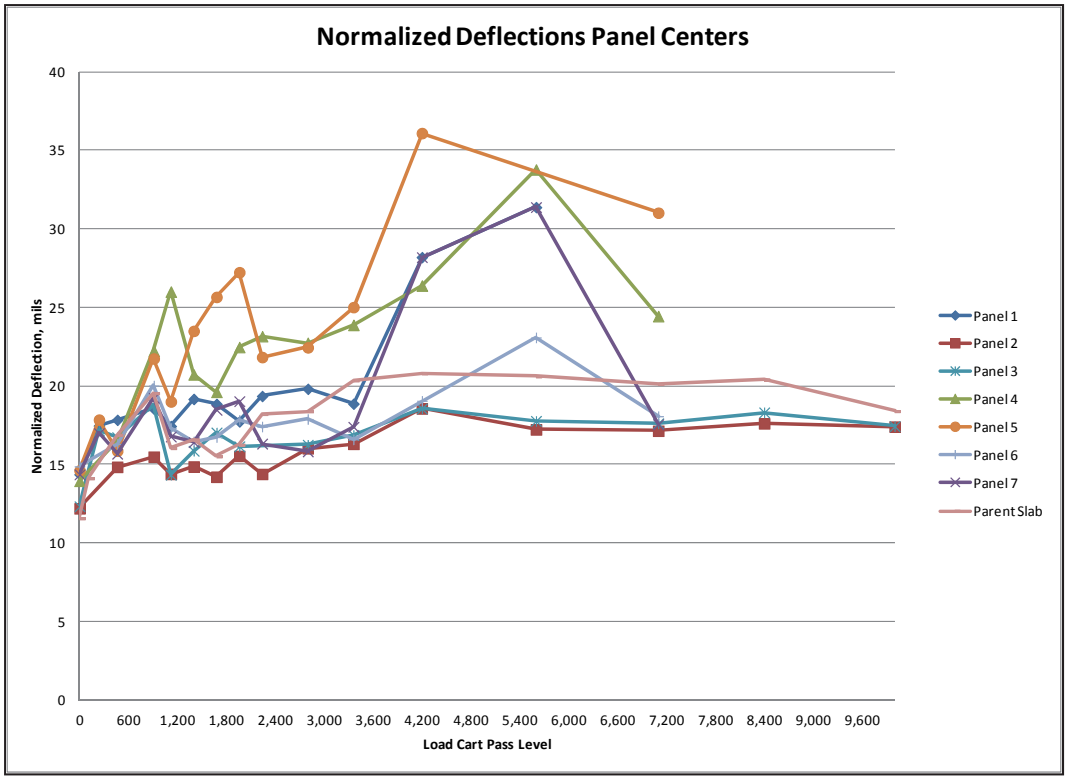

The impulse stiffness modulus (ISM) values were then computed by using the maximum force level, or load, divided by the deflection at the first sensor (center of the load plate) to provide a numerical indicator of the stiffness of the panel or slab being tested. The ISM was calculated at each interval to monitor the effect of repeated loading on the performance in the repaired areas as well as to compare this degradation to the non-repaired PCC response under repeated traffic applications. The deflection data used to calculate the ISM values were presented in Table 5.

Figure 20 shows the ISM values with trafficking for all panels and a parent PCC slab. The figure shows that both the parent slab and the repairs lose strength over trafficking. This is expected as fatigue damage increases as loadings are applied. The ISM values for Panels 2 and 3 indicate that Repair 2 was the strongest of all repairs. The ISM values indicated that the weakest panels were Panel 1 (Repair 1) and Panels 5 and 6 (Repair 3) this could indicate that the flowable fill beneath these repairs was of lesser quality compared to Repair 2.

Table 5. HWD deflection and ISM data.

Passes	Slab/Panel	ISM , kip/in.	Load, lb	Normalized D_0, mils	Deflection, mils						
					D_0	D_{12}	D_{24}	D_{36}	D_{48}	D_{60}	D_{72}
0	P1	3478.33	55375	14.37	15.92	14.30	12.68	11.11	9.69	8.62	7.48
238		2861.51	39031	17.47	13.64	12.55	11.18	9.81	8.64	7.58	6.78
462		2802.54	55210	17.84	19.70	17.71	15.79	13.84	12.17	10.73	9.41
910		2695.28	54202	18.55	20.11	18.00	15.92	14.00	12.11	10.75	9.31
1,120		2866.03	55429	17.45	19.34	17.39	15.35	13.19	11.33	9.78	8.54
1,400		2608.09	54170	19.17	20.77	18.83	16.50	14.15	12.26	10.52	9.22
1,680		2651.77	55528	18.86	20.94	19.06	16.74	14.46	12.41	10.60	9.31
1,960		2818.56	56174	17.74	19.93	17.93	15.91	13.60	11.80	9.94	8.75
2,240		2582.92	52614	19.36	20.37	18.28	16.22	13.94	12.21	10.69	9.48
2,800		2523.05	51672	19.82	20.48	18.44	16.13	13.81	12.08	10.61	9.37
3,360		2649.92	52866	18.87	19.95	18.11	15.86	13.56	11.76	10.12	8.89
4,200		1773.13	50357	28.20	28.40	24.49	20.51	16.65	13.50	10.58	9.24
5,600		1593.28	52658	31.38	33.05	27.89	22.89	18.00	13.88	10.25	8.97
0	P2	4095.81	55703	12.21	13.60	12.65	11.78	10.76	9.86	9.14	7.93
238		no data									
462		3367.29	55594	14.85	16.51	15.08	14.73	13.31	12.01	11.38	9.31
910		3226.93	55955	15.49	17.34	16.09	15.13	14.04	13.19	10.78	9.22
1,120		3472.37	56426	14.40	16.25	15.80	15.17	14.68	14.40	10.76	9.41
1,400		3363.04	55692	14.87	16.56	15.53	14.38	13.39	12.45	11.47	9.32
1,680		3516.47	56580	14.22	16.09	14.93	14.09	13.16	12.32	11.57	9.33
1,960		3216.61	55583	15.54	17.28	16.07	14.97	14.05	13.14	12.26	9.18
2,240		3473.79	54608	14.39	15.72	15.07	13.99	13.00	12.02	10.70	9.51
2,800		3118.78	51990	16.03	16.67	16.26	14.81	13.98	12.94	11.60	10.19
3,360		3065.72	53742	16.31	17.53	16.91	15.82	14.41	13.43	12.16	10.07
4,200		2693.14	50631	18.57	18.80	18.48	17.69	16.81	16.23	11.94	10.58
5,600		2901.87	54323	17.23	18.72	18.18	17.90	17.38	17.01	10.59	9.42
7,100		2916.13	54969	17.15	18.85	18.64	18.48	17.72	17.09	16.40	9.65
8,400		2838.35	54695	17.62	19.27	18.99	18.75	18.28	18.13	11.81	10.39
10,000		2871.74	55999	17.41	19.50	17.46	15.70	13.92	12.30	11.02	7.95

Passes	Slab/Panel	ISM , kip/in.	Load, lb	Normalized D_0, mils	Deflection, mils						
					D_0	D_{12}	D_{24}	D_{36}	D_{48}	D_{60}	D_{72}
0	P3	4051.79	55550	12.34	13.71	12.65	11.56	10.37	9.07	8.16	7.20
238		2915.03	55648	17.15	19.09	18.39	16.70	14.80	12.96	11.37	9.22
462		2986.79	55166	16.74	18.47	17.46	16.00	14.14	12.47	10.86	9.45
910		2661.78	55791	18.78	20.96	19.91	18.62	17.07	15.78	12.44	10.44
1,120		3484.78	54049	14.35	15.51	17.41	16.11	14.74	13.76	10.94	9.50
1,400		3149.62	54520	15.87	17.31	16.56	15.27	13.78	12.65	11.05	9.60
1,680		2935.98	52877	17.03	18.01	17.24	15.99	14.53	13.52	12.60	10.10
1,960		3094.36	55451	16.16	17.92	17.43	16.29	14.80	13.88	13.20	10.15
2,240		no data									
2,800		3076.02	52077	16.25	16.93	16.62	15.42	14.15	12.91	11.63	10.18
3,360		2962.64	52735	16.88	17.80	17.35	16.20	14.86	13.49	12.00	10.33
4,200		2693.14	50631	18.57	18.80	18.48	17.69	16.81	16.23	11.94	10.58
5,600		2813.13	52296	17.77	18.59	18.51	17.65	16.77	16.17	11.93	10.40
7,100		2837.43	52691	17.62	18.57	17.88	17.02	15.81	15.01	12.42	10.96
8,400		2729.80	52767	18.32	19.33	18.85	17.93	16.84	16.07	15.27	10.23
10,000		2867.69	55375	17.44	19.31	17.58	15.77	13.68	11.53	10.91	8.74
0	P4	3582.48	54991	13.96	15.35	14.25	12.89	11.44	10.11	9.31	7.77
238		no data									
462		3034.58	56777	16.48	18.71	17.59	15.93	14.15	12.40	10.73	9.17
910		2248.64	55429	22.24	24.65	22.71	20.31	18.33	16.52	14.16	12.20
1,120		1923.11	44847	26.00	23.32	21.34	18.24	14.83	13.46	9.90	7.17
1,400		2412.06	55791	20.73	23.13	20.94	18.11	15.70	13.65	12.26	10.41
1,680		2548.54	55813	19.62	21.90	21.35	18.49	15.86	14.09	12.68	10.97
1,960		2224.85	56667	22.47	25.47	22.90	19.94	17.56	16.00	14.54	12.54
2,240		2158.24	52877	23.17	24.50	22.25	19.03	15.77	13.24	11.33	9.97
2,800		2198.31	51990	22.74	23.65	20.94	17.62	14.47	12.06	10.17	8.93
3,360		2093.45	52713	23.88	25.18	23.85	19.96	16.19	13.46	11.52	9.99
4,200		1894.68	53392	26.39	28.18	25.34	21.47	18.06	15.48	13.07	11.47
5,600		1480.31	54520	33.78	36.83	31.69	27.02	22.52	19.12	15.40	13.48
7,100		2045.72	54498	24.44	26.64	27.38	23.16	18.98	15.72	13.08	11.27

Passes	Slab/Panel	ISM , kip/in.	Load, lb	Normalized D_0, mils	Deflection, mils						
					D_0	D_{12}	D_{24}	D_{36}	D_{48}	D_{60}	D_{72}
0	P5	3419.07	55594	14.62	16.26	14.92	13.47	11.86	10.27	8.84	7.46
238		2800.51	55254	17.85	19.73	18.90	17.58	16.17	14.72	13.55	10.57
462		3150.63	55199	15.87	17.52	16.40	15.00	13.40	11.79	10.38	8.75
910		2299.04	54947	21.75	23.90	22.48	20.49	18.44	16.57	15.22	11.20
1,120		2630.42	55002	19.01	20.91	20.13	18.42	16.44	14.95	13.86	10.70
1,400		2127.43	52888	23.50	24.86	22.59	19.52	16.87	15.07	13.87	10.42
1,680		1948.14	54509	25.67	27.98	26.36	22.95	19.70	17.33	15.98	11.88
1,960		1835.60	55068	27.24	30.00	28.24	24.70	21.24	18.38	16.32	12.22
2,240		2289.78	52001	21.84	22.71	21.45	17.79	14.29	11.37	9.71	8.56
2,800		2226.91	50818	22.45	22.82	20.91	17.31	13.74	10.98	9.41	8.13
3,360		1998.65	51825	25.02	25.93	24.50	20.43	16.56	13.75	11.97	9.17
4,200		1385.26	49634	36.09	35.83	31.61	27.20	23.01	19.36	16.96	12.14
5,600		no data									
7,100		1611.55	53874	31.03	33.43	30.23	25.33	20.92	17.98	16.44	11.28
0	P6	3361.60	53315	14.87	15.86	14.20	12.88	11.67	10.59	9.26	8.15
238		no data									
462		3065.57	55824	16.31	18.21	16.97	15.43	13.48	11.88	10.84	8.78
910		2496.77	55703	20.03	22.31	21.63	20.55	19.33	18.04	10.80	9.27
1,120		2885.66	56963	17.33	19.74	19.65	18.94	18.11	17.48	11.20	9.82
1,400		3036.51	56054	16.47	18.46	17.90	16.99	15.80	14.95	14.21	9.35
1,680		2985.98	57062	16.74	19.11	18.80	17.96	17.10	16.28	11.22	9.87
1,960		2802.81	56897	17.84	20.30	20.05	19.29	18.59	18.09	12.22	10.77
2,240		2871.29	53808	17.41	18.74	17.89	16.38	14.80	13.48	11.72	10.31
2,800		2794.57	53041	17.89	18.98	18.42	16.80	15.20	13.82	11.99	10.53
3,360		3011.84	54936	16.60	18.24	17.47	15.96	14.63	13.38	11.31	9.96
4,200		2623.75	53918	19.06	20.55	20.58	19.85	18.85	18.04	13.41	11.29
5,600		2165.91	56032	23.09	25.87	26.28	25.98	25.17	24.71	13.83	12.11
7,100		2766.75	55999	18.07	20.24	19.76	19.19	18.25	17.50	11.33	9.59
0	P7	3478.33	55375	14.37	15.92	14.30	12.68	11.11	9.69	8.62	7.48
238		2941.77	54717	17.00	18.60	17.67	16.47	15.27	13.96	12.85	7.07

Passes	Slab/Panel	ISM , kip/in.	Load, lb	Normalized D_0, mils	Deflection, mils						
					D_0	D_{12}	D_{24}	D_{36}	D_{48}	D_{60}	D_{72}
462	P7	3187.69	55944	15.69	17.55	16.43	15.02	13.59	12.20	10.47	8.93
910		2598.79	55900	19.24	21.51	20.80	19.90	18.93	17.87	16.92	8.76
1,120		2979.76	54619	16.78	18.33	18.62	17.96	17.20	16.67	8.48	7.04
1,400		3044.11	55068	16.43	18.09	18.26	17.56	16.69	16.04	15.32	7.32
1,680		2705.71	55440	18.48	20.49	20.91	20.12	19.34	18.56	17.80	8.67
1,960		2627.44	56306	19.03	21.43	21.07	20.48	19.82	18.94	18.15	8.91
2,240		3062.59	53381	16.33	17.43	16.57	15.09	13.39	11.95	10.19	8.67
2,800		3156.97	51869	15.84	16.43	16.16	14.57	12.91	11.49	10.13	8.49
3,360		2873.52	52844	17.40	18.39	17.50	16.22	14.74	13.59	10.69	7.93
4,200		1773.13	50357	28.20	28.40	24.49	20.51	16.65	13.50	10.58	9.24
5,600		1593.28	52658	31.38	33.05	27.89	22.89	18.00	13.88	10.25	8.97
7,100		2847.55	43653	17.56	15.33	15.00	14.73	14.19	13.82	7.18	6.12
0	Slab	4318.71	57007	11.58	13.20	12.47	11.69	10.76	9.87	8.81	7.62
112		3539.72	56317	14.13	15.91	15.54	14.66	13.51	12.35	11.01	9.77
238		No data									
462		2961.01	55134	16.89	18.62	17.60	16.50	15.19	13.71	12.32	10.93
910		2559.35	56229	19.54	21.97	20.59	19.10	17.24	15.55	13.89	12.13
1,120		3116.25	55407	16.04	17.78	16.19	15.72	14.36	12.94	11.44	10.03
1,400		3013.23	55112	16.59	18.29	17.28	16.21	14.85	13.56	12.15	10.91
1,680		3221.23	44453	15.52	13.80	14.35	13.33	12.27	11.17	10.08	9.02
1,960		3075.09	57412	16.26	18.67	18.14	16.95	15.53	14.64	13.43	12.39
2,240		2745.23	54630	18.21	19.90	19.40	18.60	17.56	16.52	15.35	13.55
2,800		2719.18	42963	18.39	15.80	15.56	15.08	14.29	13.58	12.72	10.90
3,360		2456.20	53447	20.36	21.76	21.24	20.55	19.57	18.69	17.07	14.44
4,200		2403.91	52910	20.80	22.01	20.87	19.60	17.97	16.46	14.93	13.33
5,600		2425.64	55353	20.61	22.82	21.85	20.96	19.17	17.96	16.12	14.52
7,100		2483.45	55977	20.13	22.54	21.45	20.23	18.99	17.77	16.37	14.79
8,400		2449.94	56667	20.41	23.13	22.22	21.52	20.10	18.85	16.63	14.74
10,000		2717.45	45789	18.40	16.85	15.95	14.46	12.90	11.66	10.11	8.94

Figure 20. ISM versus load cart passes.

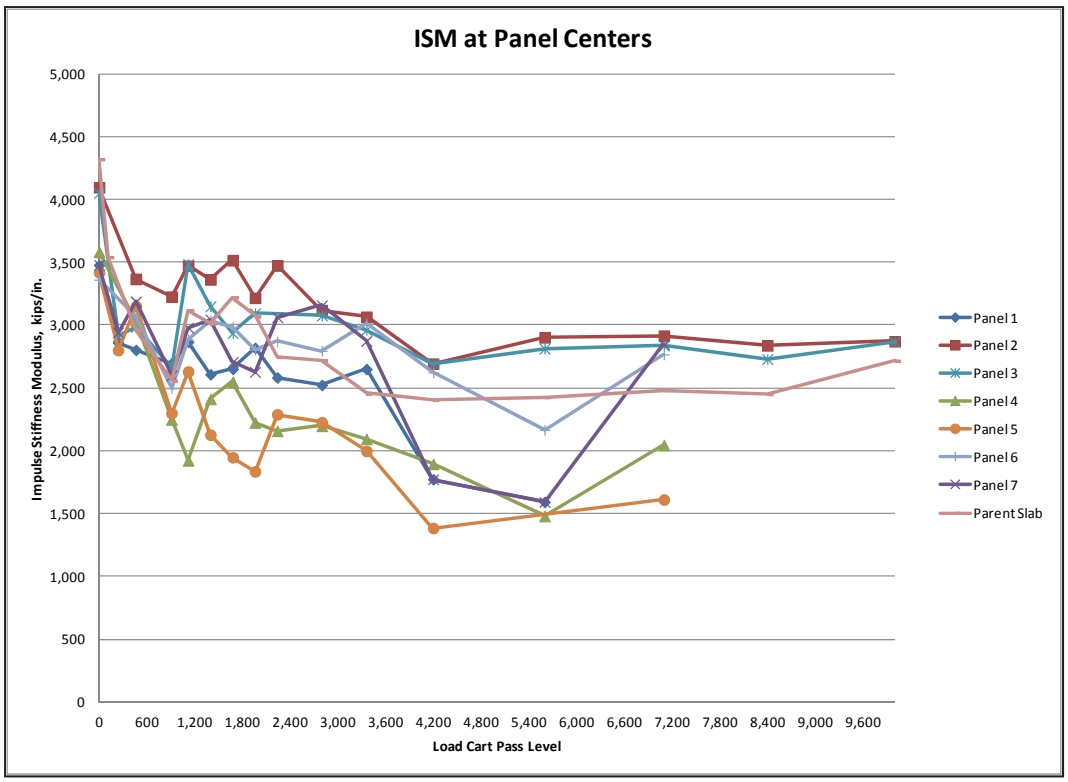

Load transfer efficiency (LTE)

Load transfer (joint) testing was conducted on the longitudinal and transverse joints of precast panels and surrounding PCC slabs using the HWD. In PCC pavements, dowel bars, aggregate interlock, and foundation characteristics all contribute to distributing the load of aircraft between slabs at the joints. How well these mechanisms transfer the load, or the load transfer efficiency (LTE) of the joints, is commonly measured during evaluation of PCC airfield pavements. Decreased load transfer will result in high stresses at the slab edges and corners and may cause distresses such as faulting, corner breaks, and spalling along the joint. The minimum LTE threshold for joints perpendicular to the direction of traffic is typically 70 percent, and this threshold was used in the evaluation of the prototype Air Force precast panel design (Ashtiani 2010).

LTE can vary over the life of the pavement because of changes in temperature causing the joint to open or close due to expansion or contraction of the PCC, number of repetitions of load, foundation support, aggregate particle angularity/ interlock, and the quality of the load transfer devices (IPRF 2011). To reduce temperature related LTE variations, measurements were

taken at the same time each day of testing to minimize temperature effects (early morning).

The three most common methods of calculating LTE are deflection-based (LTE_δ), stress-based (LTE_σ), or strain-based (LTE_ϵ) and can be calculated using the following formulas:

$$LTE_\delta = \delta_u / \delta_l \quad (2)$$

$$LTE_\sigma = \sigma_u / \sigma_l \quad (3)$$

$$LTE_\epsilon = \epsilon_u / \epsilon_l \quad (4)$$

where:

δ_u = deflection of the unloaded side of the joint
δ_l = deflection of the loaded side of the joint
σ_u = bending stress in the unloaded slab
σ_l = bending stress in the loaded slab
ϵ_u = bending strain in the loaded slab edge at the joint
ϵ_l = bending strain in the unloaded slab edge at the joint

Equation 2 is the most widely used due to the availability and acceptance of NDT equipment such as the HWD for pavement evaluation, which can measure slab edge deflections. Equation 3 and 4 rely on accurately measuring the stress and strains through instrumentation or through theoretical modeling. Stress or change in stress can be estimated from these calculated or measured strains.

For this investigation, a deflection based LTE was used based on the HWD deflection data. Stress and strain based load transfer calculations were intended to be conducted using data collected by strain gauges. Unfortunately, the gauges were destroyed during the initial passes of the load cart, and the data could not be collected.

In order to calculate LTE_δ, the HWD was used to conduct joint tests during the same data collection intervals described previously for calculating ISM. In the joint test, the HWD load was applied at one side of a joint close to the edge of a slab (or panel), and the deflections were measured by seven geophones located at a spacing of 12 in. on the adjacent slab or panel. The

deflections at the maximum drop load were used to calculate LTE. These measurements were used to produce deflection basins like those shown in Figure 21 (good LTE) and 22 (poor LTE). Good LTE results in an almost no slope between Sensors 1 and 2. Poor LTE results in large differences between deflections measured at Sensors 1 and 2 and a steep slope.

Figure 21. Deflection basin example good LTE.

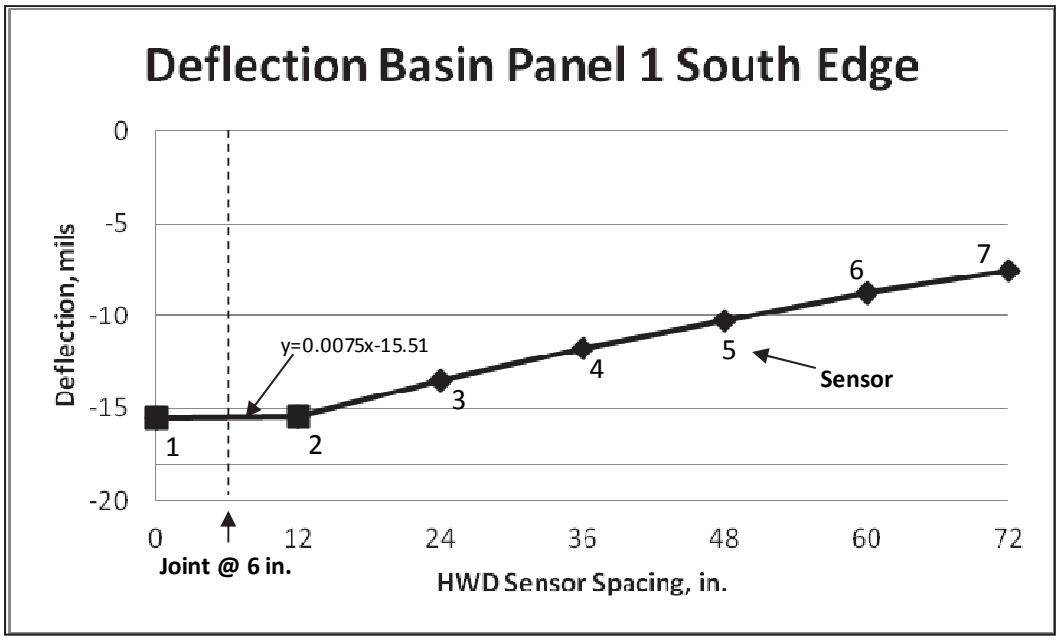

Figure 22. Deflection basin example poor LTE.

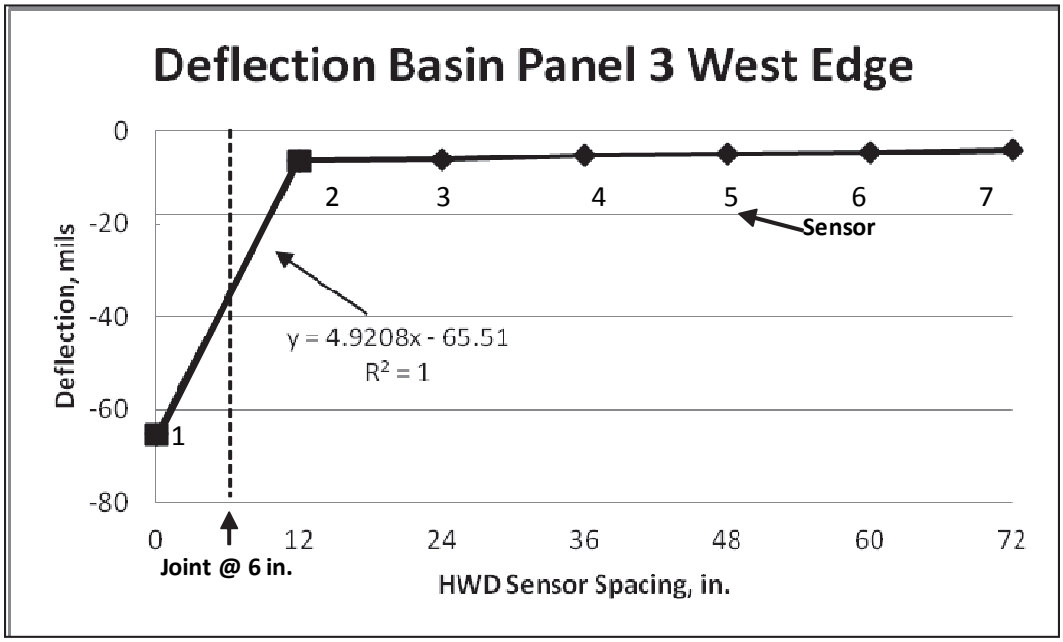

Load transfer mechanisms

In general, in PCC pavements there are two main mechanisms used for load transfer. The first is aggregate interlock. Joints constructed in PCC pavements use shallow cuts to initiate a crack from the surface to the bottom of the pavement. Beneath this cut, a full-depth crack propagates, separating the pavement into two slabs each with rough vertical faces. These rough vertical faces, in contact, produce aggregate interlock through friction. If the spacing is large or the surfaces of the faces are smooth, then aggregate interlock contributes less to transferring load, and the LTE will be reduced. The second mechanism for providing load transfer is the installation of dowel bars. These devices allow transfer of load across a joint through bending of the dowel bars and allow the pavement to expand and contract. If the joint opening is not large, then both aggregate interlock and dowel bar mechanisms can contribute to load transfer. In addition to these two mechanisms, the base and foundation can contribute to load transfer of the PCC. If the base material is strong, then the foundation material may contribute by resisting shear and vertical deformations under the slab.

For this investigation, load transfer was provided by dowels precast in the panels on the transverse joints. No dowels were provided along the longitudinal joints. For the transverse joints, it was thought that the primary load transfer mechanism would be through load transfer dowels with lesser effects attributed to aggregate interlock or foundation support. For the precast slabs, the spacing between the panels and the surrounding pavement was 0.375 to 0.5 in., and both the PCC panel and the parent PCC had relatively smooth surfaces. Thus, it was thought that aggregate interlock would contribute minimally to load transfer, unless the two faces were in close contact, causing the faces to roughen through contact and loading repetitions and contribute more shearing resistance.

Along the longitudinal joints, no load transfer dowels were installed, and it was assumed that load transfer would be poorer unless panels and the parent PCC slabs were in close contact. It was also assumed that there would be less joint shear face roughness for aggregate interlock effects between panels and the surrounding PCC and the panels to each other to allow good LTE. Thus, the LTE was expected to be lower along the longitudinal joints due to the lack of aggregate interlock and the lack of dowels.

LTE calculation

The change in LTE with increasing traffic levels for Repairs 1, 2, and 3 are presented in Figures 23, 24, 25, and Figure 26. As shown in the figures, the LTE generally decreased gradually with increasing traffic, and the LTE was better for the doweled joints (N and S joints) compared to the undoweled joints (E and W joints). Some measurements were encountered where the LTE increased temporarily before decreasing again. This is most likely due to changes in the slab temperatures during testing causing the joints to close during warmer temperatures.

The lowest LTE was calculated after 5,600 passes for Repair 3 in the longitudinal joints between Panels 4 and 5 and Panels 6 and 7 with LTE of 10 percent and 15 percent, respectively. No load transfer mechanism was used between the panels, and the installed construction joint width was 0.5 in. At early test ages, LTE was expected to come from base support or from shearing friction between the panels when the joints were closed. Initially high LTE values of 98 percent were calculated for several of the panels' north and south joints prior to traffic application with reductions over the life of the panel. High LTE was expected initially for these joints, as they were doweled.

For Repair 1, the E joint's LTE dropped rapidly after the initiation of traffic (90 percent before traffic to 20 percent at after 5,600 passes). This is not unexpected, as this was a longitudinal joint (no dowels). The high early LTE was attributed to the initial contact of the panel to the surrounding PCC during installation through temporary contact provided by flowable fill and rapid-setting grout used to seal around the panel and the dowel slots during field installation. During trafficking, the bond was weakened or destroyed due to the crushing of the material located in the narrow joint openings by traffic movement of the panel and PCC. While the individual LTE values varied during trafficking between the N and S joints, the maximum and minimum LTE values were very similar with 99 to 74 percent for the N joint compared to 99 to 77 percent for the S joint. These LTE measurements are above the minimum recommended threshold of 70 percent for transverse joints. The W joint performed similarly to the N and S joints with LTE ranging in the 90 percent and higher range to the 70 percent range, indicating that the joint may have experienced load transfer through contact of the panel and the parent PCC.

Figure 23. Load transfer efficiency for Repair 1 (Panel 1) with traffic.

Figure 24. Load transfer efficiency for Repair 2 (Panels 2-3) with traffic.

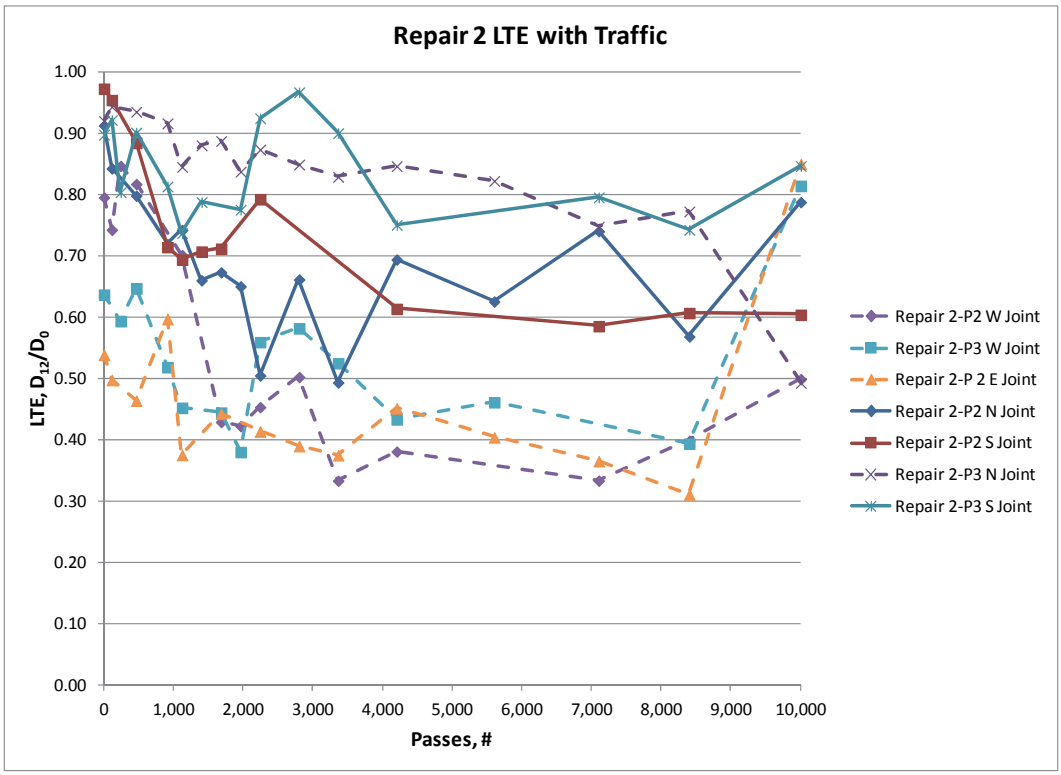

Figure 25. Load transfer efficiency for Repair 3 (Panels 4-5) with traffic.

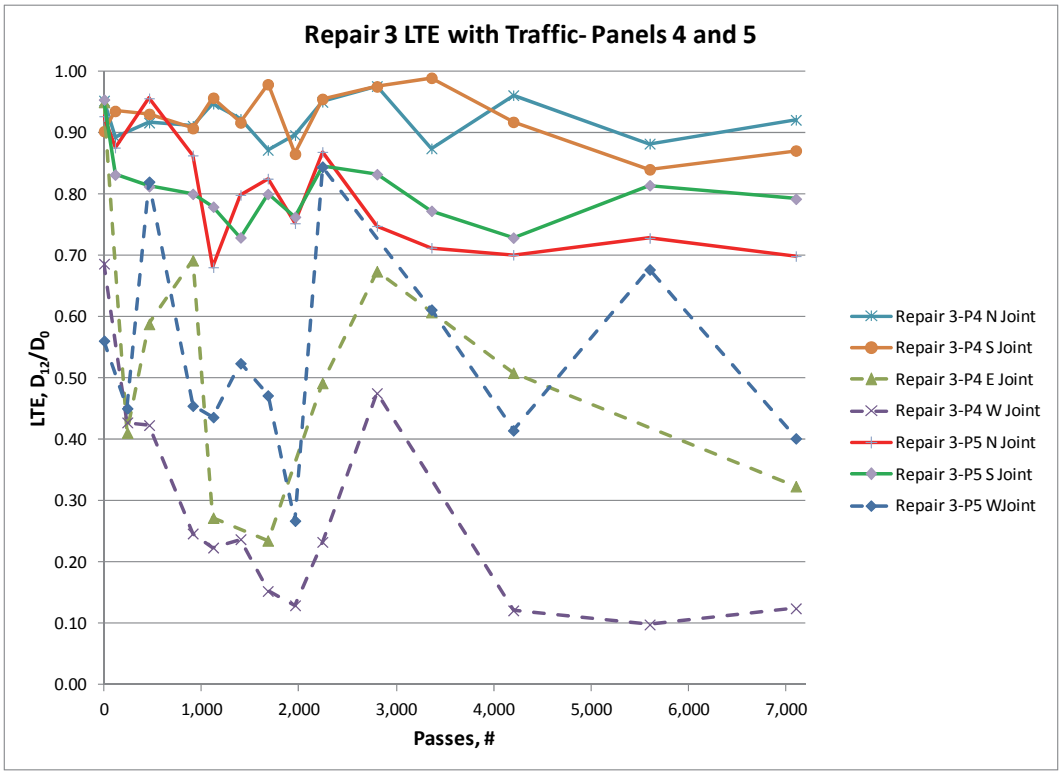

Figure 26. Load transfer efficiency for Repair 3 (Panels 4-5) with traffic.

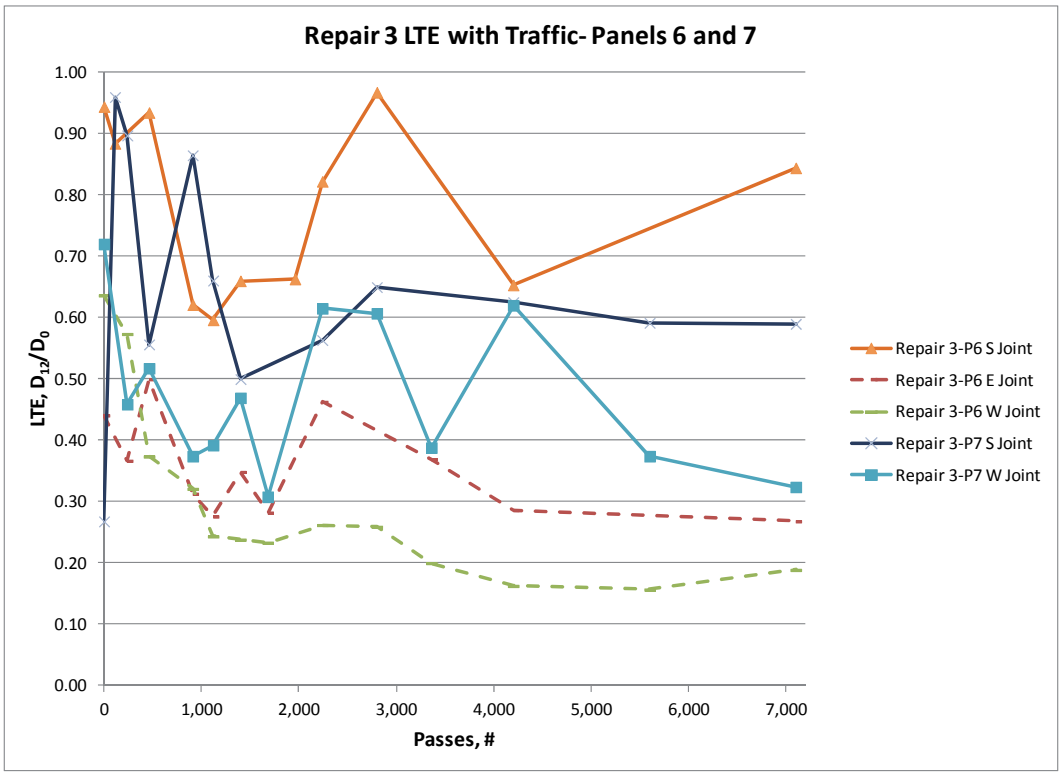

For Repair 2, the N and S joints (transverse- doweled) had better LTE than the E and W joints (longitudinal- undoweled). Overall, the longitudinal joint between the panels (Panel 2 W joint (center)) performed worse than the other joints for this repair with a maximum LTE of 65 percent and minimum of 38 percent. Additionally, the LTE for this repair was poorer than for the single-panel Repair 1. This was attributed to the larger joint openings for this repair compared to Repair 1. The panel sizes were the same, but Repair 1 had a joint opening of approximately 0.375 in., while Repair 2 had joint openings of approximately 0.5 in. Panel 2 had a maximum LTE of 84 percent and minimum LTE of 62 percent for the N joint and 97 percent maximum and 59 percent minimum for the S joint. Panel 3 had a maximum LTE of 97 percent and minimum LTE of 75 percent for the N joint and 92 percent maximum and 80 percent minimum for the S joint. The E and W joints had similar values with Panel 3 W joint with a maximum of 64 percent and a minimum of 33 percent, while Panel 2's E joint had a maximum LTE of 60 percent and minimum of 37 percent. The transverse joints (N-S) with the exception of Panel 2's N and S joints were above the minimum 70 percent threshold.

For Repair 3, the center (longitudinal) joint between the panels had the lowest LTE compared to the other joints with initial values less than 70 percent and the lowest values of less than 20 percent after 5,600 passes. The N joints of Panels 4 and 6 performed similarly to each other with maximum LTE of 90 percent for Panel 4 and 97 percent for Panel 6, and a minimum LTE of 88 percent and 84 percent for the N joints of Panels 4 and 6, respectively. Panel 7 had the lowest LTE for its S joint with a minimum of 50 percent (below the minimum threshold). This could indicate loss of support on the S end. As with Repair 2, the longitudinal joints had poorer LTE than the transverse joints. The maximum LTE for the E joints were 90 percent for Panel 4 and 52 percent for Panel 6 with minimums of 51 percent and 28 percent, respectively. The W joints had LTE maximums of 82 percent for Panel 5 and 72 percent for Panel 7. The minimum LTE for the W joints of Panels 5 and 7 were 27 percent and 31 percent, respectively.

For comparison, the LTE was calculated prior to traffic and after 10,000 passes on the parent slabs in locations shown previously in Figure 17. The majority of the slabs had LTE values greater than 70 percent prior to and after traffic with the exception of test locations 3, 10, and 11. These locations had LTE values well below the threshold level before and after traffic,

indicating that there was poor load transfer between slabs in these locations. These slabs were not doweled on the transverse joints, as shown in Figure 27.

Figure 27. Dowel layout for precast slab test section.

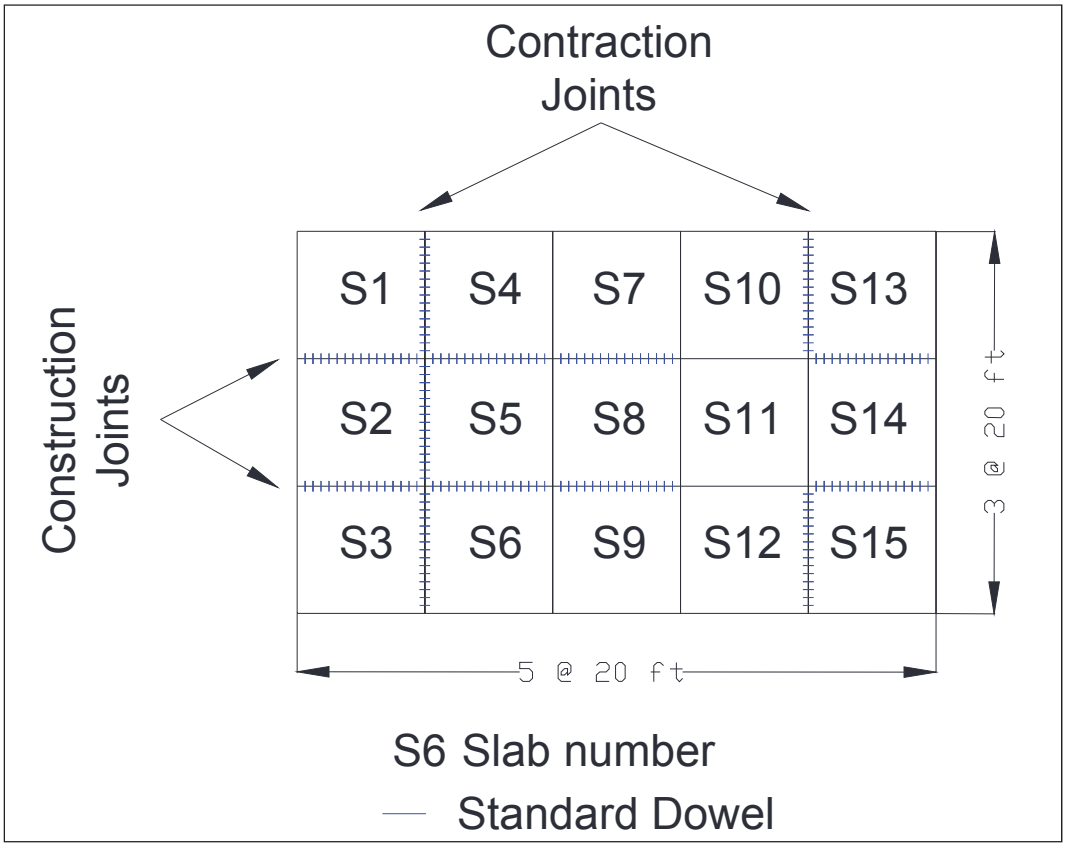

Table 6. Load transfer FWD test data parent PCC slabs prior to repair.

Passes	HWD Reference Number	Direction	LTE	Load, lb	Normalized D_0	Deflection, mils	
			D_{12}/D_0		mils	D_0	D_{12}
0	2	N-S	0.90	55,846	22.6963	25.35	22.75
0	3	N-S	0.19	53,852	38.2808	41.23	7.89
0	4	N-S	0.90	55,670	20.406	22.72	20.38
0	9	N-S	0.98	54,608	18.8617	20.60	20.14
0	10	N-S	0.29	54,772	30.3075	33.20	9.70
0	11	N-S	0.23	54,235	31.0224	33.65	7.69
0	12	S-N	0.95	55,210	18.19	20.09	19.17
0	13	E-W	0.78	53,556	31.88	34.15	26.80
0	14	E-W	0.86	54,542	23.02	25.11	21.63
0	15	E-W	0.86	55,035	20.41	22.46	19.42

Passes	HWD Reference Number	Direction	LTE D_{12}/D_0	Load, lb	Normalized D_0 mils	Deflection, mils D_0	D_{12}
0	21	W-E	0.98	54,991	18.48	20.32	19.90
0	22	W-E	0.84	54,750	20.48	22.43	18.90
10,000	2	N-S	0.95	54,520	20.41	22.25	21.18
10,000	3	N-S	0.22	53,742	35.82	38.50	8.56
10,000	4	N-S	0.96	56,163	17.86	20.06	19.30
10,000	9	N-S	0.96	55,670	19.14	21.31	20.43
10,000	10	N-S	0.53	55,561	24.18	26.87	14.36
10,000	11	N-S	0.25	53,458	31.87	34.07	8.50
10,000	12	S-N	0.96	56,481	15.57	17.59	16.91
10,000	13	E-W	No Data				
10,000	14	E-W	0.80	53,852	25.96	27.96	22.29
10,000	15	E-W	No Data				
10,000	21	W-E	0.91	53,786	20.79	22.36	20.33
10,000	22	W-E	0.33	52,691	44.69	47.09	15.33

The LTEs of the panels were predicted by simulating a joint load test using a Skarlatos rigid joint model. The model simulates two infinite slabs connected by a single joint of infinite length. The measured deflection basins for the panels were used to estimate the panel modulus of elasticity (*E*), joint stiffness factor (*JSF*) and modulus of subgrade reaction (*k*) prior to traffic and at failure. *AGG** is a nondimensional stiffness of the joint. During the simulations, E was varied between 4 and 6 x 10^6 psi (reasonable range for PCC pavement), and the *JSF* was varied between 100 (excellent load transfer) to 0 (no load transfer). *k* was varied between 100 and 276 pci (the measured test section *k* value). Predicted deflection basins were compared to measured deflections for each joint type (transverse and longitudinal) to determine which modeled joint behavior(s) best reproduced the measured joint behaviors. A subset of the predicted deflection basins compared to the average longitudinal joint behavior of the repairs prior to traffic is presented in Figure 28.

While none of the simulated basins exactly matched the measured basins, the best predicted basins were obtained when *E*=5 x 10^6 psi, *JSF*=100, and *k*=200 pci for the initial calculation of LTE on the transverse joints (prior to traffic). This high joint stiffness factor of 100 indicated high load transfer (>90 percent). For the longitudinal joints, the joint stiffness factor was reduced to 4 for the initial calculation of LTE. A joint stiffness factor of 4 is representative of good load transfer of approximately 70 percent.

Figure 28. Predicted deflection basins for longitudinal joints prior to traffic.

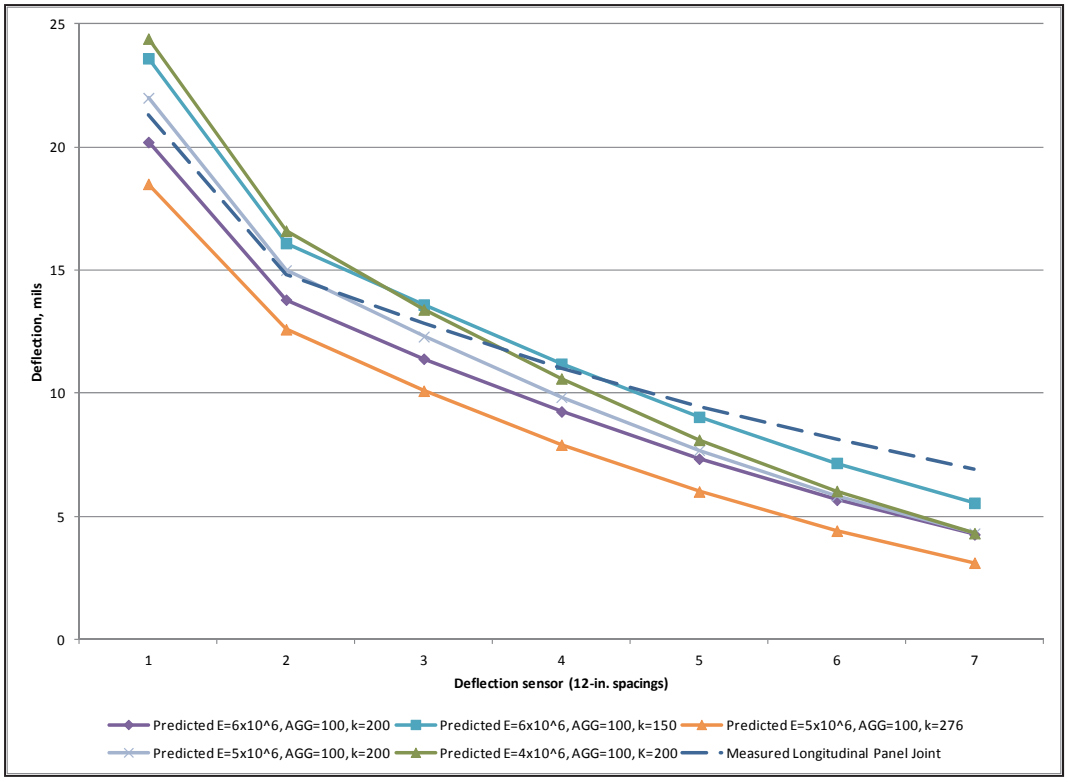

For the LTE at failure, estimating the inputs required additional trials. The measured deflections at failure were compared to the predicted deflections by varying the E between 2 and 5 x 10^6 psi and JSF between 0 and 2. The predicted deflections most closely matched the measured deflections for the transverse joints when E=3 x 10^6, k=100 pci, and JSF=4. For the longitudinal joints, the measured basins most closely matched those predicted using E=3 x 10^6, k=100 pci, and JSF=2. These values are not unreasonable considering the deterioration of the transverse joints evidenced during trafficking would result in a loss of joint stiffness. For the longitudinal joints, JSF=2 was reasonable, as they were undoweled. The reduction in the subgrade modulus was also not an unusual assumption, as the flowable fill will crack under loading imparting more stress to the subgrade. By matching deflection basins at joints, it was determined that initially the measured basins were similar to estimated, but that at failure, the basins were not. Furthermore, the deflections past the third sensor where overestimated by the model. This is due to differences in the panel repair and parent PCC structures such as PCC thickness and base materials.

Stiffness

Joint stiffness was calculated directly from the HWD joint test data using a procedure developed by Byrum (2011). This parameter is the amount of force (lb) transferred per inch of joint length, per inch of joint vertical deflection difference with units of lb/in./in. This numerical value represents how much load is transferred through a joint. The magnitudes of the joint vertical deflections under traffic or under HWD loadings are a function of the subgrade strength and the slab thickness.

This HWD predicted joint stiffness procedure uses the deflection basins from a joint load test. The equation calculates total joint stiffness magnitude in units of lb/in./in.

$$k_j = \frac{P(LTE_\delta)}{[(1+LTE_\delta)(D_0 - D_{12})(1+i)(1)\left(66 + 60 * \frac{D_{72}}{D_{12} - D_{72}}\right)]} \quad (5)$$

where:

k_j = joint stiffness (lb/in./in.)
P = HWD drop load (lb)
LTE_δ = deflection based load transfer efficiency or deflection (D_{12}/D_0)
D_0 = deflection under the HWD load plate (sensor 0) 6 in. from the joint (in.)
D_{12} = deflection measured at the first sensor spaced 12 in. from the load plate and 6 in. from the joint (in.)
D_{72} = deflection measured at the last sensor (in.)
i = percent increase factor needed to project the sensor readings to the joint

In order to determine the i percent increase factor, the assumed deflection basin at a joint was examined. At a joint, a deflection difference from the discontinuity of the joint between the first and second sensors as shown in Figure 29 is expected. The i factor is the percent increase needed to project the sensor readings taken 6 in. on either side of the joint out to the joint line. The method recommended by Byrum was to use the slope of the line on the unloaded side multiplied by the distance between the sensor and the slab edge divided by the deflection measured at the sensor on the unloaded

Figure 29. Joint deflection difference at a joint (Byrum 2011).

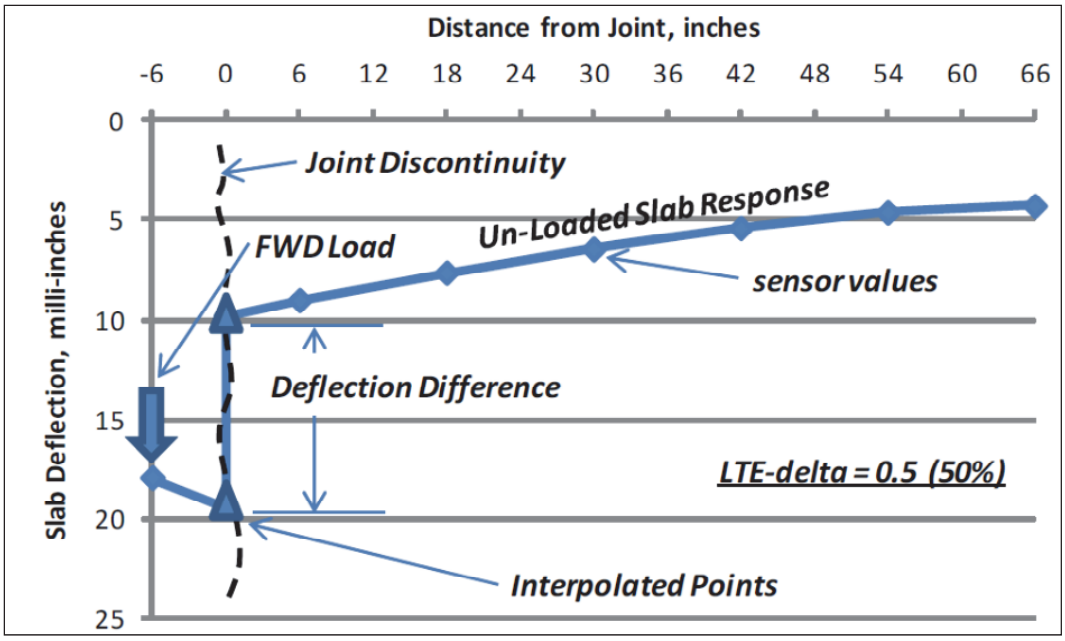

side (D_{12}). Using this procedure and the joint test data, the average value of $\acute{\iota}$=0.06 was calculated with a minimum of 0.03 and maximum of 0.07. This factor was used for determining the joint stiffness of all tested joints in the current project. This factor also matches Byrum's that was based on numerous PCC airfield pavement HWD data.

A chart of calculated LTE and joint stiffness for the panels is provided in Figure 30 separated by joint location. This figure presents HWD tests taken in the mornings following the completion of traffic intervals as described previously. In general, the lowest joint stiffness values were for the transverse (E-W) joints with low LTE values. Transverse joints including the N and S and Center joints had the highest LTE values, but joint stiffness varied substantially even with similar LTE values due to deflection measurements and load. Overall, a very good trend between the LTE and joint stiffness is shown with an R^2 value of 0.99 in the curve fit for the data in Figure 31.

In the study conducted by Byrum (2011), joint stiffness values for traditional airfield concrete slabs ranged from 0 to 250,000 lb/in./in. with the highest joint stiffness values measured during warm weather. Joint stiffness values for this investigation varied from 268 to more than 350,000 lb/in./in. The highest stiffness values were calculated when the load transfer was over 90 percent.

Figure 30. LTE versus joint stiffness.

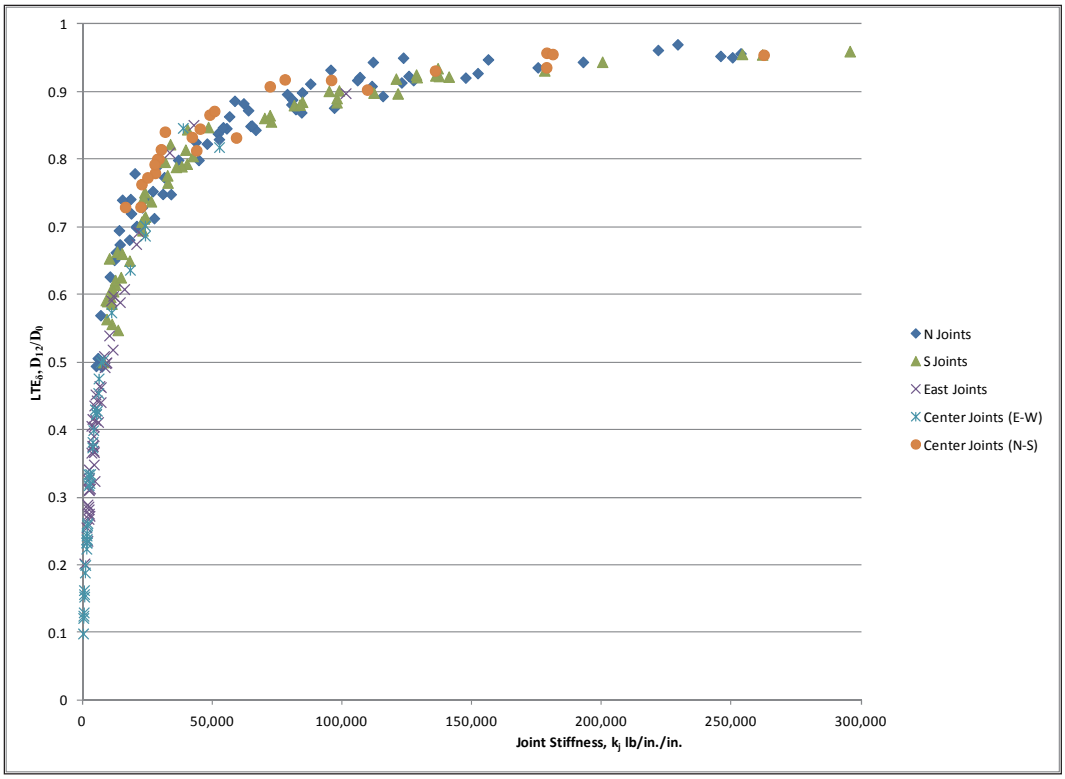

Figure 32 through Figure 36 show the change in joint stiffness for the various repairs. As with the LTE, the joint stiffness tended to decrease with increasing traffic with the lowest values for the longitudinal (E and W joints) due to the lack of load transfer. Some values increased instead of decreasing with increasing traffic, most likely due to closing of the joints caused by expansion of the panels during traffic caused by thermal effects. Figure 37 shows a comparison for the pre-traffic stiffness values for each panel and at failure. As expected, the stiffness is greatly reduced after the panels failed.

Corner deflection

Corner deflection tests were conducted on selected panel corners for each repair. Tests were conducted for Repair 1 in Panel 1, Repair 2 in Panel 2, and Repair 3 in Panels 4 and 7. The HWD was used to conduct this test with the load plate placed near the corner of the slab in the direction of traffic. Corner deflections were monitored, as deflections in the corners of the panels were expected to be higher than those measured in the center of the panel based on traditional pavement design concepts. Deflections were normalized to 50,000 lb to show comparisons between the numerous load

Figure 31. Curve fit for LTE versus joint stiffness.

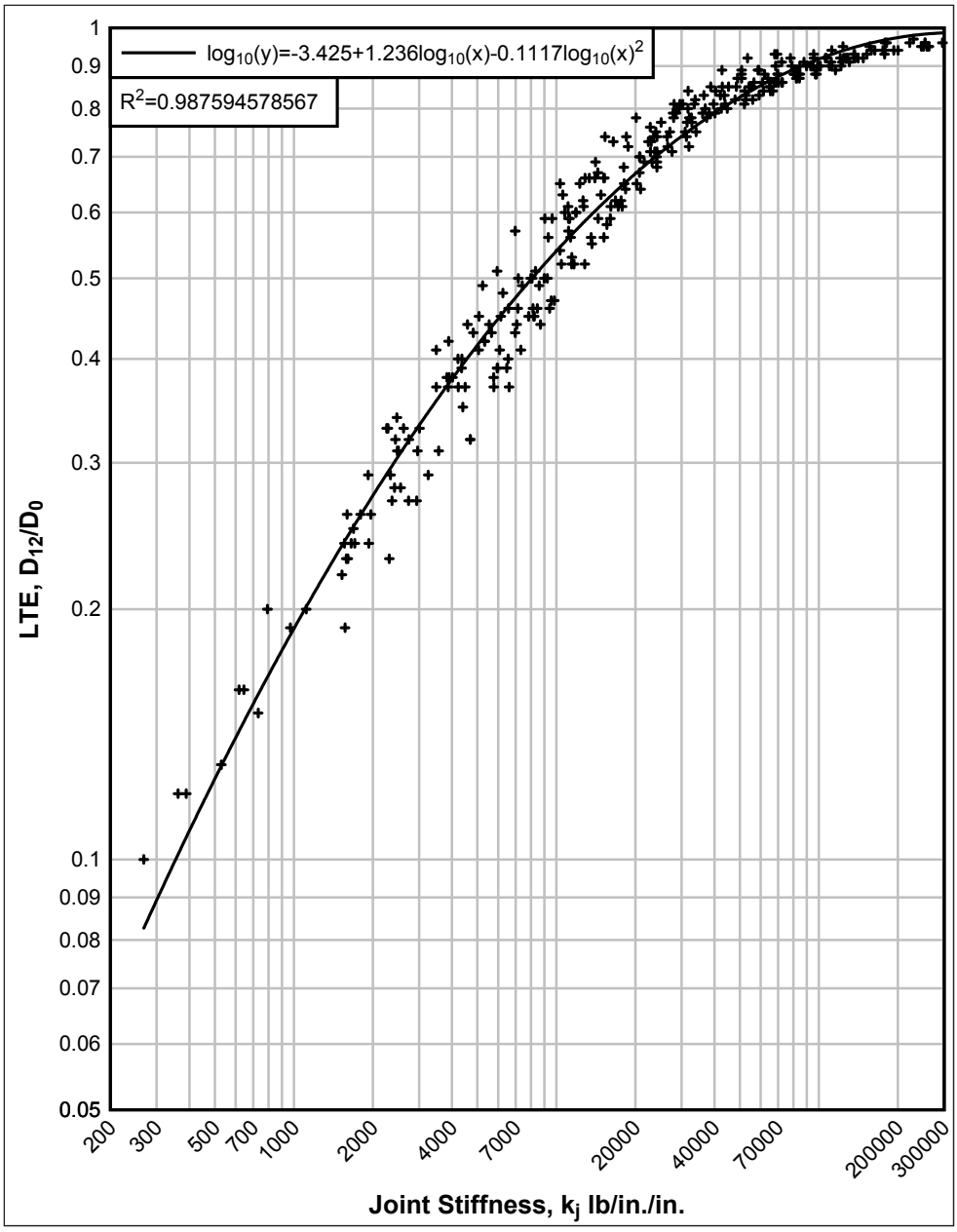

applications and measured deflections. Figure 38 shows the deflections for the panels. As can be seen, the deflections at the corners increased with increasing traffic application as a general trend. For comparison, Figure 39 presents the center deflections, and Figure 40 presents the edge deflections. As expected, the corner deflections were higher than the center deflections and higher than the doweled joints, but similar to the undoweled joints as traffic increased. This indicates that the panels deflect in a manner similar to that of the parent PCC.

Figure 32. Repair 1 joint stiffness with traffic.

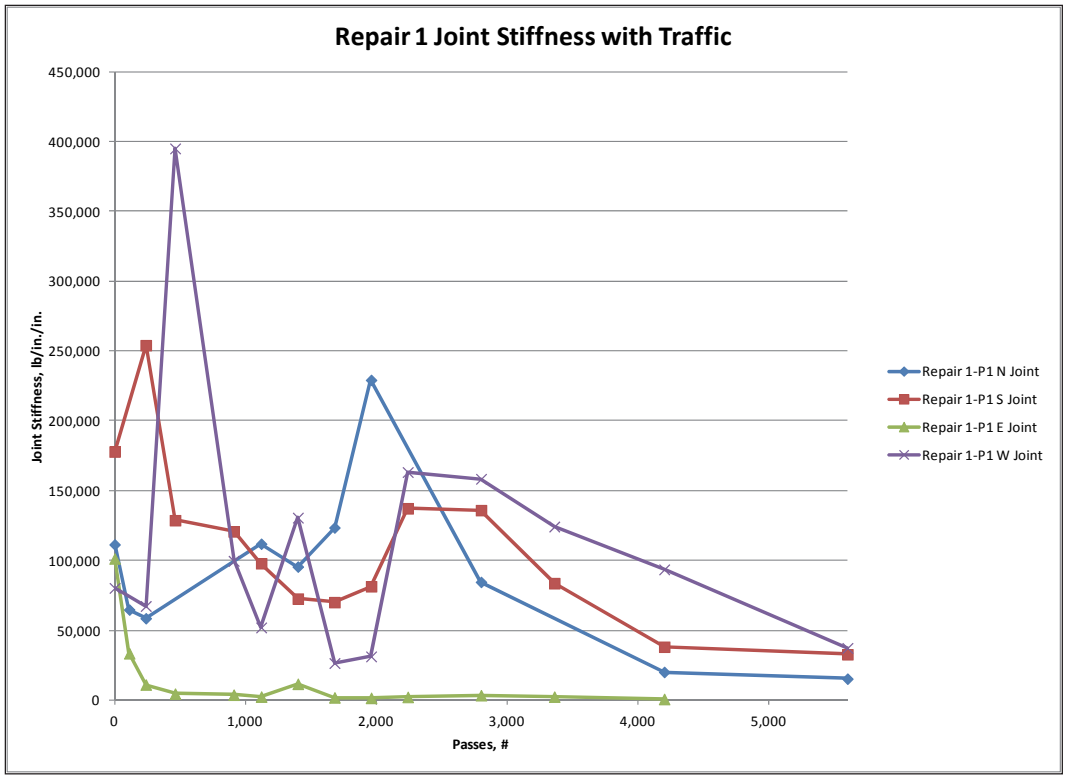

Figure 33. Repair 2, N and S joint stiffness with traffic.

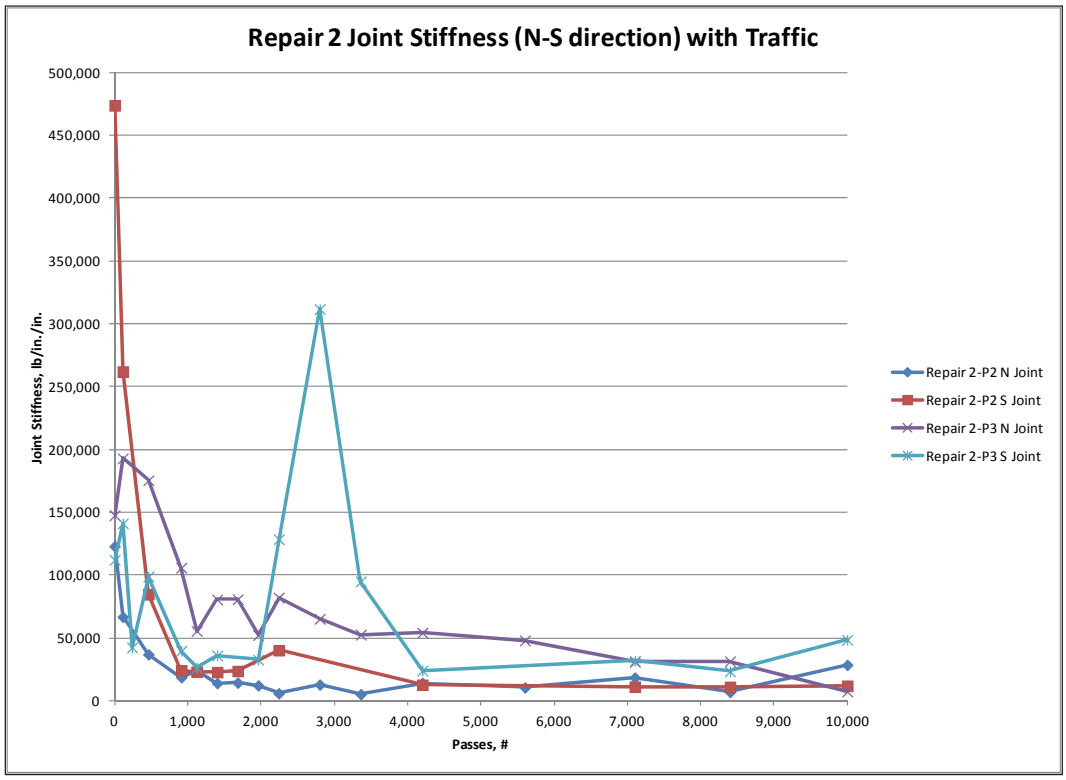

Figure 34. Repair 2, E and W joint stiffness with traffic.

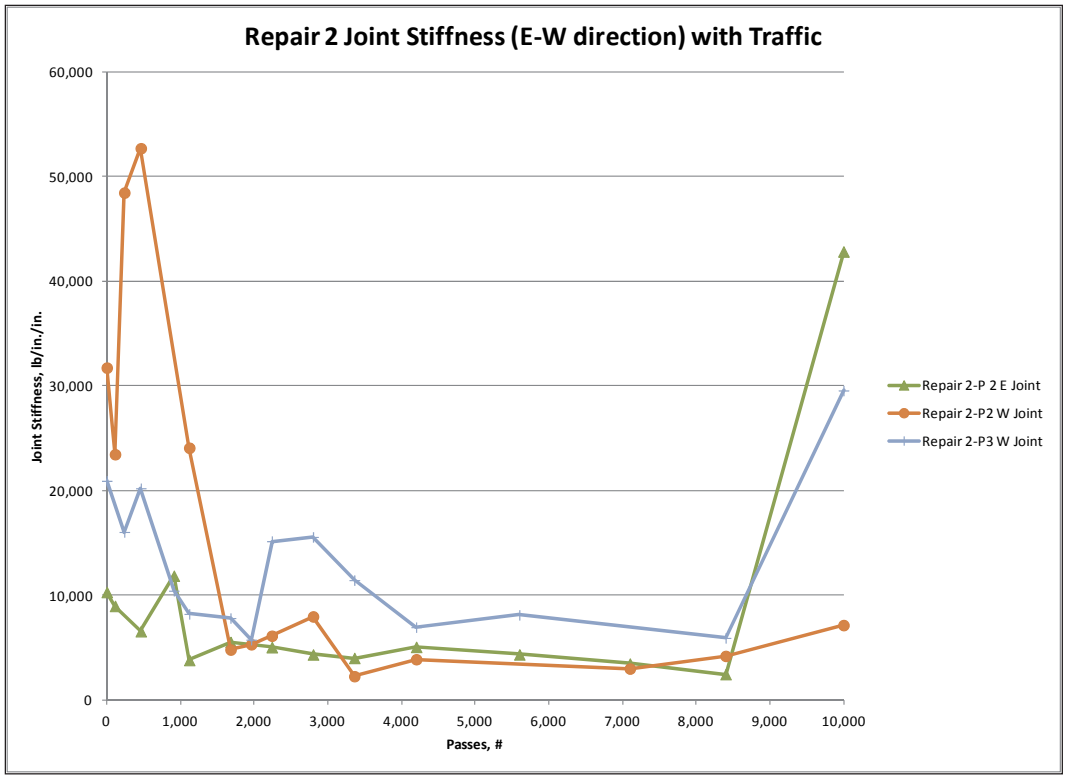

Figure 35. Repair 3, N and S joint stiffness with traffic.

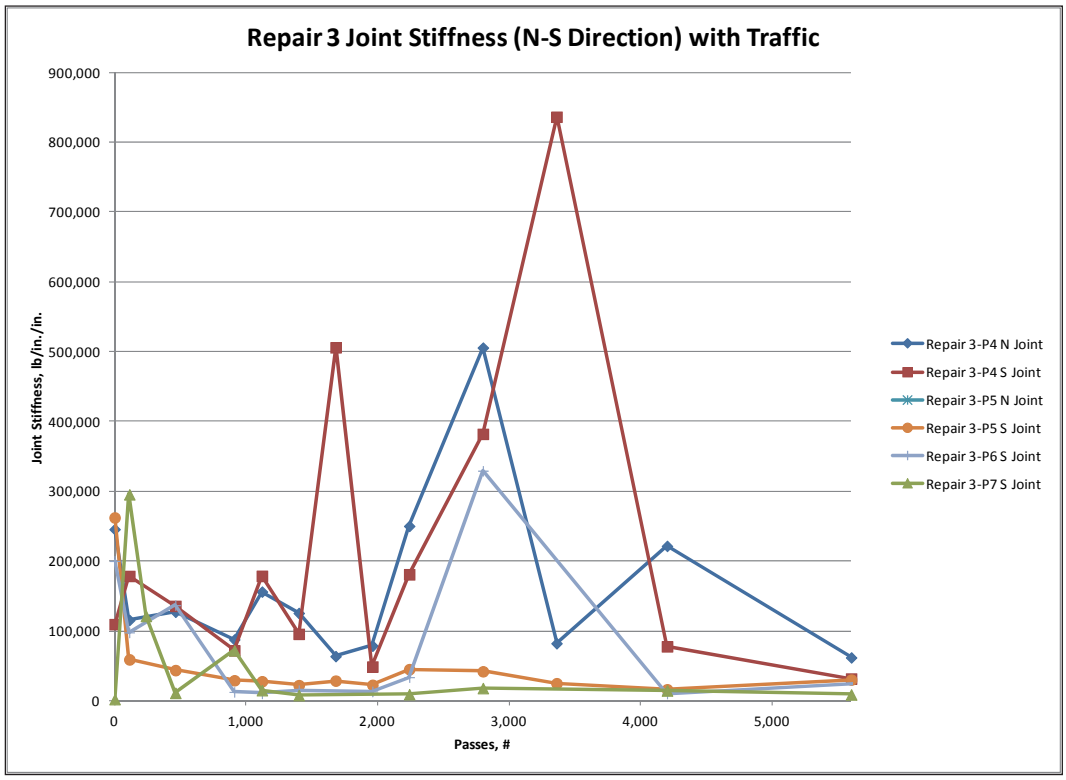

Figure 36. Repair 3, E and W joint stiffness with traffic.

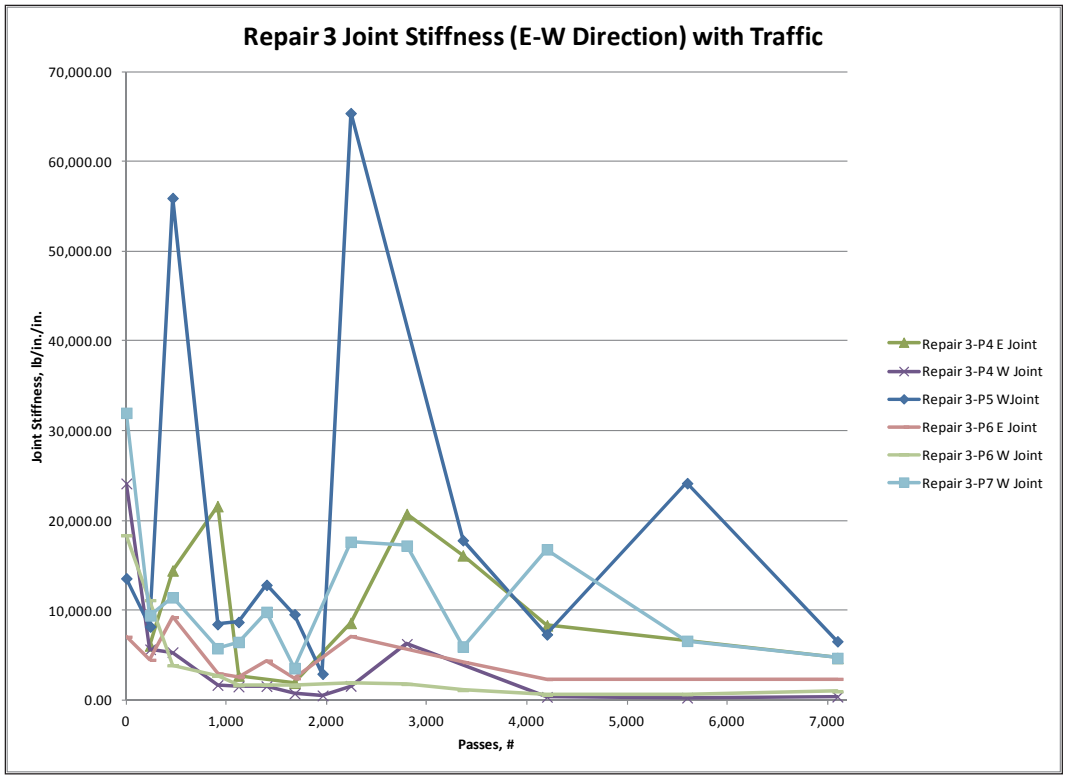

Figure 37. Pre-traffic and after failure joint stiffness.

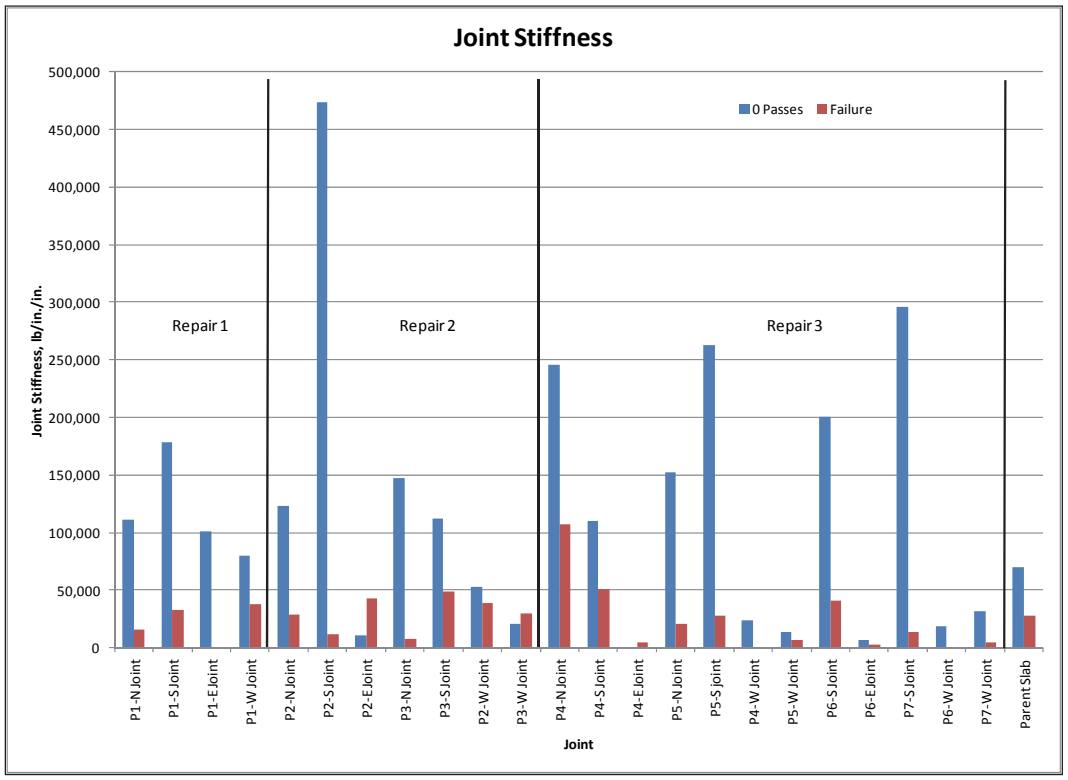

Figure 38. Corner deflections for selected panels.

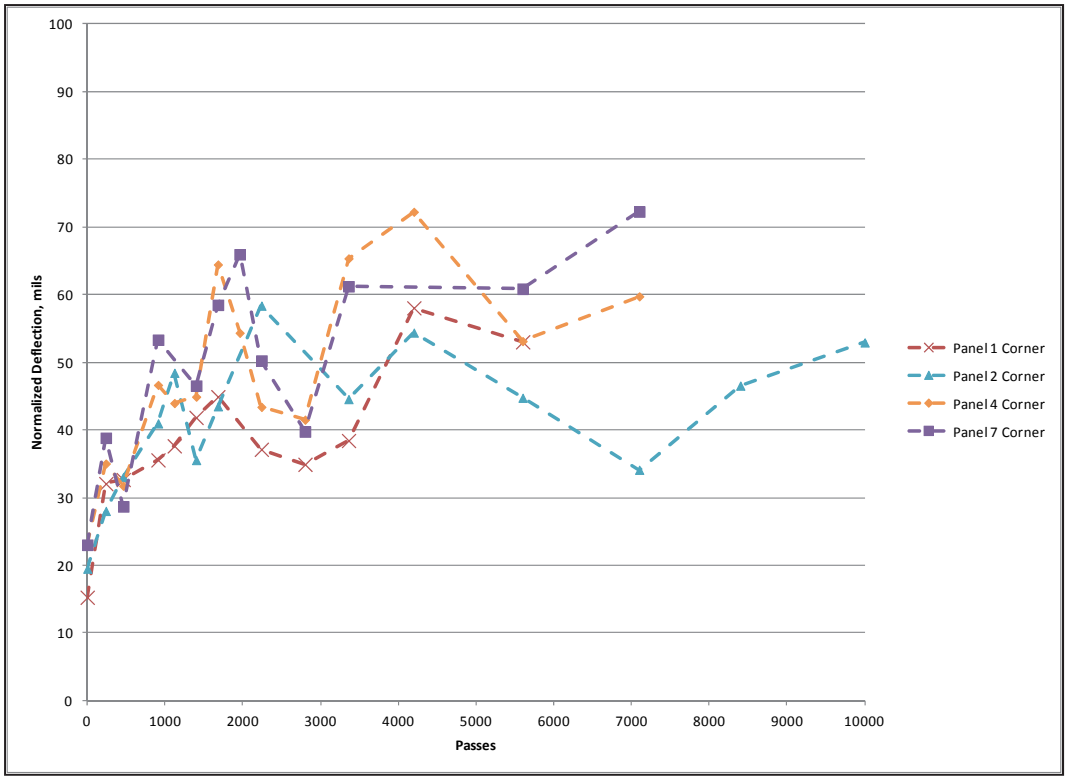

Figure 39. Center deflections.

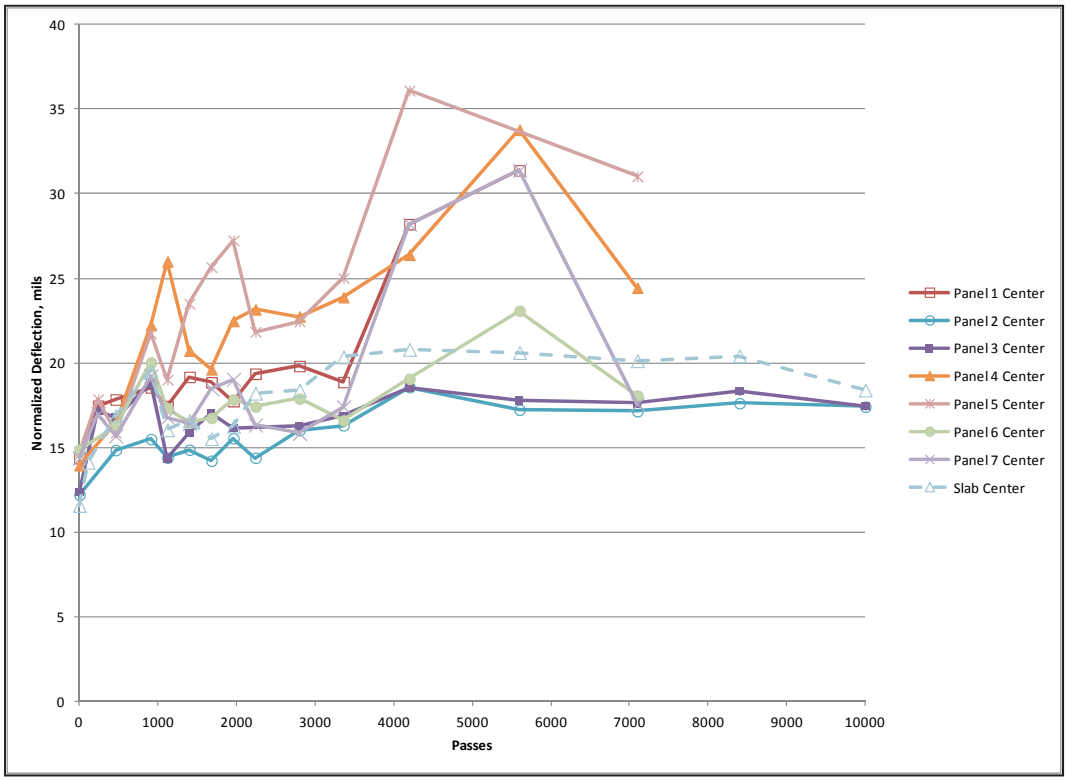

Figure 40. Edge deflections.

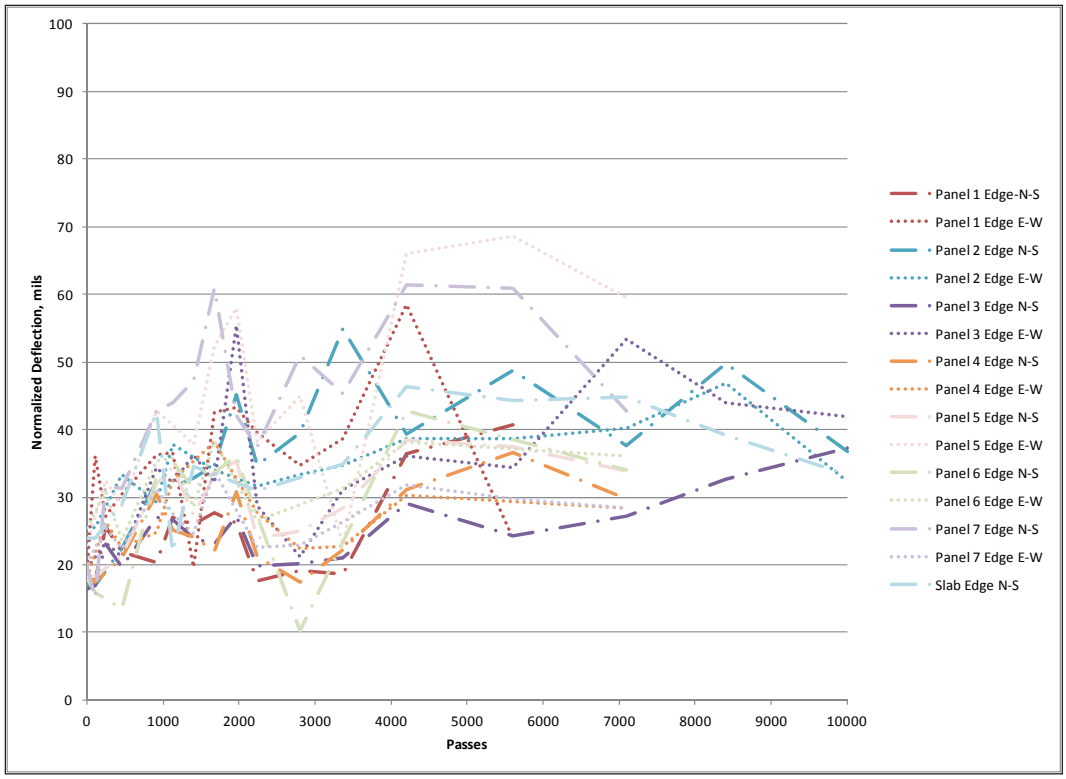

8 Instrumentation Results

The EPC and strain gauge data collected during trafficking were used to determine stresses and strains in the repairs as a function of traffic. Locations of instrumentation and the installation process were presented in Chapter 3. Despite proper installation, instrumentation is susceptible to damage due to loading of the load cart and to temperature changes. Strain gauges are particularly susceptible. Several of the installed gauges were damaged during installation and trafficking, including EPCs in the center of Panels 1, 2, 3, and 7 and all of the surface strain gauges. Data collected from the remaining instrumentation is presented in this chapter.

EPC data

EPC data were collected during the pass intervals described previously. An example of the raw EPC data prior to processing is presented in Figure 41. The data presented is one complete pattern of C-17 traffic (28 passes). The EPCs under the centers of Panels 1, 2, 3 and 7 were destroyed during the initial traffic applications, thus no comparisons between corner and center deflections in the same panel could be made. Each EPC curve was normalized to only show the influence of the load cart. The peak pressure values (maximum vertical stress) for each traffic interval measured were then identified and were plotted in Figure 42. As can be seen in the figure, a slight increase in peak vertical stress was observed after 500 traffic applications, but the overall trend was flat.

The initial center panel peak pressure readings (vertical stress) were measured in the range of 3.5-5.5 psi. These measurements were slightly less than theoretical prediction for center slab vertical stress using fundamental PCC theory calculated as 6.9 psi and less than predicted vertical stress using linear elastic analysis (LEA), which were 7.8-11.1 psi. Using 2D finite element model software (ISLAB2000), the predicted vertical stress was 4.6 psi, similar to the measured stress range. The panel center stress measurements also were similar to the control measurements on a PCC slab (initially 5.1 psi). The initial corner peak vertical stress measurements were in the range of 9-10 psi; these were close to calculated vertical stress measurement of 6.0 psi using ISLAB2000. No control tests were conducted on the PCC for comparison.

Figure 41. Example of EPC data collection.

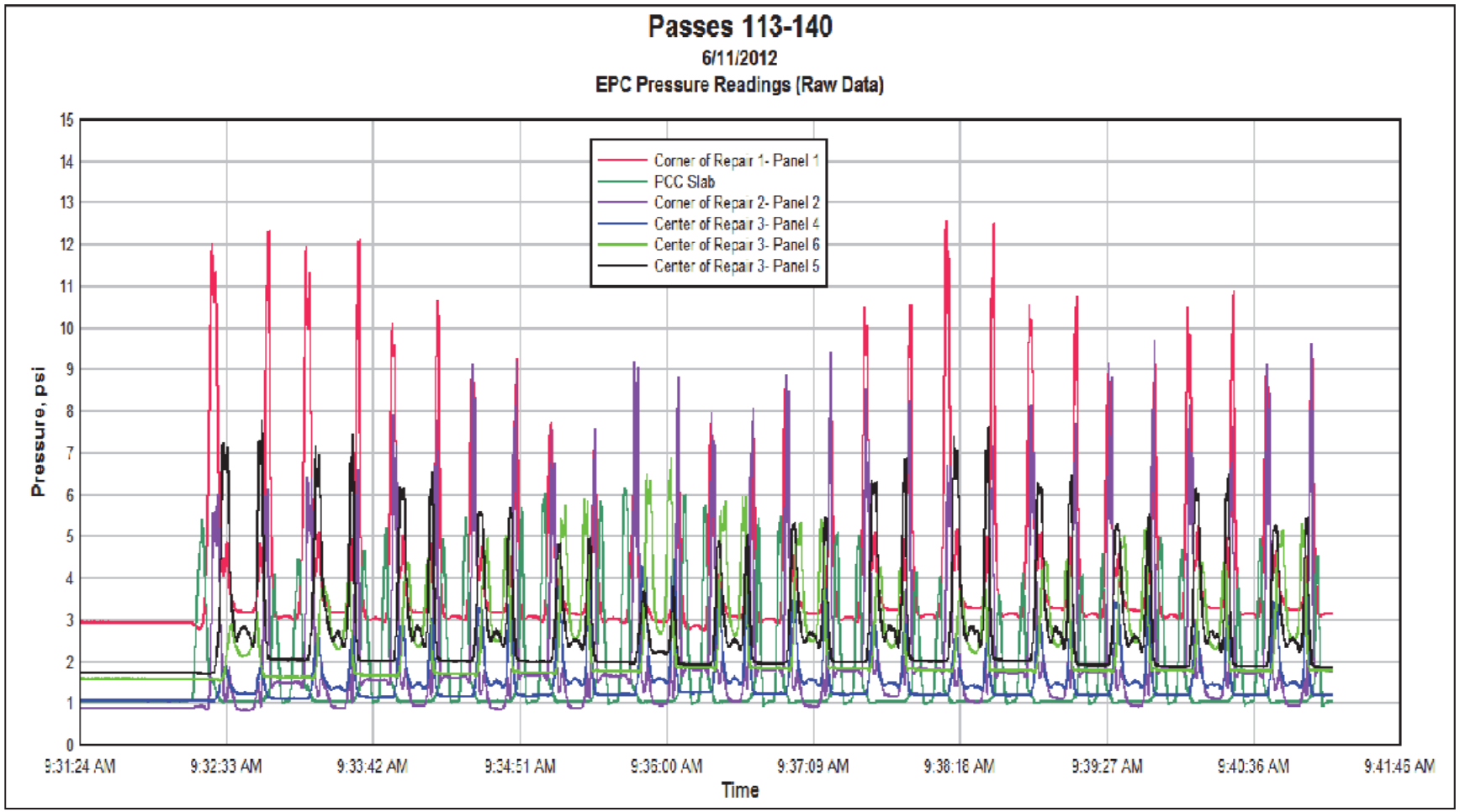

Figure 42. Peak pressure distribution with traffic passes.

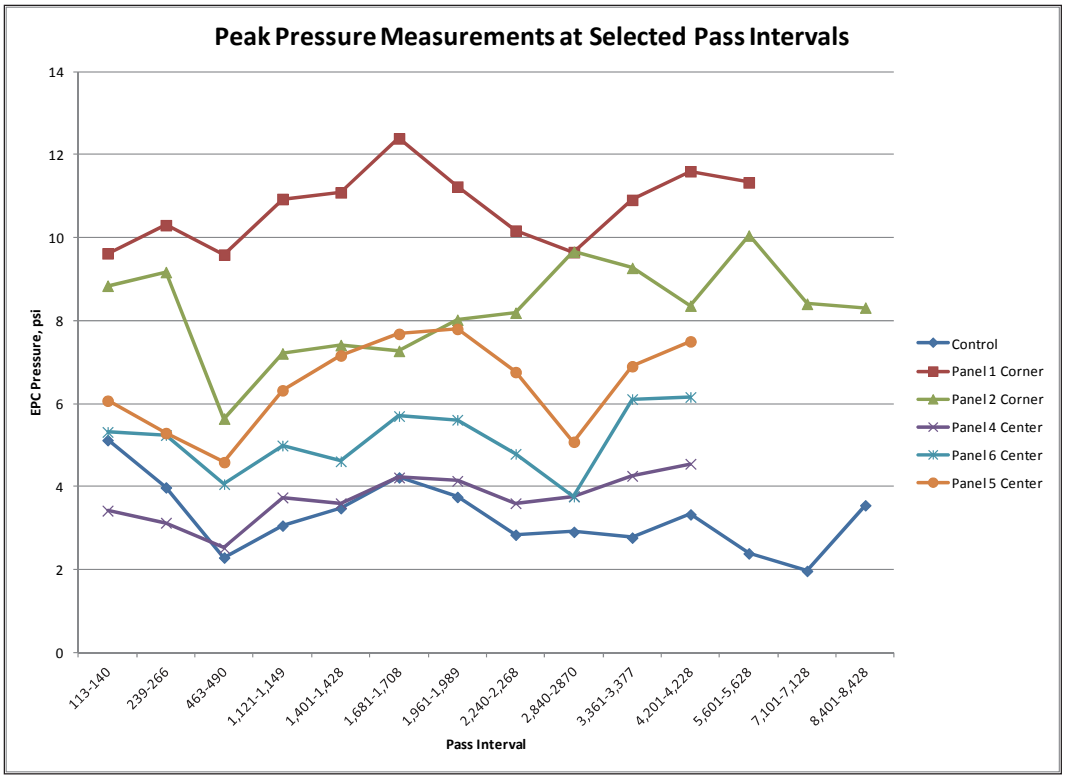

Strain gauge data

The surface of the test section and the edges of select panels were instrumented with strain gauges as described in Chapter 3. During the first few passes of the load cart, the surface strain gauges were destroyed. Only limited data were recorded. Figure 43 presents data collected by the surface strain gauges on Repair 2 panels. Gauges 5 and 7 were located on the parent PCC side of joint, and Gauges 6 and 8 were located on the panel side of the joint. The response of the pavement edge can be seen in the strain gauge plot of Figure 43. As the load cart wheels approached Panel 2, the parent PCC edge was put under compression (positive peak of Gauge 7), and the panel edge was put under tension (negative peak of Gauge 8). As the load cart departed the PCC, the panel edge was then put into compression (seen in the decreasing strain of Gauge 7 and positive peak of Gauge 8). The peak positive and negative surface strains for the first five passes, the only data collected are presented in Figure 44. The data labels for the *x*-axis indicate which side the strain gauge was placed. For example, the first label "PCC Panel 3" is the measured strain for the strain gauge mounted on the PCC side of the joint with Panel 3. Likewise, "Panel Panel 3" is the measured strain for the strain gauge mounted on the panel side of the joint.

Figure 43. Surface strain gauge data example.

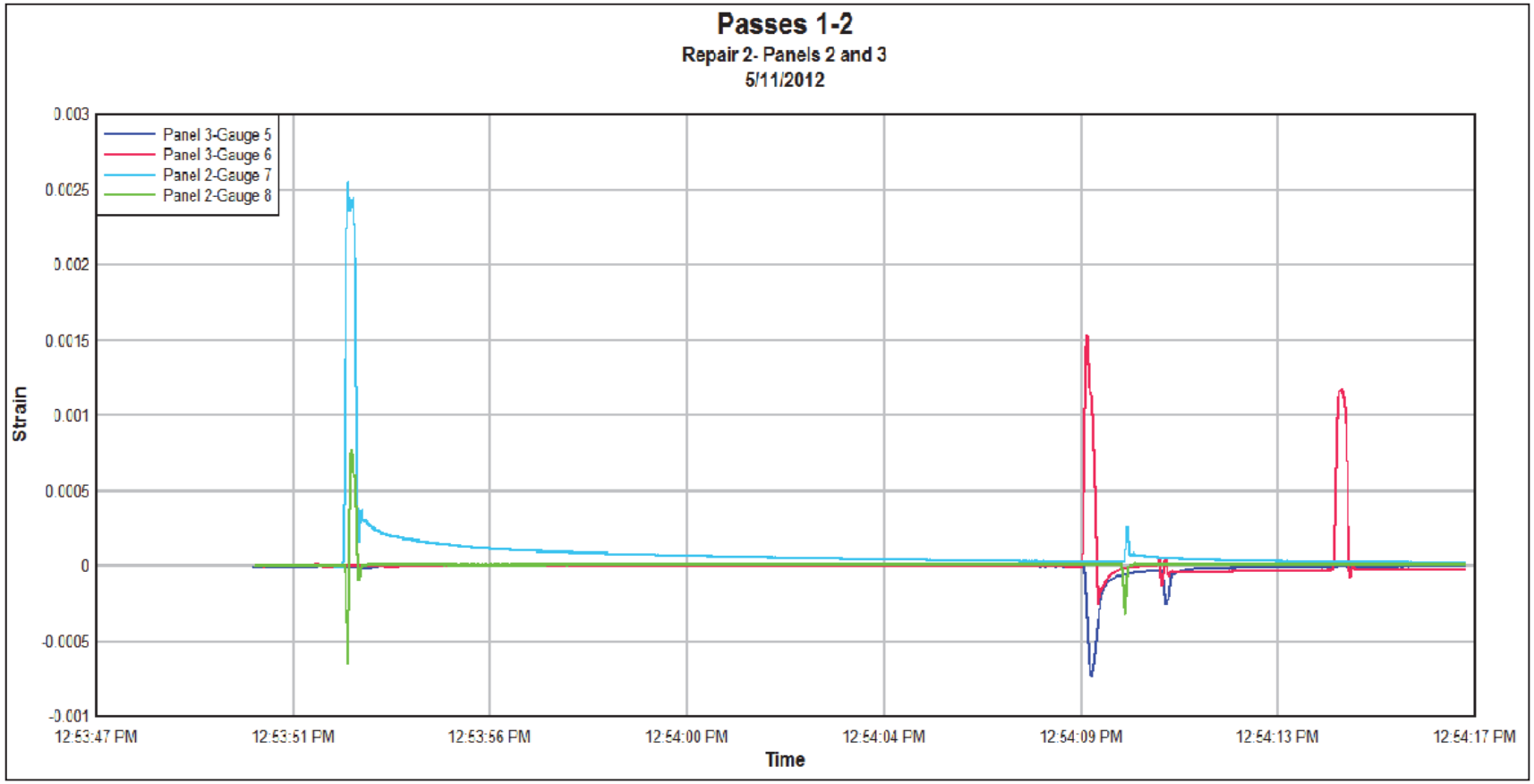

Figure 44. Surface strain peak measurements for passes 1-5.

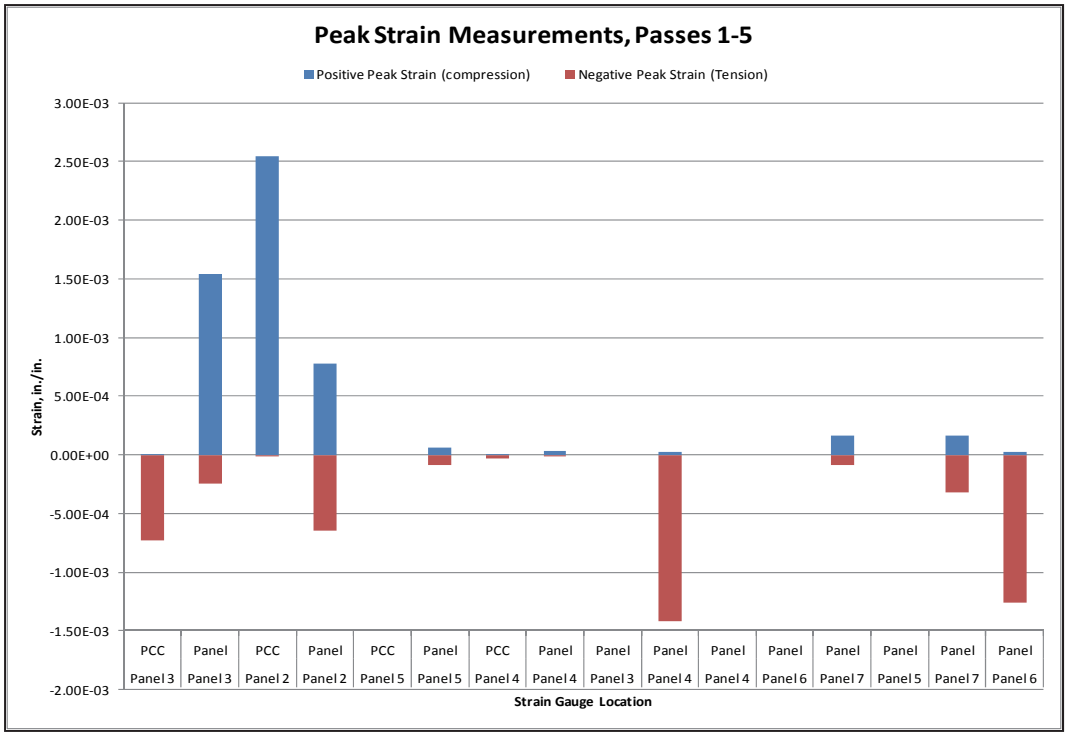

The strain gauges mounted on the edges of Panels 5 and 6 were not destroyed during trafficking and allowed monitoring of edge strains on the sides of the panels for both the transverse and longitudinal joints at selected traffic intervals. An example plot of the strain data collected during passes 463-490 is presented in Figure 45 for Panels 5 and 6 in Repair 3. Peak positive (tension) and negative (compression) strains for selected pass intervals are presented in Figure 46. In general, the strains increased with increasing traffic. The highest strains were measured for Panel 6 in the bottom strain gauge on the transverse joint.

The average initial strain measurement on the panel side of the joint was 3.5E-04. Compared to the strain predicted using ISLAB2000, the predicted strain (1.66E-4) was less than the measured strain. For the PCC side of the joint, the average strain was -2.6E-04 (measured) compared to -1.47E-04 (predicted). For the edge strains, the measured strains were projected to the surface and bottom of the panel, as the strain gauges were placed 1 in. from the top and bottom of the panel. For transverse joints, the maximum strain at the top of the panel was -4.5e-05 (measured) compared to -1.7E-05 (predicted), and the maximum strain at the bottom of the panel was 5.7E-05 (measured) compared to 1.9E-04 (predicted). Comparing the predicted and measured values, in general, the model under-predicted the strains measured in the panels for both for surface and edge strains at the joints.

Figure 45. Edge strain gauge data example.

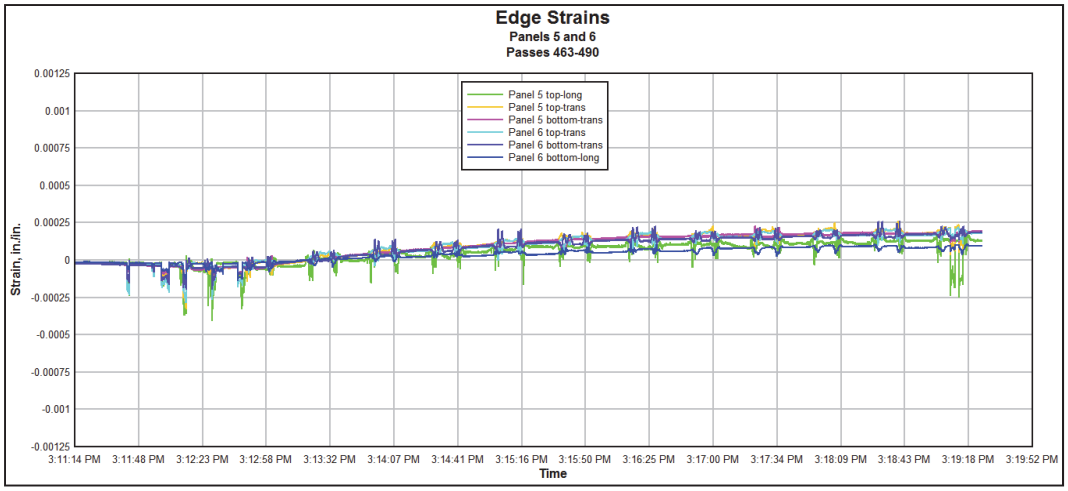

Figure 46. Peak strain measurements.

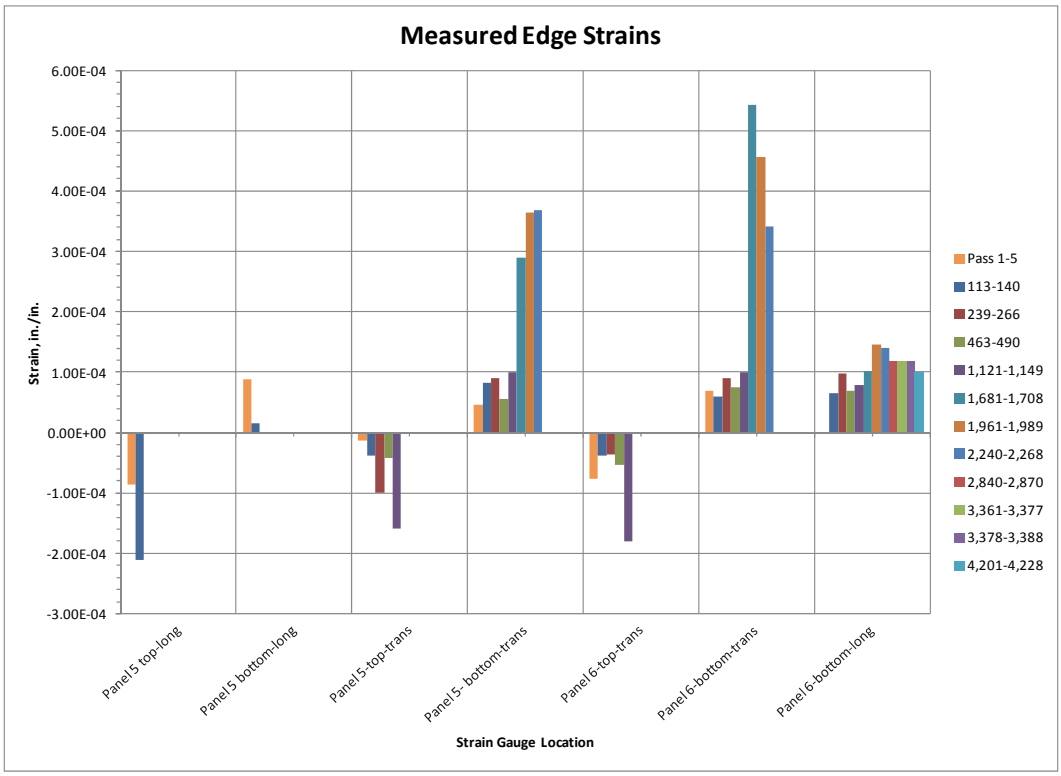

In comparing the measured and predicted stresses and strains, in general, the panels performed similarly to PCC slabs in terms of initial stress measurements. The predicted strain measurements at the joints were less than measured. This may be due to differences in the thickness of the panel and surrounding slab in addition to the differences in base composition.

9 Analyses of Results

Table 7 presents a summary of the repair failures and deflection measurements and calculations performed from HWD data including LTE, peak deflections, effective backcalculated moduli, ISMs, and joint stiffness moduli. Table 8 presents a summary of the instrumentation data including measured vertical pressures from the EPCs and strains from strain gauges. Comparisons of the panels' performance are provided for each repair in this chapter. Additionally, comparisons of the precast panel repairs in terms of cost, speed of repair, and performance are provided and compared to other Air Force expedient airfield pavement repair methods.

Repair 1-single-panel repair

Repair 1 performed the worst under C-17 traffic of the three repairs. The parent slab began deteriorating within the first 112 passes, and cracking and spalling progressed during the first 1,000 passes. Distresses noted in the panel were located adjacent to the parent slab deterioration after 2,800 passes. After this point, the repair began to crack, with spalling noted along the joints. After 5,600 passes, the panel was in shattered condition, with FOD production not easily controlled through sweeping in both the panel and the parent slab. The panel at failure is presented in Figure 47. Also seen in the figure are cracks in the parent slab extended from the overcuts from initial sawing efforts. During field placement of the panel, it was noted that the flowable fill was very wet, and it did not appear to be the same quality as the specified mixture design or the other two repairs' batches. The corner break seen in Figure 47 and the shattered slab condition of the precast panel could indicate a weak base beneath the slab. Also in this figure, the dowel receptacle deterioration is evident.

The roughness criteria were not exceeded for this repair with a maximum recorded elevation difference of 0.375 in. from the installation elevation. The maximum deflection was measured as 0.625 in. along the NE corner, where the spalled edge within the corner break is evident in Figure 47 after 5,600 passes.

As can be seen in Table 7, the LTE decreased from installation to failure for Repair 1 from approximately 90 percent for the transverse (doweled) joints (N and S) to approximately 75 percent. For the longitudinal (undoweled)

Table 7. Summary of repair failures and HWD data.

Repair	Panel	Failure Detail	Passes-to-Failure, #	Initial LTE, % (Jt. Direction)	Final LTE, % (Jt. location)	Peak Center Defl., mils	Peak Corner Defl., mils	ISM, kip/in.	Initial Jt. Stiffness, lb/in./in.	Final Jt. Stiffness, lb/in./in.
1	1	Shattered Slab and parent slab failure	5,600	90.8 (N)	74.0 (N)	14.37 (initial) 31.38 (final)	15.27 (initial) 53.03 (final)	3,478 (initial) 1,593 (final)	111,464 (N)	15,330 (N)
				93.1 (S)	76.5 (S)				177,972 (S)	32,817 (S)
				89.7 (E)	20.2 (E)				101,403 (E)	793 (E)
				87.7 (W)	77.5 (W)				80,331 (W)	37,378 (W)
2	2	Spalled joints and spalled corners along doweled edges	10,000	91.3 (N)	78.8 (N)	12.21 (initial) 17.41 (final)	19.5 (initial) 52.93 (final)	4,096 (initial) 2,872 (final)	122,923 (N)	28,528 (N)
				97.3 (S)	60.5 (S)				473,627 (S)	11,883 (S)
				53.9 (E)	85.1 (E)				10,318 (E)	42,830 (E)
	3			92.0 (N)	49.3 (N)	12.34 (initial) 17.44 (final)	no data	4,052 (initial) 2,868 (final)	147,583 (N)	7,413 (N)
				89.8 (S)	84.7 (S)				112174 (S)	48,451 (S)
				81.8 (E)	84.6 (E)				52687 (E)	38,711 (E)
				63.7 (W)	81.5 (W)				20932 (W)	29,557 (W)
3	4	Spalled joints and spalled corners along doweled edges	7,100	95.3 (N)	92.1 (N)	13.96 (initial) 24.44 (final)	23.12 (initial) 59.74 (final)	3,582 (initial) 2,046 (final)	245,804 (N)	106,815 (N)
				90.1 (S)	87.1 (S)				109,712 (S)	50,796 (S)
				95.0 (E)	32.4 (E)				no data	4,698 (E)
	5			92.7 (N)	69.9 (N)	14.62 (initial) 31.03 (final)	no data	3,419 (initial) 1,612 (final)	152,262 (N)	20,726 (N)
				95.4 (S)	79.2 (S)				262,457 (S)	27,845 (S)
				68.7 (E)	12.5 (E)				24,130 (E)	389 (E)
				56.1 (W)	40.2 (W)				13,563 (W)	6,550 (W)
	6			94.4 (S)	84.4 (S)	14.87 (initial) 18.07 (final)	no data	3,362 (initial) 2,767 (final)	200,262 (S)	40,413 (S)
				44.1 (E)	26.8 (E)				7,065 (E)	2367 (E)
	7			95.6 (S)	54.7 (S)	14.37 (initial) 17.56 (final)	23.04 (initial) 72.28 (final)	3,478 (initial) 2,848 (final)	295,624 (S)	13,656 (S)
				63.6 (E)	18.9 (E)				18,344 (E)	969 (E)
				72.0 (W)	32.39 (W)				31,996 (W)	4,698 (W)

Table 8. Summary of instrumentation data.

Repair	Panel	Peak Corner Vertical Stress, psi	Peak Vertical Center Stress, psi	Peak Positive Panel Surface Strain (Passes 1-5)	Peak Negative Panel Surface Strain (Passes 1-5)	Peak Positive Edge Strains	Peak Negative Edge Strains
1	1	9.62 (initial) 11.33 (final)	No data	No data	No data	No data	No data
2	2	8.84 (initial) 8.31 (final)	No data	7.76E-04	6.47E-04	No data	No data
	3	No data	No data	1.54E-03	2.49E-04	No data	No data
3	4	No data	3.42 (initial) 4.55 (final)	3.01E-05	1.38E-06	No data	No data
	5	No data	6.07 (initial) 7.50 (final)	6.60E-05	8.44E-05	3.69E-04	-2.12E-04
	6	No data	5.32 (initial) 6.16 (final)	No data	No data	5.42E-04	-1.79E-04
	7	No data	No data	1.64E-04	9.05E-05	No data	No data

Figure 47. Repair 1 at failure condition.

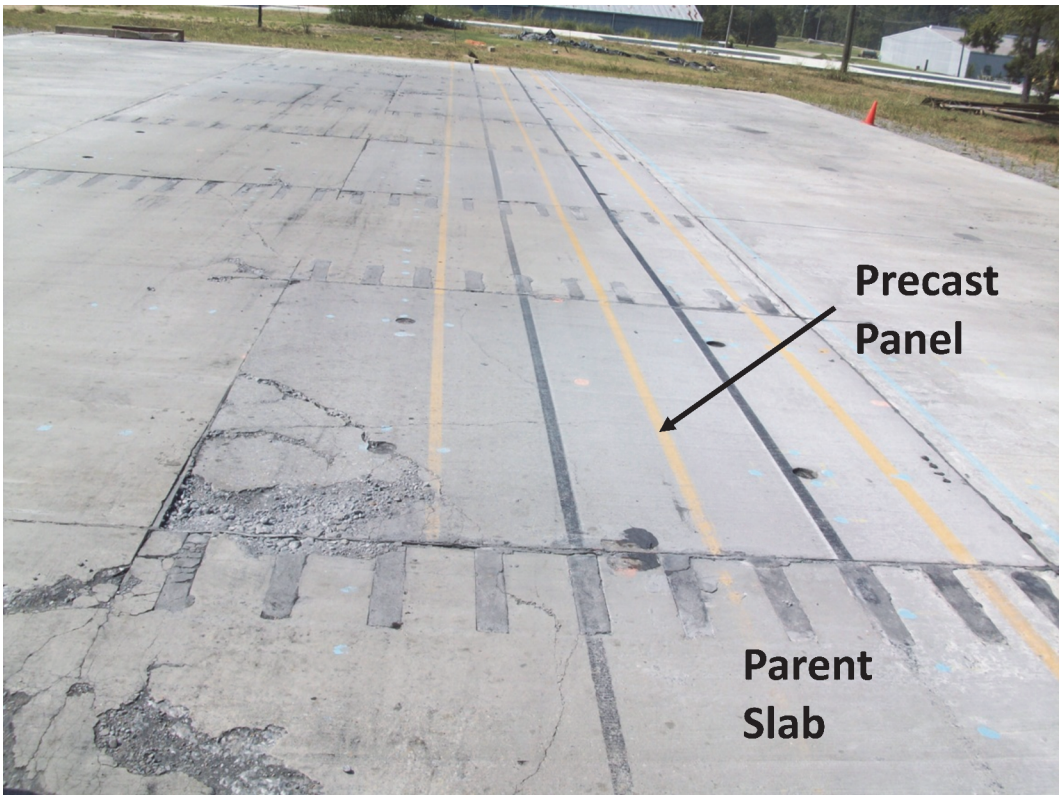

joints, the initial LTE was approximately 88 percent, but this reduced to 20 percent for the E joint and 78 percent for the W joint after 5,600 passes. For the transverse joints, the LTE met the general PCC guidance of at least

70 percent, indicating that the dowel preparation was acceptable as meeting the requirements for general PCC requiring load transfer.

The maximum panel center deflection measured after 5,600 passes was 31.38 mils (normalized to 50,000 lb for all measurements), which was an increase from the initial measurement of 14.37 mils. The corner deflections showed an even greater increase from 15.27 to 53.03 mils between 0 and 5,600 passes. The initial peak center deflections prior to traffic for all the panels were similar (12 to 15 mils). The final center deflection for Panel 1 in Repair 1 was higher than the final deflections measured for the other panels. This was not unexpected, as the panel was in shattered condition. The maximum peak deflection in the center of the panel appeared to be around 30 mils based on the measurements at failure. Correspondingly, the maximum peak corner deflection appeared to be 50 mils.

ISMs for Panel 1 were similar to Repair 3, but less than Repair 2's initial and final values. As with increasing deflections with increasing traffic, the ISMs decreased with increasing traffic with higher deflections measured at similar load levels.

The calculated joint stiffnesses for each joint decreased during trafficking with initial and final values presented in Table 7 for each panel. The initial joint stiffnesses measured were in the range of 80,000 to 180,000 lb/in./in. with high initial LTE. Because of the use of LTE in the calculation of joint stiffness, it was expected to have high initial values. At failure, the joint stiffnesses were much lower with a range of 15,000 to 33,000 lb/in./in., with the exception of the E joint, which was much lower (793 lb/in./in.) corresponding to the low final LTE value of 20.2 percent. Other factors in the calculation of stiffness included the deflection measured by the 72-in. HWD sensor, thus incorporating sublayer influences, in addition to the near surface deflections at the load plate and first sensor not accounted for in LTE calculations. The joint stiffness values (initial and final) for Repair 1-Panel 1 indicated that overall, this repair had weaker transverse joints than the other repairs. The data indicated that Repair 2 had the overall highest joint stiffness values at failure despite having similar initial values to Repair 3.

Measured vertical (EPC) stress for the SE corner was low ranging from 10 psi (initially) to 11 psi (failure) as seen in Table 8. No EPC measurements were available for the center of the panel, nor were surface or edge strain

data available due to instrumentation failure. In general, the vertical stress increased with traffic, indicating that the repair was deteriorating with traffic.

Despite failing the earliest of all the repairs with only 5,600 passes, the repair performed reasonably well under C-17 traffic, with traffic applications suitable for sustainment repair activities on contingency airbases requiring 5,000 passes. The passes to failure recorded for this repair were fewer than anticipated based on previous traffic tests on this type panel performed by the Air Force in 2007 using an F-15E load cart. Under that traffic, the panel did not deteriorate after 1,508 passes (Ashtiani et al. 2010). The C-17 load cart presented a more complex loading situation. Based on the traffic results, the repair configuration of a single-panel repair was determined to be suitable for C-17 traffic for at least 5,000 passes.

Repair 2- double-panel repair

Repair 2 showed the best performance of the three repairs withstanding 10,000 passes of C-17 traffic. As with Repair 1, cracks extended from the overcuts in the surrounding parent PCC and propagated during traffic. After 1,960 passes, cracking began to occur on the NW corner of Panel 2. The northern edge of the repair suffered spalling and cracking across both Panels 2 and 3. After 10,000 passes, the repair was considered failed due to the high-severity spalling at the center joint between the panels on the N end and spalling on the S end. The repair was also considered failed from the cracking and spalling of the patched dowel receptacles. Panel 2 at failure is presented in Figure 48. Similar cracking and spalling were located on Panel 3.

The roughness criteria were not exceeded for this repair with a maximum recorded elevation difference of 0.150 in. from the installation elevation. The maximum recorded elevation measurement was 0.3125 in. (negative) along the NW corner of Panel 2, where the spalled edge is evident in the figure.

As can be seen in Table 7, the LTE decreased from installation to failure for Repair 2 from a range of approximately 90 to 97 percent for the transverse joints (N and S) down to a range of approximately 50 to 85 percent. The lowest LTE was for the N joint of Panel 2, which had significant cracking and spalling along this joint as shown in the previous figure; for the longitudinal joints (E-W), the initial LTE ranged from approximately 54 to

Figure 48. Repair 2-Panel 2 at failure condition.

80 percent. The LTE increased from 54 percent to 85 percent for the E joint of Panel 2, indicating that the joint had better LTE possibly due to expansion or movement of a panel. The E and W joints of Panel 3 also increased in LTE from the initial measurement, most likely also due to expansion or movement of the panels causing closer contact of the panel to the parent PCC leading to increased LTE. For the transverse joints, the LTE prior to traffic met the general PCC guidance of at least 70 percent, indicating that the dowel preparation was acceptable as meeting the minimum requirements for general PCC requiring load transfer. After 10,000 passes, the S joint of Panel 2 and the N joint of Panel 3 had LTE values less than the minimum requirement.

The maximum panel center deflection measured following 10,000 passes was 17.41 mils for Panel 2 and 17.44 mils for Panel 3, which were small increases from the initial deflection measurements of 12.21 and 12.34 mils, respectively. The corner deflections of Panel 2 showed an increase from 19.5 to 52.93 mils at failure. The initial peak center deflections from these panels were similar to the other panels with a range of 12 to 15 mils.

ISMs for Panel 2 initially were 4,095 kip/in. and decreased to 2,872 kip/in. after 10,000 passes. These were similar to the ISMs measured for Panel 3 with an initial measurement of 4,052 reducing to 2,868 kip/in. As mentioned for Repair 1, the initial and final ISMs for panels in Repair 2 were higher than those for Repair 1 or Repair 3. This is attributed to better flowable fill used for this repair.

The calculated joint stiffnesses for each joint decreased during trafficking with initial and final values presented in Table 7 for each panel. The initial joint stiffnesses measured were in the range of 10,000 to 180,000 lb/in./in. with high initial LTE. Because of the use of LTE in the calculation of joint stiffness, high initial values were expected. At failure, the joint stiffnesses were much lower with a range of 10,000 to 470,000 lb/in./in., with smaller values corresponding with lower LTE measurements along the longitudinal joints of both panels. The joint stiffness values (initial and final) indicated that Repair 2 had the overall highest joint stiffness values at failure despite having similar initial values to Repair 3.

Measured vertical EPC pressures for the SW corner of Panel 2 were low, with little change between initial and final measurements (approximately 8 psi). No EPC measurements or edge strains were available for Panels 2 and 3 due to instrumentation failure. The peak positive surface strain measured during the first five passes of traffic on Panel 2 were 7.76E-03 in./in. and on Panel 3 were 1.54E-03 in./in., which were higher than those measured on panels from Repair 3. The peak negative surface strains were 6.47E-04 and 2.49E-04 in./in. for Panels 2 and 3, respectively, in similar range to the peak negative values. No edge strain data were available due to instrumentation failure. In general, the vertical EPC pressure readings increased with traffic, indicating that the repair was deteriorating with traffic.

Repair 2 withstood the most passes to failure. Based on the traffic results from this study, the repair configuration of a double-panel repair was determined to be suitable for C-17 traffic for 5,000 to 10,000 passes.

Repair 3- quad-panel repair

Repair 3 withstood 7,200 passes of C-17 traffic. As with Repairs 1 and 2, cracks extended from the overcuts in the surrounding parent PCC and propagated during traffic. After 1,400 passes, cracking began to occur on the SE corners of Panels 6 and 7 on the S end of the repair. The N edge of the repair suffered spalling and cracking across both Panels 4 and 5. The

spalling of the S edge and the dowel slots continued until the repair was considered failed after 7,200 passes from the high-severity spalling on the S edge of the repair and the dowel receptacles. Panels 6 and 7 at failure on the S edge of the repair are presented in Figure 49. The cracking as a result of overcutting the parent slab and the deterioration of the dowel receptacles are also shown in this figure.

Figure 49. Repair 3 South edge at failure condition and cracking extending from overcut in parent slab.

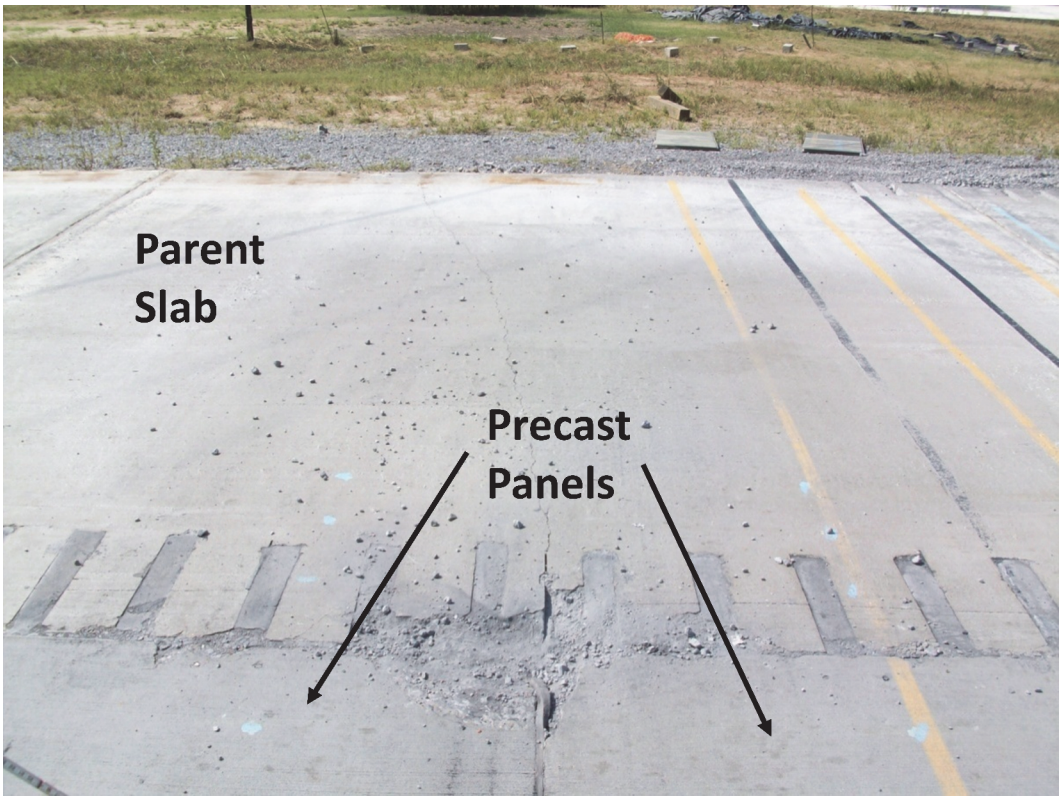

The roughness criteria were not exceeded for this repair with a maximum recorded elevation difference of 0.375 in. from the installation elevation. The maximum elevation measurement was 0.625 in. along the NE corner of Panel 4.

As can be seen in Table 7, the LTE decreased from installation to failure for Repair 3 from a range of 90 to 96 percent for the transverse joints (N and S) down to approximately 55 to 92 percent. The largest decrease was measured for Panel 7 on the S edge of the repair. This is not unexpected by the severity of the spalling and cracking on this side of the repair. For the longitudinal joints, the initial LTE ranged from 44 to 95 percent. The lowest LTE was for the E joint of Panel 6 of 44 percent. The panels decreased from their initial

values to 12.5 to 33 percent. The lowest values were measured along the E joint of Panel 5 and Panel 7. For the transverse joints, the LTE prior to traffic met the general PCC guidance of at least 70 percent, indicating that the dowel preparation was acceptable as meeting the requirements for general PCC requiring load transfer. After 7,200 passes, the S joint of Panel 7 had LTE values less than the minimum requirement. As mentioned previously, this is not unexpected due to the severity of the spalling and cracking along this joint.

The maximum panel center deflections measured following 7,200 passes were 13.96 mils for Panel 4, 14.62 mils for Panel 5, 14.87 mils for Panel 6, and 14.37 mils for Panel 7 initially. The final peak center deflections were higher for Panels 4 and 5 with 24.44 mils for Panel 4 and 31.03 mils for Panel 5. The final peak center deflections for Panels 6 and 7 were 18.07 and 17.56 mils, respectively. The corner deflection of Panel 4 was also measured, showing an increase from 23.12 to 59.74 mils at failure. The corner deflections measured for Panel 7 were similar with 23.04 mils measured initially and 72.78 mils at failure.

ISMs for the panels were similar initially with an approximated value of 3,500 kip/in. The ISMs decreased with traffic to a range of 1,600 to 2,800 kip/in. These are similar to the ISMs of Repair 2.

The calculated joint stiffnesses for each joint decreased during trafficking with initial and final values presented in Table 7 for each panel. The initial joint stiffnesses measured were in the range of 7,000 to 262,000 lb/in./in. with high initial LTE corresponding to high joint stiffness values. At failure, the joint stiffnesses were much lower with a range of 400 to 107,000 lb/in. /in. with smaller values corresponding to lower LTE measurements along the E and W joints of both panels.

Measured vertical EPC pressures for the centers of Panels 4, 5, and 6 were measured to be initially 3.42, 6.07, and 6.16 psi, respectively. At failure, these measurements only increased slightly to 4.55, 7.50, and 6.16 psi, respectively. No corner stresses were measured, and no center stresses were available for Panel 7 due to instrumentation failure. The peak positive surface strain measured during the first five passes of traffic on Panels 4, 5, and 7 were 3.01E-05, 6.60E-05 and 1.64E-04 in./in., respectively. The peak negative surface strains for the same panels were 1.38E-06, 8.44E-05, and 9.05E-05 in./in.

This repair withstood more passes to failure than Repair 1 but fewer than Repair 2. Based on the traffic results, the repair configuration of a quad-panel repair was determined to be suitable for C-17 traffic for at least 5,000 passes.

Comparison of precast repair method to other expedient repair methods

The precast panel repair method was also compared to expedient repair alternatives developed for the US Air Force and US Navy that have been investigated in recent years for airfield damage repair. These repair alternatives include a proprietary rapid-setting material cap placed over various backfill materials (foam, injected foam, flowable fill, and aggregate). The repairs are compared in this section in terms of timing, performance, and cost.

Work task timing

The timing data presented is based on average repair times from numerous field investigations facilitated and planned by the ERDC between 2006 and 2010. Various sized repairs were conducted, and the times to complete each repair including distressed area removal, preparation of backfill material, placing the rapid-setting cap, and curing of material were recorded.

The process for preparing the repair area using these methods is slightly different, requiring saw cutting the perimeter of the repair areas, breaking the surface PCC into smaller pieces, and excavating the PCC and any sub-layer material as required. The process of lifting the damaged pavement using drilled concrete expansion anchors was not used prior to the precast panel investigation.

For the previously investigated expedient repair methods, the comparison was conducted by calculating the average time to saw cut a PCC area, the average time to excavate 1 ft^3 of material (including the PCC and underlying materials using standard construction equipment), the average time to backfill 1 ft^3 of material, and the average time to place and cure 1 ft^3 of capping material. The average times were then used to calculate the time required to complete a 10-ft by 10-ft by 14-in. repair. The repair cap was assumed to be 10 in. for the rapid-setting material, and 4 in. for the backfill materials. This repair size corresponded to a single-panel repair (although the precast repair does not require as much backfill). As can be seen in

Figure 50, all repair types can be conducted in 4 to 6 hr (including curing). The precast panel repair compared well to the other repair options in terms of timing. The precast panel timing was based on an estimate using an optimized placement procedure developed and presented in the Phase I report (Bly et al. 2013).

Figure 50. Comparison of times to complete a 10-ft by 10-ft repair.

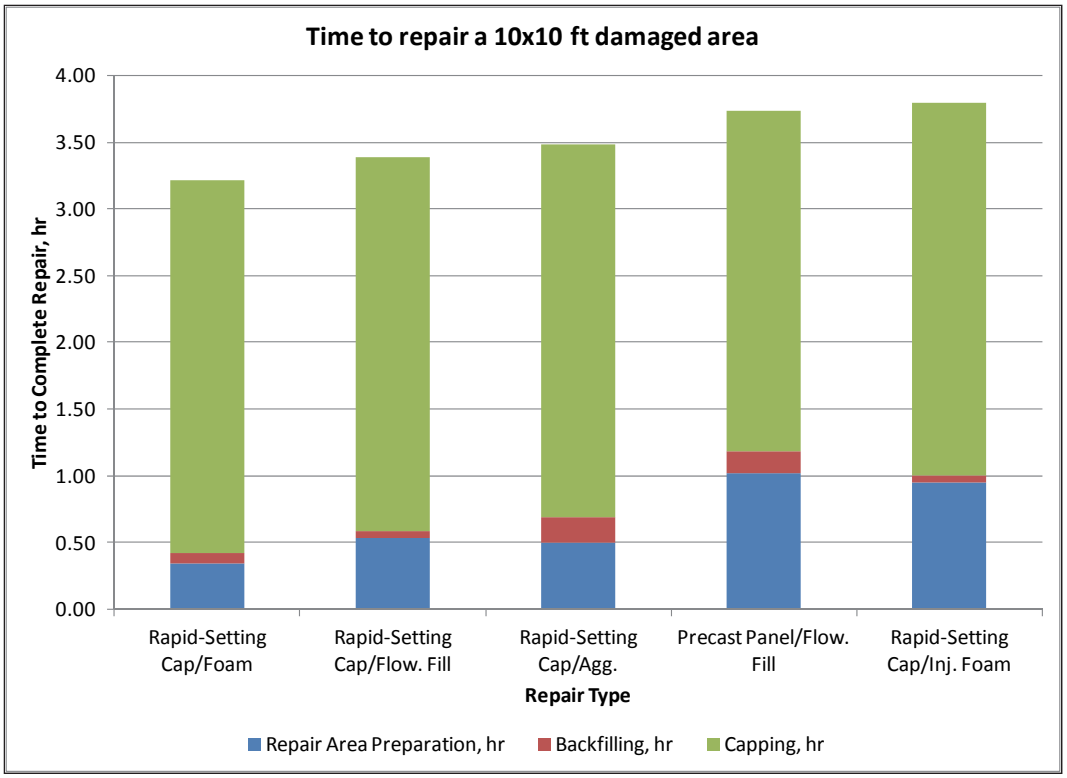

Cost and performance

The expedient repair types considered were also trafficked using simulated aircraft traffic and live aircraft testing including the C-17 and F-15 during the last several years through various full-scale field tests. The performance of these repairs indicated that all repair options were capable of supporting at least 100 passes of aircraft with several repairs being suitable for over 5,000 passes. The performance of the repairs is presented in Table 9. The total material cost to complete a 10-ft by 10-ft by 14-in. repair similar to the single precast panel repair used in the current investigation is also presented in this table. Neither the equipment nor labor costs are included for any repair.

Table 9. Comparison of repair methods in terms of performance, timing, and cost.

Repair Type	Repair Detail	Passes to Failure, #	Time to Complete Repair, hr	Estimated Material Cost
Rapid-Setting Cap/Aggregate	10 in. cap 4 in. compacted aggregate	5,000+	3.5	$1,380
Rapid-Setting Cap/Foam	10 in. cap 4 in. foam	1,000	3.2	$6,055
Rapid-Setting Cap/Injected Foam	10 in. cap debris	1,000	3.8	$6,020
Rapid-Setting Cap/Flowable Fill	10 in. cap 4 in. flowable fill	5,000+	3.4	$1,865
Precast Panel/Flowable Fill	11 in. panel 3 in. flowable fill	5,000+	3.7	$2,500
Traditional PCC (full-depth)	14 in. PCC	5,000+	28 days	$555

The cost of the precast panel repair was the cost to fabricate a single precast panel including PCC, rebar, dowels, flowable fill backfill (3 in.), and the dowel and joint sealing materials. The estimated costs were $2,500 for a standard panel and $2,550 for a terminal panel. As can be seen in the table, the least expensive repair is the traditional cast-in-place PCC; however, rapid return to traffic cannot be obtained using this method. Combining cost, performance, and speed, the precast slab is the third best option for rapid repair of those considered. Since the precast panel method's attributes are similar to other DoD expedient repair methods, this repair technique is suitable for conducting airfield PCC repairs. The greatest utility repair teams may find with this technique is that the amount of rapid-setting material supplies required are minimized compared to the other methods, and minimal upkeep is needed to maintain an operational rapid repair system.

10 Conclusions and Recommendations

As detailed in Chapter 1, attributes for an acceptable expedient PCC pavement repair system using precast panels included:

- Is easily fabricated under adverse field conditions,
- Uses locally available materials,
- Is capable of long-term storage,
- Is ready for use in a moment's notice,
- Allows for rapid installation in multiple repair geometries,
- Minimizes equipment required for installation,
- Minimizes specialized training, and
- Provides sufficient service life under the prospective aircraft traffic.

The Phase I report evaluated the precast panel system for the first seven attributes and provided recommendations and conclusions for the final system (Bly et al. 2013). This report evaluated the panels to determine if they could provide sufficient service life under simulated aircraft traffic. The original repair system was previously field tested under F-15E load cart trafficking for 1,508 passes without any notable distresses. The performance of the new panel system under C-17 simulated traffic was evaluated in this report. In addition to the panels' performance under traffic, the panel repair concept was compared to other previously tested expedient repair methods in terms of speed, cost, and performance.

Based on the preparation, performance of the panels under C-17 traffic, repair speed, and cost, the following conclusions and recommendations are made:

Conclusions

- The precast panel repair method provided repairs capable of supporting at least 5,000 passes of C-17 traffic.
- The precast panel system design was suitable for conducting a variety of repair sizes.
- The connection of the panels using the standard and terminal panels performed well under traffic application.

- The flowable fill backfill provided adequate support for the panels under C-17 traffic. Differences in flowable fill quality contributed to variances in repair performance under traffic.
- The failure of the panels was the result of spalling along the doweled joints both in the panel and in between and within the dowel receptacles in the parent PCC.
- All partially removed parent slabs cracked into smaller, square slabs, where cracking initiated from overcutting used to remove the damaged portion of the pavement.
- The panels performed similarly to traditional PCC in terms of measured deflections and stresses to predicted values; however, the models and equations used could not account for differences in panel and parent PCC pavement structures.
- Higher LTE was measured for the transverse doweled joints than the longitudinal undoweled joints.
- The LTE of the panels corresponded well to the stiffness of the joints, indicating that the joint spacing and use of dowels contributes more to the higher LTE and stiffness than sublayer effects or aggregate interlock.
- The precast panel method was comparable to the previously approved repair methods in terms of speed.
- The cost of the precast panel repair was slightly more expensive than the rapid-setting cap over flowable fill or aggregate methods, but it is less expensive than the rapid-setting materials over foam methods.

Recommendations

- Further research into the most efficient doweling design is recommended. Modifications should investigate minimizing the dowel slot receptacles in terms of the number and/or volume required to reduce the amount of spalling and cracking. Dowel diameter and panel thickness are also factors in modifying the dowel design. The LTE, stiffness, and instrumentation measurements may be useful for modeling various design alternatives and developing more realistic models for pavement repairs.
- Based on the cracking and spalling of the dowel patching material used in this field testing, further investigation into proper selection of dowel patching materials should be explored. Currently, DoD certified products are recommended for use; however, these requirements may not be stringent enough to provide adequate performance with this repair method.

- Methods for repairing spalled joints should be developed and evaluated to determine if the life of the panels may be extended through small repair efforts.
- To help control cracking developed from overcutting the parent PCC during installation of the panels, it is recommended that the parent PCC slabs where portions of the slab are removed be saw cut (and sealed) to similar dimensions.
- Additional field testing of the repair method is recommended to determine if the estimated time savings can be obtained using the optimized repair method used for the comparison. Field testing should also focus on the use of the minimum rated 15-ton crane, and perspective personnel assignments required utilizing the system.
- Based on the performance of the panels, the speed of the repairs, and the cost, the panel repair method is suitable for conducting airfield PCC repairs where rapid-setting materials or other repair methods are not available.

References

Ashtiani, R., C. Jackson, A. Saeed, and M. Hammons. 2010. *Precast concrete panels for contingency rigid airfield pavement repairs*. AFRL Technical Report AFRL-RX-TY-TR-2010-0095. Tyndall AFB, FL: US Air Force Research Laboratory.

Bly, P. G., L. P. Priddy, C. J. Jackson, and Q. S. Mason. 2013. *Evaluation of precast panels for airfield pavement repair-Phase I: System optimization and test section construction*. ERDC/GSL TR-13-24. Vicksburg, MS: US Army Engineer Research and Development Center.

Byrum, C. R. 2011. Direct Calculation of Pavement Joint Stiffness using Falling Weight Deflectometer Joint Load Tests. *Transportation Research Board Annual Meeting Compendium of Papers Online*, National Research Council, Washington, DC.

Innovative Pavement Research Foundation (IPRF). 2011. *Joint load transfer in concrete airfield pavements: Summary report*. Report IPRF-01-G-002-05-2. Rosemont, IL: IPRF.

Ioannides, A. M., L. Khazanovich, and J. L. Becque. 1992. Structural Evaluation of Base Layers in Concrete Pavement Systems. *Transportation Research Record 1370*, National Research Council, Washington DC.

REPORT DOCUMENTATION PAGE

Form Approved
OMB No. 0704-0188

1. REPORT DATE *(DD-MM-YYYY)*	2. REPORT TYPE	3. DATES COVERED *(From - To)*
September 2013	Report 2 of a series	

4. TITLE AND SUBTITLE

Evaluation of Precast Panels for Airfield Pavement Repair; Phase II: Results of Accelerated Pavement Testing

5a. CONTRACT NUMBER

5b. GRANT NUMBER

5c. PROGRAM ELEMENT NUMBER

6. AUTHOR(S)

Lucy P. Priddy, Peter G. Bly, Christopher J. Jackson, and Tony N. Brogdon

5d. PROJECT NUMBER

5e. TASK NUMBER

5f. WORK UNIT NUMBER

7. PERFORMING ORGANIZATION NAME(S) AND ADDRESS(ES)

U.S. Army Engineer Research and Development Center
3909 Halls Ferry Road, Vicksburg, MS 39180; and
Applied Research Associates
Aircraft Operating Surfaces Research Group; Engineering Science Division;
104 Research Road, Bldg. 9742, Tyndall AFB, FL 32403

8. PERFORMING ORGANIZATION REPORT NUMBER

ERDC/GSL TR-13-24

9. SPONSORING / MONITORING AGENCY NAME(S) AND ADDRESS(ES)

Headquarters, Air Force Civil Engineer Center
Tyndall Air Force Base, FL 32403-5319

10. SPONSOR/MONITOR'S ACRONYM(S)

11. SPONSOR/MONITOR'S REPORT NUMBER(S)

12. DISTRIBUTION / AVAILABILITY STATEMENT

Approved for public release; distribution is unlimited

13. SUPPLEMENTARY NOTES

14. ABSTRACT

During the period May through August 2012, researchers of the U.S. Army Engineer Research and Development Center (ERDC) in Vicksburg, MS conducted accelerated pavement testing using a C-17 load cart to evaluate the performance of a precast portland cement concrete (PCC) pavement repair system. The system was originally developed by the Air Force Research Laboratory (AFRL) in 2009 but was modified in a joint venture between AFRL and ERDC in 2011 and 2012 as Phase 1 of this project. Three PCC precast panel repairs were performed using the modified system. The precast repairs evaluated were a single-panel, a double-panel, and a quad-panel repair, which simulated repairing a quarter, a half, and a full pavement slab, respectively. Simulated C-17 traffic was applied to the repaired surfaces to determine if the precast panel repairs were suitable for withstanding aircraft traffic for emergency or contingency airfield operations. This report presents the results of accelerated pavement testing including the passes-to-failure, surface deterioration, load-transfer efficiency, deflections, and stress-strain measurements during trafficking. Results of this investigation will be used to further refine the design of the precast panel repair system.

15. SUBJECT TERMS

Airfield repair
Airfield rigid pavements
Expedient Repair
Field testing
Precast concrete
Precast panels
Precast slabs
Rapid concrete repair

16. SECURITY CLASSIFICATION OF:			17. LIMITATION OF ABSTRACT	18. NUMBER OF PAGES	19a. NAME OF RESPONSIBLE PERSON
a. REPORT	b. ABSTRACT	c. THIS PAGE			19b. TELEPHONE NUMBER *(include area code)*
Unclassified	Unclassified	Unclassified		97	